UNIVERSITY OF CENTRAL OKLAHOMA

GRADUATE COLLEGE

MOISTURE-WICKING PROPERTIES OF FABRIC AND THEIR EFFECT ON BLOOD AND THE ANGLE OF IMPACT

A THESIS

SUBMITTED TO THE GRADUATE FACULTY

in partial fulfillment of the requirements for the

Degree of

MASTER OF SCIENCE, FORENSIC SCIENCE

By

DIAH JOHNSON
Edmond, Oklahoma
2022

MOISTURE-WICKING PROPERTIES IN FABRIC AND THEIR EFFECT ON BLOOD AND THE ANGLE OF IMPACT

A THESIS APPROVED FOR THE
MASTER OF SCIENCE, FORENSIC SCIENCE

BY

Diah Johnson

Dr. Mark McCoy, Chair

Mr. Craig Gravel

Dr. Cynthia Murray

Mr. Austin Kress

Thank you.

To the UCO professors who have helped me along the way.

To my parents, Michael and Kristin, for their unwavering support of me and my academic ambitions. I couldn't have done this without you.

To Carolyn and Anna for being my sounding board when words were hard.

To Mrs. Dettmann, my 7th grade teacher, who fostered my love of science and encouraged my dream of becoming a forensic scientist. I did it!

To Kenzie and Paige for providing comedic relief and moral support.

To Mary Anne, my life-saver of an editor, whom without this paper would not exist.

To Kaleb, my love, for the sacrifices you've made while I chased this dream.

Thank you to everyone who has made this possible.

Table of Contents

List of Tables

List of Figures

Abstract

The use of angle of impact calculations within bloodstain pattern analysis is limited to researched surface types which currently include smooth, non-porous materials and cotton. The purpose of this study was to determine if the existing equation for angle of impact could accurately be applied to moisture-wicking polyester. This study used posterboard as a control and tested three different polyester fabrics (100% polyester, 80% polycotton, and 20% polycotton). Bovine blood was dropped onto each of the four surfaces at 10° increments from 10° to 90°. The resulting stains were measured with digital calipers used in conjunction with drafting dividers. The measurements were analyzed using ANOVA and Tukey's multiple comparisons test to determine and evaluate the significant differences between the surface types and the actual angles. The results showed that polyester significantly affected the ability to calculate angle of impact to within ±5°. The wicking property of polyester distorted the stains disproportionately so the angle of impact calculations were inaccurate at some angles. All three polyester samples had accurate calculations from 10° to 40°, but outside of that range, calculations were inconsistent and inaccurate. This information broadens the understanding of bloodstain analysis and can assist analysts in understanding the weight of their findings.

Chapter 1: Introduction

Bloodstain Pattern Analysis

The main focus of bloodstain pattern analysis is to determine what happened at a crime scene. Analysts can examine the characteristics of bloodstains and identify, with varying accuracy, what weapons were used and the direction of force, as well as where people and objects were located during a bloodshed event. They can also get an idea of how people moved through a scene, which is important when trying to reconstruct a crime scene. Blood maintains a spherical shape while moving through the air (Gravel & White, 2019) which means blood behavior can be predicted and reproduced. Analysts are able to reverse engineer bloodstains to better interpret what happened at a scene. Having reliable knowledge on the behavior of blood has revolutionized crime scene reconstruction.

Statement of the Problem

In order for bloodstain analysis to be admissible in court, there needs to be reference data to validate it. Most studies conducted on bloodstain pattern analysis were done on smooth, non-porous surfaces, but not many surfaces found at a crime scene fall into this category. Any blood found on textured surfaces, such as tile or carpet flooring and upholstered furniture, cannot currently be used for analysis purposes. A common places to find blood at a crime scene is on clothing, but the analysis of bloody clothing is quite limited. Most of the previous research involving fabric was qualitative, focused on the interaction of the blood with the fabric, instead of quantitative, examining the stains for reproducible properties often used for reconstruction purposes.

Background and Need

Research on bloodstain patterns has come a long way, but it still has a long way to go. Balthazard's 1930s studies on stain characteristics used smooth, flat surfaces, which is great as a control but is very limited in application. The use of angled targets opened the door to identifying area of origin (Balthazard, 1939). Kirk's use of bloodstain pattern analysis in a 1950s court case (Kirk, 1955) inspired MacDonell's research in the 1970s to modernize old methods, calculate angle of impact and explore how surface texture can affect stain patterns (MacDonell, 1971). In the 2000s, research was conducted on how surface texture, and more specifically fabric, distorts bloodstains (Holbrook, 2010) and causes misinterpretation by analysts (Reynolds & Silenieks, 2016).

The textile industry is large and continues to grow as new fiber blends are created that change the properties of the fabric. Many properties can change the way bloodstains look, and absorption is one of them (Slemko, 2003). Polyester is often used in athletic clothing for its moisture-wicking properties to keep the wearer dry (Knapp, 2018). Since moisture-wicking prevents absorption (Knapp, 2018), the accuracy of analysis on polyester and its blends is called into question. The Organization of Scientific Area Committees for Forensic Science has requested more research on the effect of fabric on blood to better analyze the stains (FSSB, 2015). The fact that the absorption level of fabric distorts bloodstains is known (Slemko, 2003), but the effect that distortion has on the ability to calculate things like angle of impact is still largely unknown.

Research is needed on the quantitative properties of blood on fabric to determine whether the angle of impact can accurately be calculated on the different fabric types. Gaps in the research can lead to subjective interpretations and erroneous conclusions.

Purpose of the Study

This study concentrated on the ability to calculate the impact angle of blood on fabric designed to wick moisture. Most moisture-wicking fabrics are made using synthetic fibers, such as polyester. The fibers often have special coatings to make them hydrophobic and the fabric is designed with space between the fibers to promote capillary action and move liquid to the surface (Knapp, 2018). The equation for angle of impact was discovered using a smooth, non-porous surface, and fabric texture is known to distort the shape of stains. The moisture-wicking property of the fabric used in this study had the possibility of adding to the distortion of the stain. A smooth control was used to validate the design of the experiment. Three common moisture-wicking fabrics, one pure and two blends, were tested using the existing equation for angle of impact. The calculated angles of all three targets were compared to the actual angle; acceptable error is ±5° (Bevel & Gardner, 1990).

Research Questions

The main question when designing this experiment was: can the equation used to find the angle of impact on smooth, non-porous surfaces provide accurate results on moisture-wicking polyester fabrics?

Significance to the Field

This experiment will add to the knowledge base of bloodstain pattern analysis. Experimenting with the moisture-wicking polyester will give examiners a better understanding of how blood interacts with the fabric allowing for a more accurate analysis with less subjective interpretation.

Definitions

Terms from The Organization of Scientific Area Committees for Forensic Science

Angle of Impact (Impact Angle)—The angle (alpha) at which a blood drop hits a target, relative to the plane of the target

Area of Origin—The three-dimensional location at which trajectories of spatter can be utilized to determine the location of the spatter producing event

Bloodstain—A deposit of blood on a surface

Bloodstain Pattern—A grouping of distribution of bloodstains that indicate through regular or repetitive form, order, or arrangement the manner in which the pattern was deposited

Cast-off pattern—a bloodstain pattern resulting from blood drops released from an object due to its motion

Edge Characteristics—A physical feature of the periphery of a bloodstain

Parent Stain—A bloodstain from which satellite spatter originated

Pool—A bloodstain resulting from an accumulation of liquid blood on a surface

Satellite Spatter—Smaller bloodstains that originated during the formation of the parent stain as a result of blood impacting a surface

Spatter—A bloodstain resulting from an airborne blood drop created when external force is applied to liquid blood

Target—A surface onto which blood has been deposited

Transfer Stain—A bloodstain resulting from contact between a blood-bearing surface and another surface

Void—An absence of blood in an otherwise continuous bloodstain or bloodstain pattern

(OSAC for Forensic Science, 2017)

Other Terms

Absorption—Moisture is taken into the fiber and retained

Adsorption—Moisture is held on the surface of the fiber instead of being taken into the fiber

Blotter—highly absorbent paper

Capillary Action/Effect—The rise or depression of a liquid in a small passage such as the space between fibers or the openings in a porous material

Crime Scene Reconstruction—The combined use of reasoning, physical evidence, and scientific methods to gain knowledge of the events surrounding the commission of a crime

Distortion—Asymmetrical features of a bloodstain

Dropping Distance—The distance a blood drop traveled prior to impacting a target

High Energy Spatter—Spatter resulting from a force in excess of 100 ft/sec. The stains typically measure 1mm or smaller and are generally associated with gunshots and explosions.

Leading Edge—The side of a bloodstain where the blood drop made contact with the target first when angle of impact is not 90˚

Medium Energy Spatter—Spatter resulting from a force of 5-25 ft/sec. The stains typically measure 1-4mm and are generally associated with blunt force trauma.

Moisture-Wicking—hydrophobic fibers use capillary action to move moisture to the surface

Passive Drops—A bloodstain resulting from the force of gravity up to 5 ft/sec. The stains typically measure 4mm or larger and are generally associated with a bleeding injury.

Tail—A skid mark at the terminal edge of a bloodstain

Terminal Edge—The side of a bloodstain where the blood drop made contact with the target last when angle of impact is not 90˚.

(ACSR, 2021), (Encyclopedia Britannica), (Oxford Dictionary), (TextileGlossary.com)

Limitations

Polyester was used as the focus material, but only three compositions, 100% polyester and two polycotton blends, were tested. This study could not examine every possible blend. Fabric construction influences the way blood interacts with the fabric, so the data collected is limited in application to only the materials utilized in this study.

Bagged blood has added anticoagulants to prevent the blood from clotting, which may affect the interaction between the blood and fabric. To avoid possibility of unwanted variables, the blood used was provided by a local butcher. To prevent clotting, the blood was continuously stirred.

The experiment was conducted in a laboratory setting with a controlled environment and stationary targets. Crime scenes, especially outdoors, may have environmental factors impacting the blood's interaction with the target. Crime scenes also have the added variable of motion, so it is important to make sure the area being analyzed is unaltered. Knowing the angle of impact is only helpful if the bloody object remains unaltered from the time of the crime.

The impact of blood onto a target creates edge characteristics on the bloodstain that can make measuring the stain difficult as edge characteristics are not included in the measurements. Blood on fabric tends to soak into the weave pattern causing the edge of the stain to become less defined and therefore makes measuring the stain more difficult. It is the decision of the analyst to determine where to measure on each stain. An analyst with a higher skill level may be needed to determine where to measure on the less defined stains.

The expertise of the analyst can impact the outcome of the study. The measurements for the stains may vary depending on the skill level of the analyst and their comfort with the tools. The accepted ±5° error for angle of impact helps to combat user error.

Chapter 2: Literature Review

Discovering the Basics

Balthazard was a French professor in forensic medicine and one of the first people to truly experiment with bloodstain patterns in the 1930s. He and his team performed several studies to see what information could be gathered by analyzing different characteristics of bloodstains and to determine how bloodstains could assist in the reconstruction of a crime scene.

When Balthazard and his team started experimenting with bloodstains, they quickly recognized the limitation of testing on flat targets. Instead, they switched to angled targets. With all the movement that takes place during a crime, it is more likely blood will hit a surface at an angle rather than at 90˚. They knew being at an angle would change the shape of the bloodstain and wondered whether the angle could be used to determine dropping distance. They dropped blood from a variety of known heights, and they noticed a relationship between the angle of the target and the length/width ratio of the stain; horizontal targets created circular stains, and as the targets neared vertical, the stains became increasingly elliptical (1939, p.7). By plotting the length/width ratio of the stains with their known angle, they created a graph that could be used to predict the unknown angles of stains (**Fig 1**).

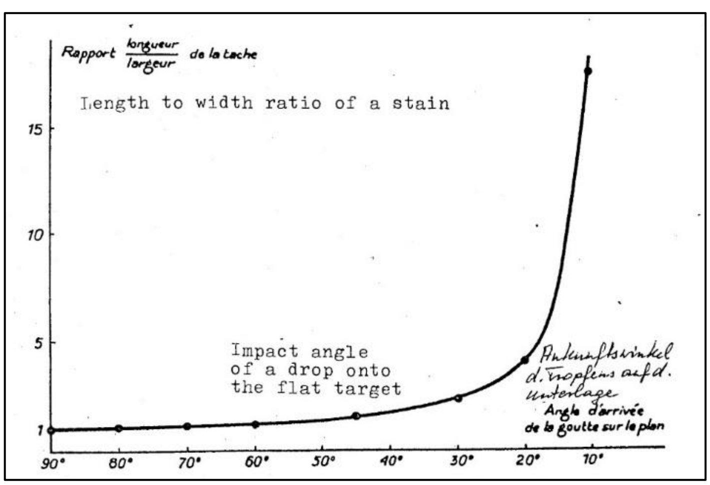

Figure 1 Graph of length/width ratio for angle of impact

Balthazard et al (1939)

One issue was that at sharper angles the blood dripped after impact creating a tail that caused the bloodstain to have an undefined terminal edge and made accurately measuring the length more difficult. Even though they were unable to determine the exact angles, they were able to estimate the angles with some room for error. These approximations proved sufficient for practical use. After the difficulty they faced when tails appeared on the stains, they focused on how to appropriately measure such stains. They dropped blood from various heights onto known angles and tried to compare the total stain length to the length of the tail. The stain/tail ratio was too inconsistent to be conclusive (1939, p.8). Although their angle of impact graph (**Fig 1**) was not perfect, their methods were sound, and their conclusions were considered accurate for their time. Despite the fact Balthazard addressed angled targets, the research was still limited to smooth surfaces.

Balthazard was interested in the practical use of bloodstain analysis, and he noticed a flaw in their previous testing method; all the tests were completed using cardboard as the target, which is not an accurate representation of crime scenes. Balthazard and his team decided to expand their research to include multiple surface types. They dropped blood at both 90° and 45° onto a variety of surfaces such as tile, parquetry (wooden mosaic), textiles, furs, metal, and a blotter. They discovered the composition of the target greatly impacted the resulting bloodstain. Five characteristics were used to describe why the different target types affected the bloodstain. The first (1) characteristic was the surface lacked adhesive properties causing the blood to retract upon impact. Smooth surfaces, such as glass and tile, displayed retracted stains, along with rubber surfaces and raincoats. The second (2) characteristic dealt with absorption. On tight fabrics like felt and furs the blood was unable to absorb so remained on the surface. Alternatively, on looser fabrics, such as cotton or paper-like materials, the blood was absorbed causing the stain to enlarge. The absorption witnessed was irregular and asymmetrical making it difficult to accurately calculate an angle of impact. The third (3) characteristic involved the texture of the surface. Porous or rough surfaces caused the blood to expand asymmetrically. The fourth (4) lumped two characteristics together: added ink or color on a surface, and holes in the surface. Both cause an interruption to the spread of the bloodstain while leaving the rest of the stain to spread unaffected. The fifth (5) characteristic was oxidation. Oxidation is a chemical reaction between the blood and the composition of the surface. Oxidation occurred when blood fell onto zinc and oxidized causing what they called a "pseudo-retraction" because of the visual similarity to retraction. With the new knowledge of how blood interacts with the target, Balthazard noted that previous data and graphs regarding bloodstains were only applicable to the material used in the experiment; data could not be assumed to be accurate on untested material (1939, p.25). Balthazard determined the interaction of blood with its target was important to consider when analyzing bloodstains.

Balthazard emphasized his findings and conclusions were only applicable in situations reminiscent of those tested. He stressed his conclusions cannot be assumed to be accurate when applied to differing scenarios. Balthazard also recognized the need for further study and acknowledged that although his tests involved vertical blood drops with known heights, it is more common the blood is a product of motion with a horizontal component, which would require solving for trajectory. He theorized a collection of bloodstain trajectories could be examined together to find a 3-dimensinal area of origin. (1939, p31). It took 30 years for Balthazard's research to be re-explored by MacDonell, mentioned later, but in the meantime, his theory on area of origin was brought to life in a US court case.

The Modern Building Blocks of BPA

A Breakthrough Case

Roughly 15 years after Balthazard's research was published, the topics he theorized played an instrumental role in an Ohio appellate court. In the case of *Ohio v Sheppard,* the jury convicted a man of violently beating his wife to death. Upon appeal, the defense team called Paul Kirk, the chair of UC Berkeley's criminology program, as an expert witness to reexamine the evidence and provide an unbiased report. The prosecution never conducted a thorough analysis of the blood patterns, and most of their other evidence from the first trial was circumstantial.

Kirk was able to visit the scene and was given access to pieces of evidence that had been previously removed in order to recreate the crime scene. The violence of the crime was evident by the amount of blood spatter all over the room. There was a two-foot void in an otherwise continuous pattern, so Kirk was able to place the attacker with great certainty in that spot within the room.

Kirk applied Balthazard's theory of area of origin (Balthazard, 1939) when he noticed the blood drops on the bed were elliptical and all pointed back to a single point on the bed with a large blood pool. After comparing the directionality of the spatter to the wounds on the body, Kirk was able to place the victim's head at the time of the beating. The blood pool indicated the head remained in that position as it was bleeding. Most of the spatter on the walls was identified as medium energy spatter, which is consistent with a beating, and fanned out from the bed making the bed the area of origin. Two stains were too large to be spatter from the victim and were found to be a blood type inconsistent with that of the victim and her husband.

Kirk noticed some of the drops on the wall pointed in directions not consistent with the beating. These drops created line patterns pointing to a space next to the bed instead of on the bed where the victim lay. Kirk experimented to duplicate these stains and concluded blood was castoff, flung from the backswing of a weapon. Knowing the location of the weapon also provided a location for the assailant. The distribution of the stain was arced and horizontal, therefore Kirk determined the weapon was swung with the assailant's left hand horizontally, like a bat. The lack of blood on the ceiling supported his horizontal swing theory since a vertical swing would cast blood onto the ceiling instead of the wall (1955). Kirk's examination of the case was objective and pointed to there being a third person involved. Kirk's testimony led to a not guilty verdict in the husband's retrial. While the case remains unsolved, a new suspect was identified but he died before a new investigation could be conducted. The *Ohio v Sheppard* case demonstrated the value of bloodstain analysis and set a precedence for the acceptance of bloodstain pattern analysis in the modern court system. The ability to use bloodstains to track the movements of a crime and to place people in relatively specific locations greatly reduced the need for unsupported guesswork. Kirk's work brought a spotlight back to bloodstain analysis, a topic forgotten in research for many years, and prompted people to continue research once more.

Resuming Research

Herbert MacDonell, a renowned forensic scientist, resumed research on bloodstain analysis after noticing a scarcity in literature in the 20 years after Paul Kirk's testimony. MacDonell started his research by examining the physical properties of blood and noted that blood outside the body is affected by gravity and air resistance, which causes the drops to form spheres in the air. To increase the validity of future experiments, he determined, with 95% confidence, the volume of a single blood drop to be 0.05 mL. He also determined the diameter of a single drop of blood to be 15-19 mm (1971, p.3-5). By defining these measurements, MacDonell eliminated a possible source of error for his tests.

Earlier studies concluded target composition affects the way blood acts upon impact, and therefore, the dropping distance cannot be determined without first examining the target. The stain in question must be compared to test data collected using the same target material. MacDonell went a step further to explore what happened when a blood drop lands on multiple surface types. He observed greater amounts of satellite spatter on the smoother surface as pictured in **Figure 2**. MacDonell concluded the cause of the spatter was a lack of capillary effects on the smooth surface. The rougher material broke the surface tension of the blood drop upon impact causing the droplet to separate and spatter outward (1971, p.8).

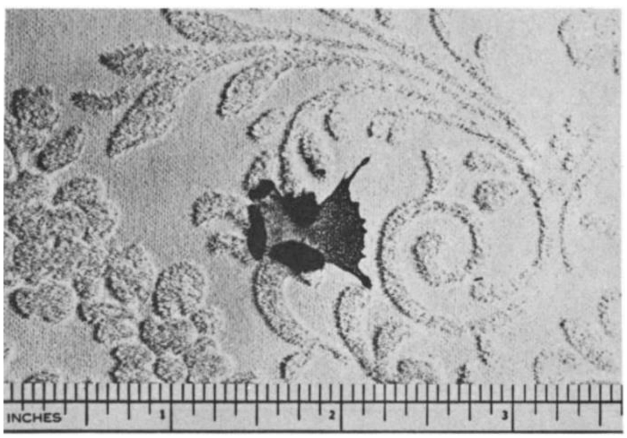

Figure 2 A single blood drop landing on soft, flocked wallpaper

MacDonell (1971)

Balthazard studied angle of impact in the 1930s, but MacDonell wanted to know whether it mattered which element was angled, the target or the blood's trajectory. For the first part, MacDonell dropped blood vertically onto smooth, angled boards and analyzed the elliptical stains. Steeper angles created longer ellipses, which made measurements for the length/width ratio more accurate. Replicating the same experiment using a blotter created the same elliptical stains. Absorption created distortion in the stains causing the measurements to not be as accurate as the board, but the length/width ratio still provided a close estimate (1971, p.11). Testing on angled targets reaffirmed previously accepted conclusions and acted more as a control for MacDonell to compare in the next part of his experiment, which involved angling the flightpath of blood.

Blood moving horizontally through the air is affected by gravity, which means the trajectory is curved and will likely not land at a 90° angle. MacDonell experimented with blood on the floor, walls, and ceiling. On the floor, blood was projected horizontally and allowed to fall. For the walls, blood was flung vertically, and both directions created similar stain patterns. Blood was flung overhead to produce stains on the ceiling. In each scenario, the length-to-width ratio measurements of the resultant ellipses provided an accurate angle of impact (1971, p.13). Knowing that the cause of an angle, the target or blood trajectory, did not affect the calculation of the angle validated the equation for use in crime scene reconstruction and in the courtroom.

MacDonell published a follow-up article in 1982, *Credit Where It's Due*, in which he amended the wording of his equation to reflect the standardized verbiage.

$$arc\ sin \frac{width\ of\ bloodstain}{length\ of\ bloodstain} = impact\ angle$$

Figure 3 Equation for Angle of Impact

Focusing on Fabric

Characteristics of Fabric

Most of the prior research involving fabric only used it for comparison purposes. In 1939, Balthazard used fabric to show how surface texture effects stain patterns, but he never looked into the specifics of why. In 2003, Slemko, a recognized bloodstain expert, decided to look specifically at the characteristics of fabric. He focused on the effect fabric treatment had on the distortion of bloodstains. The fabrics used were a mix of new, washed, and water-shielded samples. He tested transfer patterns, passive drops, and both medium and high energy spatter. Slemko discovered the treatment of the fabric mattered more than the method of bloodshed when it came to the cause of distortion.

The weave of the fabric influenced the distortion of bloodstains but was dependent on the volume of blood. A course weave caused blood to diffuse along the grain of the fabric. When spatter drops were small enough to fit on top of a thread, weave did not matter since the blood was not absorbed into the weave.

In general, both high and low absorbencies created distorted stains (**Fig 4**). Higher absorbency fabric diffused the blood and merged stains if they were near each other. Some distorted stains had a dark center surrounded by a lighter colored ring, while others, the medium and high energy spatter, had a ring of satellite spatter around the drops. Low and no absorbency fabric caused the blood to roll and drip rendering any analysis pointless.

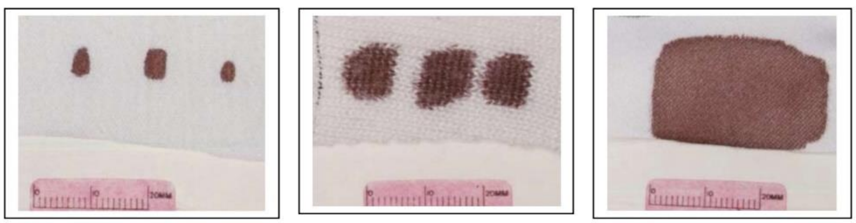

Figure 4 Three drops of blood on low to high absorbency fabric (left to right)

Slemko (2003)

Slemko noticed the absorbency of the fabric was altered when treated. Washing the fabric considerably increased the fabric's absorption (**Fig 5**), while water-shielding treatments like Scotchgard® greatly decreased absorption. The size of the stains were too distorted to differentiate medium and high energy spatter (2003).

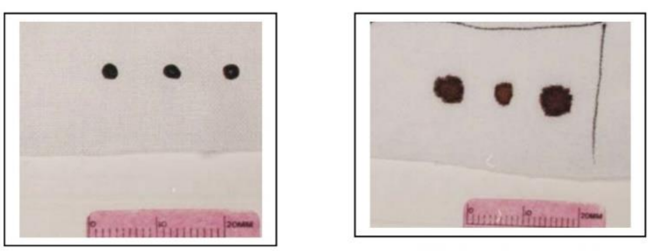

Figure 5 Absorbency of blood on new cotton (left) and washed cotton (right)

Slemko (2003)

For any accurate analysis only mid-range absorbency fabrics worked. Mid-range was not defined and is greatly subjective given the effect of fabric treatments. More testing will need to be conducted on fabric treatments and their impact on the properties of fabric and subsequent impact on bloodstain analysis.

Identifying Stain Types

Although Slemko studied bloodstains on fabric, he was not concerned with identifying the cause of the stains. In 2010, Holbrook, a bloodstain expert, decided to investigate whether any distinguishing features could be found between spatter and transfer stains. Blood on an object indicates involvement with the crime but knowing how it got there helps place it in the scene.

In general, Holbrook discovered transfer stains were only present on the top layer of thread, while spatter appeared on the underlying layers as well. The difference in blood location made separating stain types relatively easy. The difficulty presented itself when spatter drops were smaller than the width of the thread. Small spatter drops could remain on top of the thread, as they were too small to reach the lower layers, causing them to look like transfer stains. Holbrook concluded the analysis of multiple drop sizes within a stain pattern was necessary to accurately identify the cause of a stain since the size of the drops affects how it interacts with the fabric (2010). Holbrook offered some good advice, but her conclusions left the analysis of stains on fabric unreliable at best. The implication of spatter and transfer stains are very different and can completely change the story of events, so it is important to limit guesswork.

Fiber Characteristics

Since there was no reliable way to analyze blood on fabric, Li, Li, and Michielsen, textile engineering students at NCSU, researched the impact of yarn structure on stains. They spun their own yarn and created a simple textile sample to examine how the yarn structure affected the distortion of stains. They discovered the yarn characteristics were more important than the fabric characteristics when it came to stain distortion. The blood wicked along the threads of the fabric, not along the weave pattern (2017). Li, Li, and Michielsen conducted their study specifically with cotton so the results cannot be assumed to apply to all material types, but they changed the way analysts examine fabric. It was no longer valid to compare stains based on material; it was now narrowed to yarn construction. In practice, a cotton sample cannot be compared to a random cotton sample; the yarn structures have to match. Matching fibers is not conducive in the field, so samples would need to be brought back to the lab for analysis before conclusive bloodstain analysis could be done.

Bringing Fabric to Life

Research on fabric had mainly been conducted with the fabric pulled taught or lying flat, and while that produces valuable information, it is not always representative of real life. When looking at fabric it is important to consider its original positioning before analyzing. Reynolds and Silenieks encouraged consideration of three-dimensional positioning when analyzing clothing. **Figure 6** shows how clothing can mislead analysists if examined flat (2016).

Figure 6 Bloodstains on curved fabric at time of incident

Reynolds & Silenieks (2016)

Both stains were the result of a 90° drop. When the fabric is curved in its original position, shown on the left, the stains appear to result from the same blood event. Without proper positioning, the stains appear to be from different blood events, as shown on the right. Interpreting the story correctly, to the best ability, is crucial in bloodstain pattern analysis.

Applying Old Math to New Targets

Duffle, a forensic graduate student at UCO, focused on whether MacDonell's angle-of-impact equation could be accurately applied to cotton. She tested 100% cotton as well as a denim blend of 98% cotton and 2% spandex against a poster board control. All three materials were tested at the same known angles with blood dropped from a consistent height. The experimental impact angles for the fabric samples proved accurate when compared to the control board. No significant difference was discovered between the experimental angles of the control and those of the fabric samples. Duffle concluded the angle of impact equation for smooth, non-porous surfaces accurately applied to her cotton samples (2020). Duffle's study has yet to be replicated as it was just recently published, but it has great potential to widen the scope of court-approved bloodstains to include those found on cotton.

Summary

A review of the literature has shown great improvement in the knowledge of bloodstains and the analysis of bloodstains. A great deal of the past research was qualitative in nature, which provided subjective results. Further research focusing on quantitative properties, such as angle of impact, is still necessary. Quantitative research on fabric has remained a fairly untouched category aside from Duffle's 2020 study. Considering how much of a crime scene is fabric-based (clothing, bedding, pillows, furniture), having a better grasp of the role fabric plays in bloodstain analysis will provide a better picture of the events that transpired. Clothing, whether that of the victim or perpetrator, is a common source of blood evidence. The ability to place people within the scene is crucial for reconstruction; therefore it is crucial to study fabric commonly used in clothing. The rise of athletic/athleisure wear has caused polyester and polyester blends to increase in popularity. Collecting data from polyester-based fabric will determine whether the standard angle of impact equation can be applied accurately, potentially broadening the available stains for use in reconstruction and court settings.

Chapter 3: Methods

Overview

Analysts have been unable to use stains found on fabric surfaces due to limited research on the effect fabric has on bloodstains. Given the frequency that blood is found on fabric, it would be beneficial to know what information can be ascertained from such stains. The angle of impact is highly sought-after information and greatly aids in the reconstruction of a crime scene. It must be determined whether the only existing equation for angle of impact, which was developed on a smooth, non-porous surface, can accurately be applied to various fabric types. For bloodstain analysis purposes, acceptable angles of impact are ±5°.

This quantitative study focused on the ability to accurately calculate various angles of impact for blood drops found on two common moisture-wicking fabrics. For comparison purposes, poster board was used as a control. A micropipette was used to drop blood onto each of the four target materials set up at a variety of known angles. Once dry, all of the bloodstains were measured, and the impact angles were calculated. The calculated angles and the actual angles for each material were compared and analyzed for statistical significance. A difference of ±5° was considered acceptable.

Setting

The experiment was conducted at the University of Central Oklahoma (UCO) in the Forensic Science Institute's Evidence Bay. The Evidence Bay is a climate-controlled laboratory intended for forensic experimentation.

Intervention and Materials

Poster board acted as a control since the existing equation for angle of impact was developed on a smooth, nonporous surface. Polyester is commonly used for its moisture-wicking properties, so three polyester-based fabrics were tested. One sample was 100% polyester, and the other two were polycotton blends. See **Figure 7**. Laundering has been shown to affect the blood-fabric interaction (Slemko, 2003) so all fabric samples were washed and air-dried prior to testing.

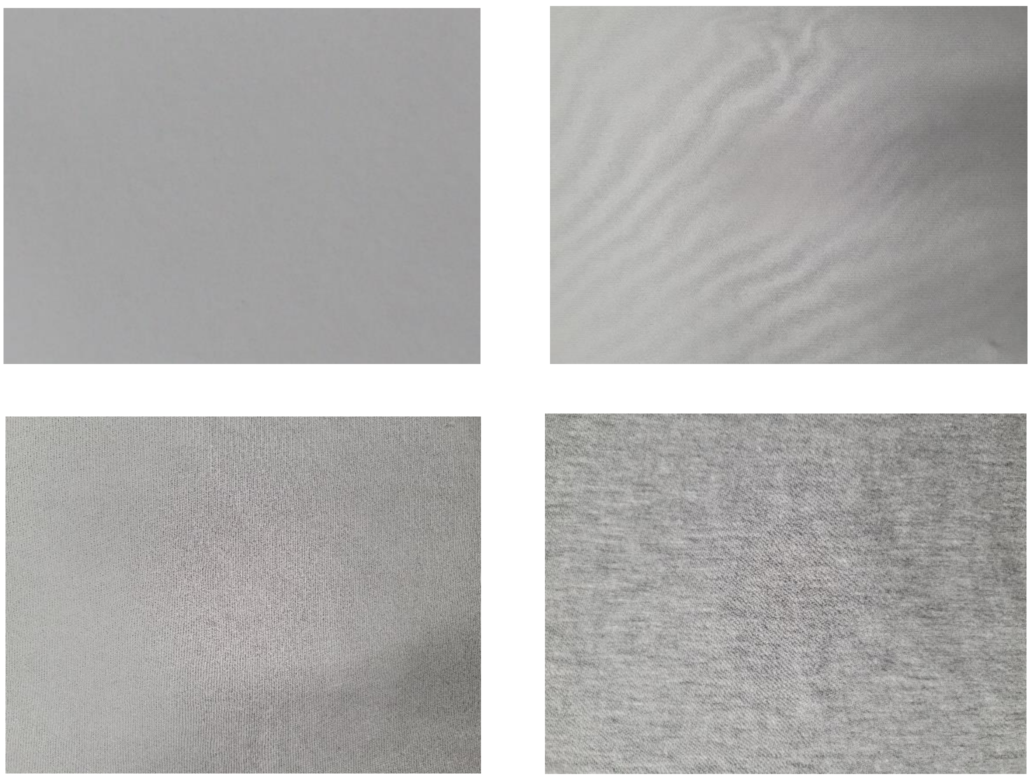

Figure 7 Materials.
Poster board, 100% Polyester,
80% Polycotton blend, 20% Polycotton blend

To maintain the integrity of the experiment and because bagged blood contains anticoagulants, the blood used was provided by a local butcher. The bovine blood was kept warm to mimic the human body and stirred continuously to prevent clotting. A micropipette was used to drop the blood as it allowed gravity to pull the drop rather than forcefully expel it.

A clipboard stand was used to hold clipboards at known angles. The stand is a two-inch by four-inch beam with slots cut at 10° increments from 10° to 80°. Clipboards were inserted into each of the slots, and the 90° clipboard was placed on the floor. The target materials were clipped to the clipboards while the blood was dropped. See **Figures 8 & 9**.

Figure 8 Empty clipboard stand

Figure 9 Clipboard stand with clipboards

Measurement Instruments

The clipboard stand was made with unknown accuracy, so an angle finder was used to measure the actual angle of each clipboard within ±0.5° accuracy. **Table 1** shows the theoretical angles with their actual angles. All calculations were made using the actual angle, although the theoretical angle will be used when discussing the experiment for the sake of ease.

Table 1: Theoretical v Actual Angle for Clipboard Stand

Theoretical Angle	Actual Angle
10	11
20	21
30	31
40	41
50	46
60	59
70	69
80	82
90	90

A wooden dowel with a test-tube clamp was used to maintain a consistent dropping distance. A drafting divider with no significant error other than user error was used to determine where on each stain to measure length and width, and digital calipers with ±0.005mm accuracy were used to measure the length and width of the stains. See **Figure 10**.

Figure 10 Tools. Digital calipers (top), drafting divider (bottom)

Duffle (2020)

Data Collection

The clipboards were used to hold the samples at known angles. The control was tested first to validate the experimental process. Samples of the control board were secured to the angled clipboards as blood was dropped at 90˚ to the ground from a known height. After depositing 14 drops on each sample, the samples were removed from the clipboards and set aside to dry. The clipboards were wiped down with paper towels to remove any residual blood before setting up the next round of samples. The same process was used with each of the fabric types.

Once dry, each stain was labeled with a letter A-P. Stains were crossed out and voided if overlapped, too close to the edge of the surface, dropped from the wrong height or otherwise interfered with. Photos of the bloodstains are shown in **Appendix E-H**. Drafting dividers and digital calipers were used to measure each stain. The right triangle analogy (**Fig 11**) was used to determine where on the stains to measure since real bloodstains are not perfect ovals (**Fig 12**). The method of using a perfect oval on an imperfect stain when calculating the angle of impact eliminates distortion but introduces systematic error. The systematic error is countered by allowing a range of acceptable angles (±5°).

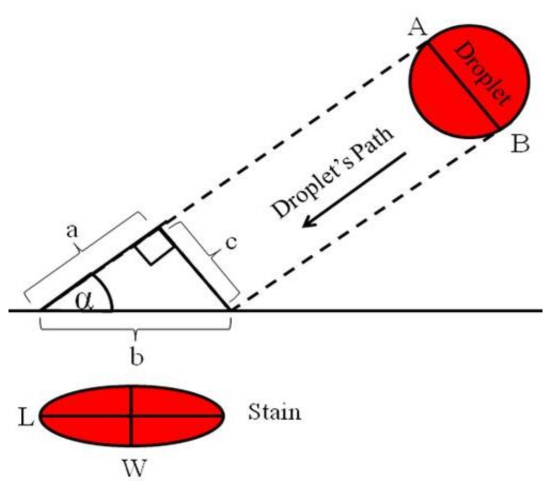

Figure 12 Right Triangle Analogy

Karnjanadecha (2010)

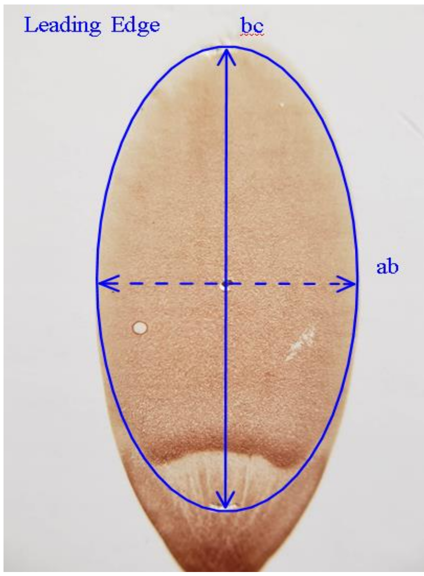

Figure 11 Bloodstain with oval overlay

Duffle (2020)

The drafting dividers and digital calipers were used in an effort to limit systematic error. The digital caliper was used to determine the widest part of the stain and displayed the measurement of the width. One end of the drafting divider was then placed at the halfway point of the width and extended to the top of the stain (leading edge). A measurement was taken of the drafting divider and then doubled to equal the length of the stain. See **Figure 13**.

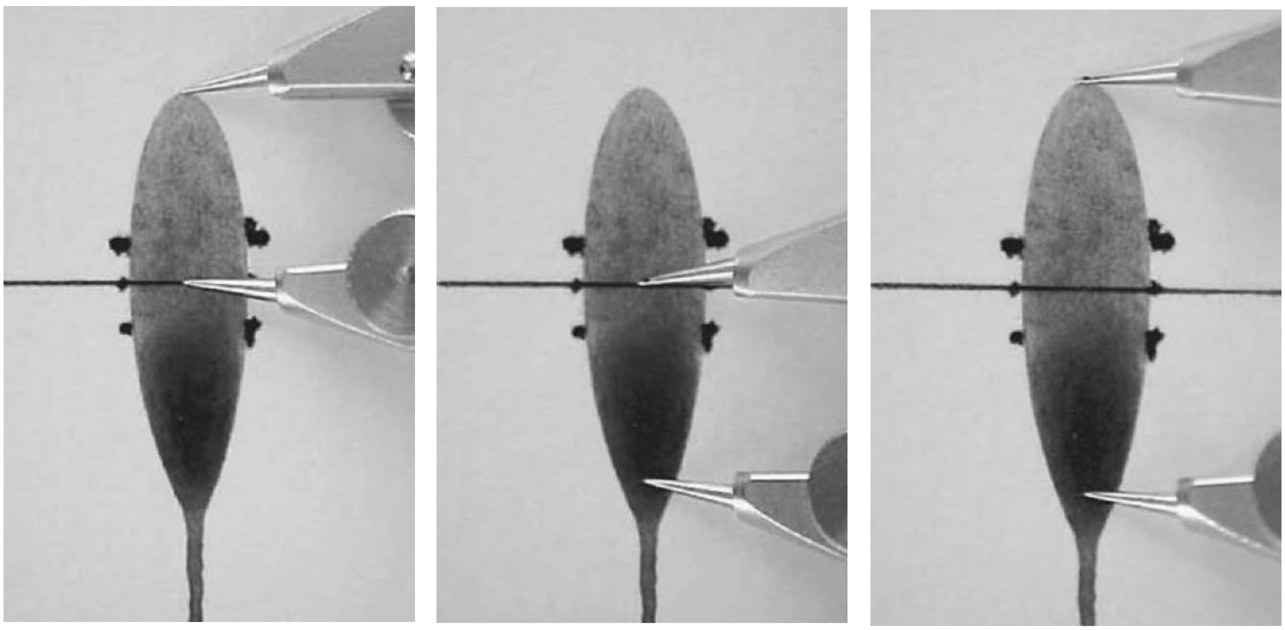

Figure 13 How to use drafting dividers to measure bloodstains

Bevel & Gardner (2001)

Data Analysis

To determine the statistical significance of the target material, the calculated experimental angles were compared to the actual angles. The absolute values of the difference between each of the calculated angles and their respective actual angles were used in an analysis of variance (ANOVA). The ANOVA compared the mean of the absolute value for each material and actual angle to determine whether differences existed. When necessary, a Tukey test was conducted to identify if the difference was significant.

Chapter 4: Results

Introduction

The main goal of this thesis was to determine whether the equation used for angle of impact on smooth, non-porous surfaces would work on porous, moisture-wicking polyester. A control was used to validate the experiment, and three polyester fabrics were used to test the equation using the methods laid out in **Chapter 3**.

The results show that for each polyester fabric, the calculated angle of impact only met the accuracy threshold of ±5° at the more elliptical range of angles.

Statistical Analysis of Data

A statistical analysis, using SAS 9.4, was conducted using the absolute value of the difference between the calculated angle and the actual measured angle to determine whether there was a significant interaction between the surface type and the actual angle of impact. For each of the four surface types (one control and three polyester fabrics), 14-15 blood drops were deposited at each theoretical angle (10°- 90°) for a total of 510 data points. Calculations for the absolute value between the calculated and actual angle, the standard deviation, and the minimum and maximum differences for each data set can be seen in **Table 2**. The measurements and raw data can be found in **Appendixes A-D**.

The Mean Difference column in **Table 2** is the mean absolute difference between the calculated and actual angles of all the drops on a surface sample. This speaks to the accuracy of the angle of impact equation at a given angle on a particular surface type. The highlighted boxes represent the highest tested angle for each surface type at which the angle of impact equation provided an acceptable result of ±5° (seen as a value of 0 to 5). The maximum accurate angle for each surface type is listed below in **Table 3**.

Table 2: Statistical Summary

Theoretical Angle (Actual)	Surface	Mean Difference	Standard Deviation	Min Difference	Max Difference
10	C	0.66	0.38	0.14	1.29
(11)	F1	1.61	1.52	0.03	4.54
	F2	1.86	1	0.10	3.09
	F3	1.38	1.13	0.04	3.67
20	C	3.14	1.78	0.67	7.24
(21)	F1	1.94	1.09	0.23	3.99
	F2	2.31	1.42	0.22	4.91
	F3	2.29	1.7	0.23	5.25
30	C	2.07	1.27	0.08	4.58
(31)	F1	2.59	1.19	0.43	4.35
	F2	2.16	1.05	0.47	3.93
	F3	3.91	2.02	0.63	8.48
40	C	2.53	1.76	0.24	6.07
(41)	F1	4.41	7.12	0.10	27.65
	F2	2.34	1.33	0.01	4.38
	F3	4.45	3.18	1.38	13.99
50	C	2.16	1.3	0.08	5.11
(46)	F1	7.79	9.73	0.50	36.50
	F2	3.66	2.29	0.05	7.55
	F3	4.21	3.34	0.13	11.92
60	C	1.92	1.54	0.23	5.16
(59)	F1	17.50	4.06	10.41	22.13
	F2	3.58	2.79	0	8.08
	F3	6.79	5.38	0.55	19.96
70	C	1.68	1.94	0.12	7.51
(69)	F1	18.59	5.9	10.00	30.45
	F2	8.08	4.54	1.62	14.59
	F3	5.73	5.61	0.45	21.00
80	C	4.31	2.29	1.02	9.21
(82)	F1	16.45	6.47	8.00	30.50
	F2	11.24	4.9	4.60	18.14
	F3	18.57	8.37	5.80	31.94
90	C	5.74	6.34	0	16.54
(90)	F1	32.04	6.53	18.57	41.96
	F2	12.69	6.64	0	22.62
	F3	29.31	8.73	10.18	46.14

Table 3: Maximum Angles for Accuracy

	Max Accurate Angle (Mean Difference < 5)
Control	80 (82)
Fabric 1	40 (41)
Fabric 2	60 (59)
Fabric 3	50 (46)

The mean of the absolute differences for each surface are shown in **Figure 14** with error bars representing the standard deviation. Any mean absolute difference point above 5 indicates the angle of impact calculation is inaccurate. The individual absolute differences used to calculate the mean absolute difference are plotted out on **Figures 15-18** for each surface type.

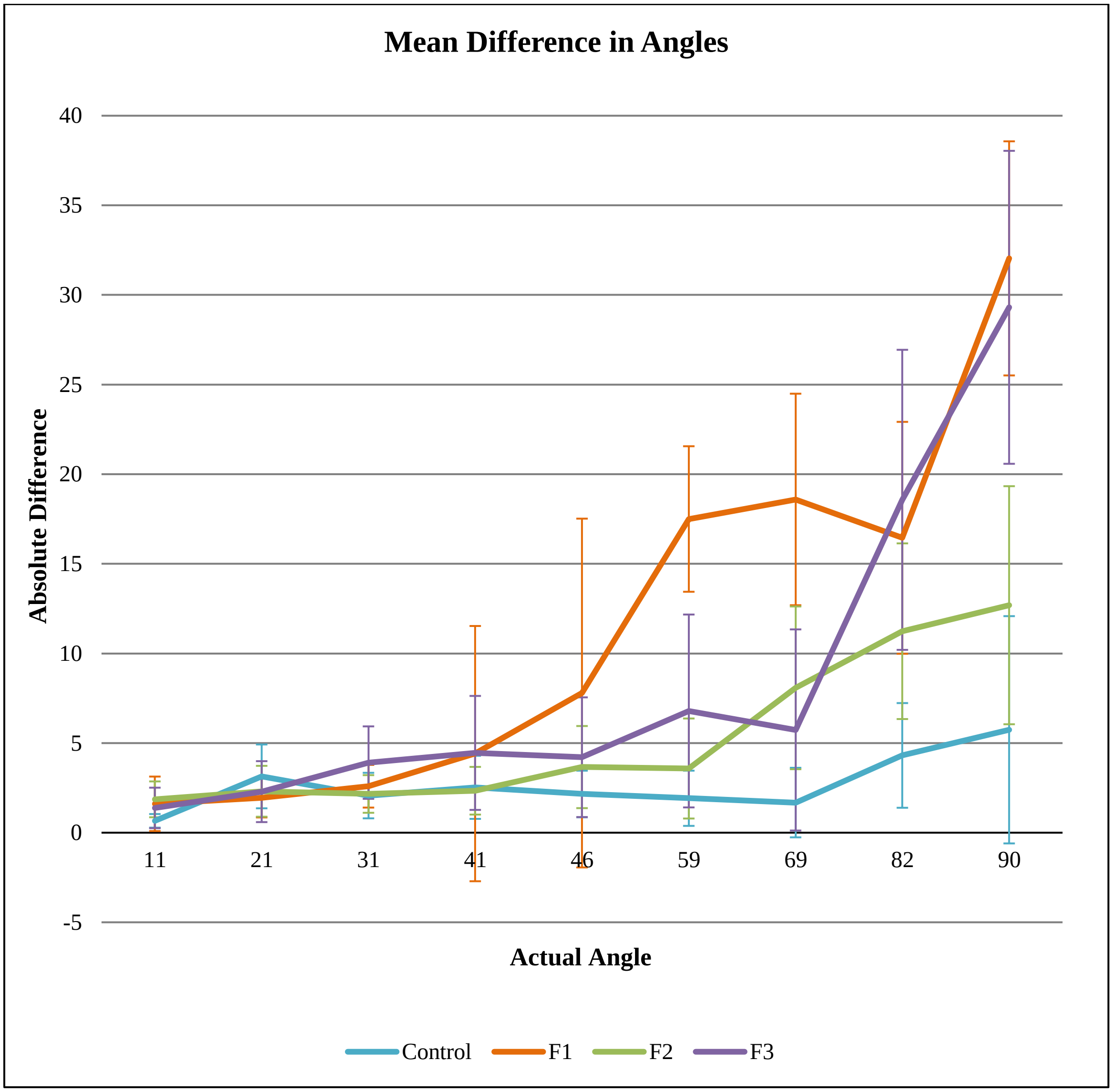

Figure 14 Comparison of Mean Difference for each surface type with Standard Deviation

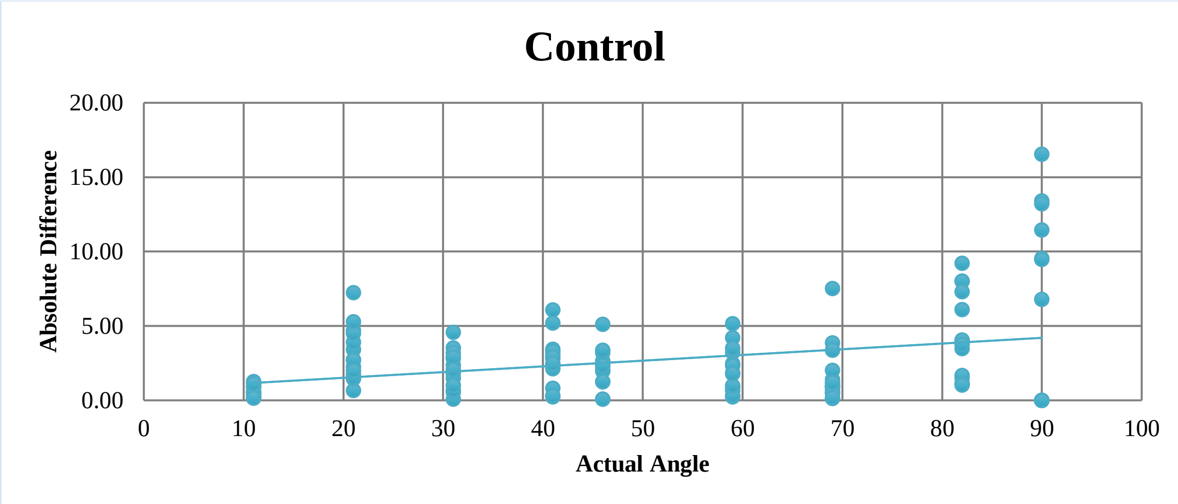

Figure 15 Absolute Difference of the Calculated and Actual angles v. Actual Angle, Control

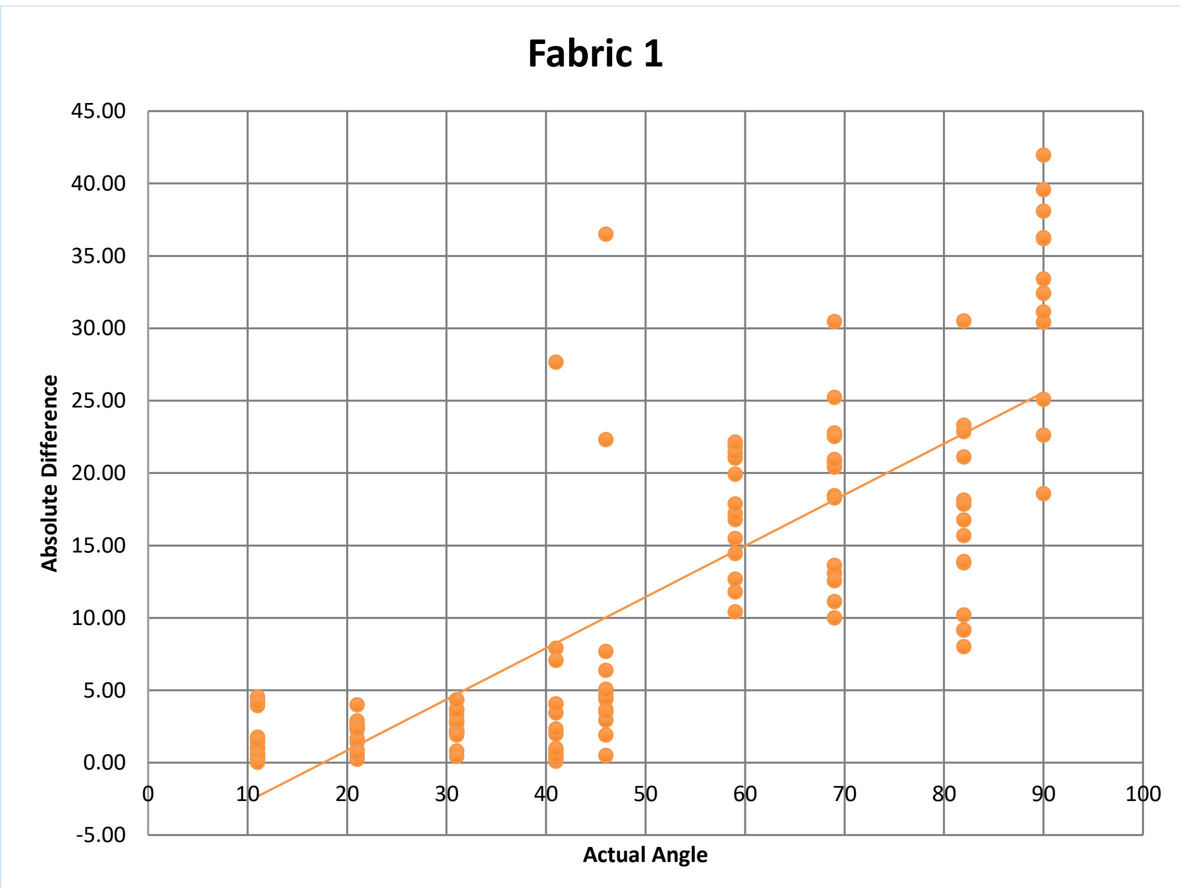

Figure 16 Absolute Difference of the Calculated and Actual angles v. Actual Angle, F1

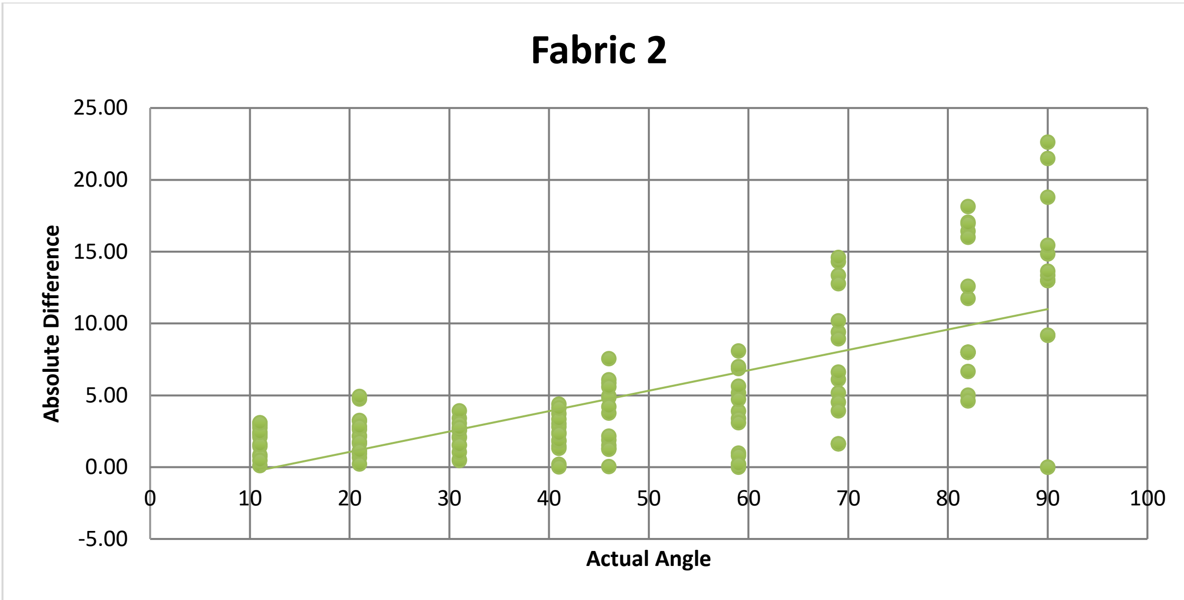

Figure 17 Absolute Difference of the Calculated and Actual angles v. Actual Angle, F2

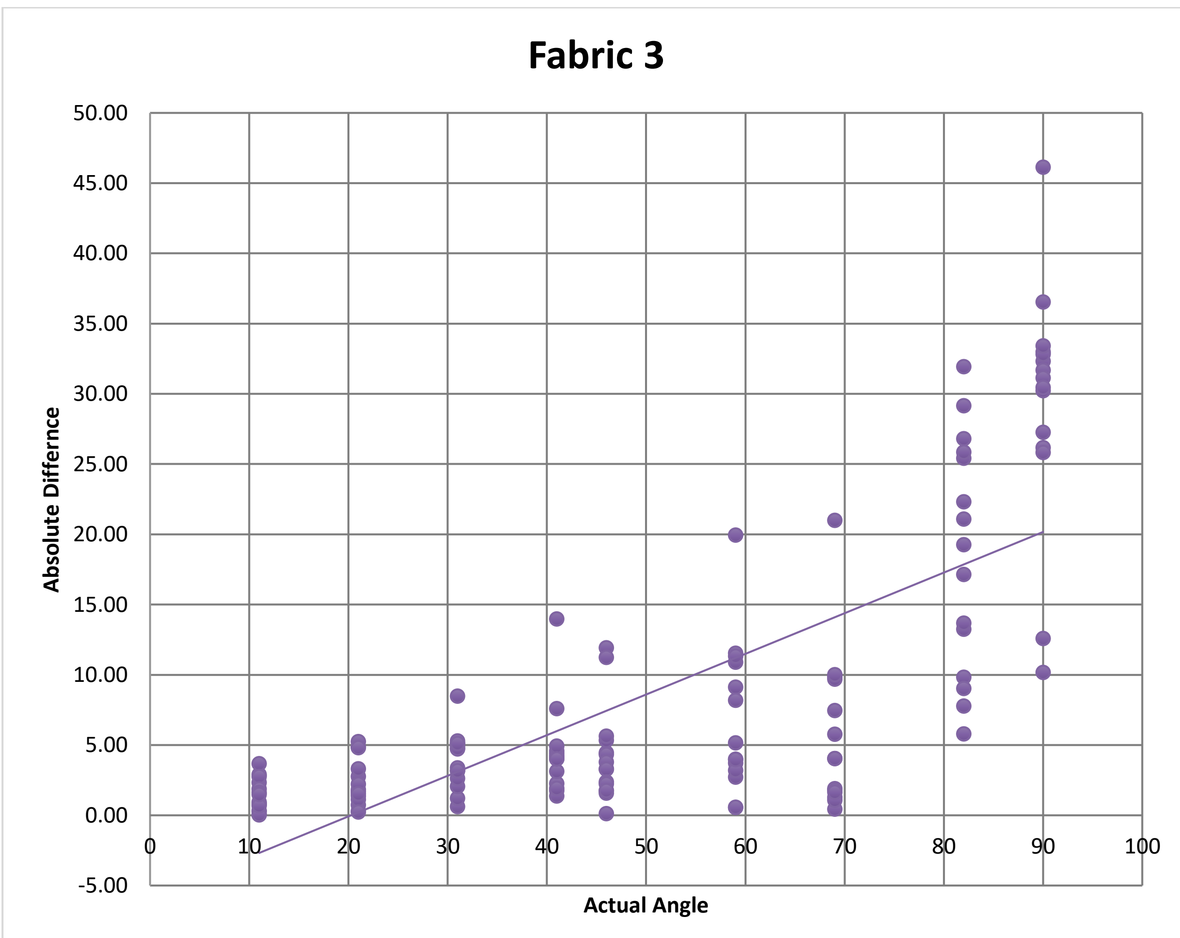

Figure 18 Absolute Difference of the Calculated and Actual angles v. Actual Angle, F3

A 2-Factor ANOVA found a significant interaction ($p<0.05$) between surface type and actual angle. 1-Factor ANOVA was used to analyze surface type and actual angle separately.

Statistical Significance Between Surface Types

Analysis between the surface types was done to compare the mean absolute differences of the four surfaces at each angle. Significant differences were found between the surface types at many of the angles (**Table 4)**. Although they are statistically significant, they are not all practically significant since there is ±5° of acceptable differences between the calculated and actual angles. The differences that are both statistically and practically significant are at angles for which the angle of impact equation was not accurate on one or more of the surfaces.

Statistical Significance Between Actual Angles

Analysis between the actual angles was used to compare the mean absolute differences of the nine angles on each surface. Significant differences were found between the angles on all of the surfaces (**Table 5)**. Although they are statistically significant, they are not all practically significant since there is ±5° of acceptable differences between the calculated and actual angles. The differences that are both statistically and practically significant are on surfaces on which the angle of impact equation was not accurate for one or more of the angles.

Table 4: Differences between Types for each Actual Angle

Actual Angle	Statistical Significance	Practical Significance
11	C with F2	No practical significance
21	No significant difference	No practical significance
31	F3 with all other	No practical significance
41	No significant difference	No practical significance
46	C with F1	F1 not accurate
59	C with F3 F1 with all other	F1 not accurate F3 not accurate
69	C with F2 F1 with all other	F1 not accurate F2 not accurate
82	C with all other F2 with F3	F1 not accurate F2 not accurate F3 not accurate
90	C with F1 and F3 F2 with F1 and F3	F1 not accurate F2 not accurate F3 not accurate

Table 5: Differences between Actual Angle for each Type

Surface Type	Statistical Significance	Practical Significance
C	90 with all except 82 82 with 11	No practical significance
F1	90 with all other 82 with 46, 41, 31, 21, 11 69 with 46, 41, 31, 21, 11 59 with 46, 41, 31, 21, 11	No practical significance
F2	90 with all except 82 82 with 59, 46, 41, 31, 21, 11 69 with 59, 46, 41, 31, 21, 11	No practical significance
F3	90 with all other 82 with all other	No practical significance

Chapter 5: Discussion

Introduction

The goal of bloodstain pattern analysis is to determine what happened at a crime scene. Analysts examine the physical characteristics of the bloodstains and use their knowledge of how blood behaves both in the air and upon impact with a surface to make their conclusions. All interpretations must be backed by research with consistent and reproducible results. The application of the angle of impact equation is limited to bloodstains on surface types that have been scientifically tested which leaves many stains unusable for analysis.

To give analysts the greatest chance to interpret the scene effectively, it is vital to maximize the number of stains available for accurate analysis. Lack of research on the effect surface type has on angle of impact calculations is a limiting factor of the current equation. Continued research is needed on the current angle of impact equation to determine its accuracy on other surface types.

The purpose of this study was to expand the knowledge base and test the angle of impact equation on moisture-wicking polyester. The control surface had accurate calculated angles at all actual angles which validated this study's methods. The moisture-wicking process distorted the shape of the bloodstains and rendered the angle of impact calculations unreliable. Even with an acceptable error range of ±5°, the results of this thesis found the accuracy of the current angle of impact equation to be inconsistent and dependent on the percentage of polyester in the fabric composition as well as the actual angle of the target surface.

Discussion

The statistical analysis for this study compared the four surface types to each other to determine if the difference in the data are statistically significant. Since angle of impact calculations have a range of error that is deemed acceptable (±5°), this study used the absolute value of the difference between the calculated angle and the actual angle when doing the ANOVA tests. A 2-factor ANOVA found a significance relationship between the surface type and the actual angle so 1-factor ANOVA examined surface type and actual angle separately.

Statistical significance does not imply practical significance. The practical significance was determined using the mean difference value. Mean difference values less than 5 indicate the calculated angle was within the 5° of accepted error and the equation was accurate. Mean difference values greater than 5 indicate the calculated angle was outside the 5° of accepted error and the equation was inaccurate.

Discussion of Surface Type Analysis

Analysis between the surface types compared the mean absolute differences of the four surface types at each angle. There were statistically significant differences at all but two angles, 21° and 41°. Since this study is only concerned with whether the angle of impact equation produced an accurate result, comparison of **Tables 2 and 4** determines whether the statistically significant differences correlate to practical significance. For instance, angles 11° and 31° had statistically significant differences but all the mean differences were less than 5 which signifies the equation was accurate and any statistical significance is practically irrelevant. Alternatively, angles 46°-90° had mean difference values that were greater than 5 which signifies the equation was inaccurate. Any statistical significance within the 46°-90° range is practically significant which indicates the equation cannot be used on the surface types mentioned for that angle.

Discussion of Actual Angle Analysis

Analysis between the actual angles compared the mean absolute differences of the nine angles on each surface. This study focused on whether the equation is accurate, the specific value for the mean difference isn't important, only whether it is above or below a value of 5. When looking at **Tables 2 and 5**, there is no correlation between angles that are statistically significant and angles that have a mean difference value above 5. The analysis of the actual angles gives no indication of the practical application for this equation.

Limitations

Polyester is moisture-wicking and hydrophobic which caused the blood to momentarily bead on the surface before absorbing into the fabric. The distorting effect of this beading can be seen in the photos of Fabric 1 and Fabric 2 (**Appendixes F and G**) as satellite spatter and segmented stains. The distortion of these stains made measuring them difficult and resulted in inaccurate angle of impact calculations at some angles.

This study found no correlation between the percentage of polyester in the surface sample and the range of angles for which the equation was accurate. This could be due to the small sample size. A larger sample size could better examine the relationship between polyester content and the ability to accurately calculate angle of impact. Further research is necessary to determine the impact fabric blends have on the analysis of bloodstains.

The human involvement in this study adds an element of human error. It is the job of the examiner to measure the length and width of the stains. Errors when measuring are amplified in the calculated angle of impact. The ±5° of acceptable error associated with the angle of impact equation is used to minimize the effect of human error.

Conclusion

This thesis was successful in that the control surface resulted in accurate angle of impact calculations at every angle which means the experimental design was valid and can be used for future research to test different surface types. The results on three polyester samples were not what was initially expected. Although the angle of impact equation was developed on smooth, non-porous surfaces, it was generally expected to provide accurate results across all surface types. The results of this thesis show that bloodstains found on 100% polyester, 80% polycotton, and 20% polycotton could not be universally analyzed using the current equation for angle of impact. Each fabric sample had a different range of angles that produced accurate results.

The moisture-wicking property of polyester disproportionately distorted the stains which altered the length/width ratio and resulted in angle of impact calculations outside of the acceptable ±5° range. This is significant to the field of forensic science because it suggests the current angle of impact equation cannot be universally applied to bloodstains. The surface type has to be considered before further analysis of a bloodstain can be conducted.

The research question at the beginning of this study asked if the equation used to find the angle of impact on smooth, non-porous surfaces provided accurate results on moisture-wicking polyester fabrics. The answer to that question is it depends. The equation provided accurate results on all three polyester samples for angles 11°-41°. For angles outside of that range, the equation yielded an unacceptable amount of error and should not be used. Although this study's results may limit the number of usable stains at a crime scene, it may increase the accuracy of the analyst's conclusions.

Future Research

In the future, the angle of impact equation will need to be tested on other fabric types, as well as other textured surfaces, to determine the accuracy of the calculations. Being able to calculate the angle of impact is helpful for crime scene reconstruction so knowing which surfaces are acceptable, or more importantly the surfaces that are unacceptable, for those calculations is vital. For surfaces on which the current equation is inaccurate, research should be done to determine if there is a different equation that can produce accurate angle of impact calculations.

Analysts need to be cautious when analyzing bloodstains on fabric, and other textured surfaces, and consider how the surface type may affect their interpretation of those stains. By continuing research and adding to the knowledge in the field, sources of known error can be eliminated to increase the confidence of bloodstain analyst's findings.

References

ACSR. (2021). Crime Scene Reconstruction. Retrieved April 9, 2021, from https://www.acsr.org

Balthazard, V., Piédeliévre, R., Desoille, H., & Dérobert, L. (1939). Étude des Gouttes de Sang Projeté [Research on Blood Spatter] (K. Schmidt, Trans.). Presented at *XXII Congrés de Médecine Légale.* Paris.

Bevel, T. & Gardner, R. M. (1990). Bloodstain Pattern Analysis: Theory and Practice—A Laboratory Manual. *TBI Inc., Oklahoma City, OK*, 38.

Bevel, T., & Gardner, R. M. (2001). Bloodstain Pattern Analysis: With an Introduction to Crime Scene Reconstruction. (2nd ed.). *CRC Press.*

Duffle, L. (2020). The Wicking of Blood in Fabrics and the Effect It Has on the Angle of Impact. [unpublished master's thesis]. University of Central Oklahoma.

Encyclopedia Britannica (2009). Newton's laws of motion. In Britannica. Retrieved April 9, 2021, from https://www.britannica.com/science/Newtons-laws-of-motion

Forensic Science Standards Board (FSSB). (2015). Interaction of Blood and Fabrics. *OSAC Research Needs Assessment Form*. OSAC for Forensic Science

Gravel, C. & White, M. (2019). Bloodstain Pattern Analysis: Level 1 Lab Manual. *Cognella, Inc.*

Holbrook, M. (2010). Evaluation of Blood Deposition on Fabric: Distinguishing Spatter and Transfer Stains. *International Association of Bloodstain Pattern Analysts News*, 26(1) 3-12. Retrieved from https://www.iabpa.org/docs/March_2010_News.pdf

Kittipat, Boonkhong & Karnjanadecha, Montri & Aiyarak, Pattara. (2010). Impact Angle Analysis of Bloodstains Using A Simple Image Processing Technique. Songklanakarin Journal of Science and Technology. 32.

Kirk, P. L. (1955). Affidavit of Paul Leland Kirk. *1954-1955 Post-Trial Motions and Ohio Eighth District Court of Appeal***.** 10. Retrieved from https://engagedscholarship.csuohio.edu/sheppard_eight_district_1950s/10

Knapp, K. (2018). What does moisture-wicking mean? Retrieved March 26, 2021, from https://www.rei.com/blog/hike/what-does-moisture-wicking-mean

Li, X., Li, J., & Michielsen, S. (2017). Effect of yarn structure on wicking and its impact on bloodstain pattern analysis (BPA) on woven cotton fabrics. *Elsevier*. doi:10.1016/j.forsciint.2017.04.011

MacDonell, H. L. & Bialousz, L.F. (1971). Flight Characteristics and Stain Patterns of Human Blood. Law Enforcement Assistance Administration, U.S. DOJ, Washington.

MacDonell, H. L. (2011). Credit Where It's Due. *Journal of Forensic Identification, 61(3)*, 210-221. Retrieved from http://proquest.com/docview/867849853?accountid=14516

OSAC for Forensic Science. (2017). Terms and Definitions in Bloodstain Pattern Analysis. ASB Technical Report 033.

Reynolds, M. & Silenieks, E. (2016). Consideration for the Assessment of Bloodstains on Fabrics. *Journal of Bloodstain Pattern Analysis, 32(2)*, 15-20. Retrieved from https://iabpa.org/uploads/files/iabpa%20publications/December%202016%20JBPA.pdf

Slemko, J. (2003). Bloodstains on Fabrics: The Effects of Droplet Velocity and Fabric Composition. *IABPA* News. 3-11.

TextileGlossary.com. (n.d.). What is "Absorbancy". Retrieved April 9, 2021, from https://www.textileglossary.com/terms/absorbency.html

Appendix A: Raw Data—Control

Type	Sample ID	Width (mm)	Length (mm)	Calc Angle (rad)	Calc Angle (deg)	Actual Angle (deg)	Absolute Difference (deg)
C	C90a	15.2	15.2	1.57	90.0	90	0.00
C	C90b	14.3	14.3	1.57	90.0	90	0.00
C	C90c	15.1	15.1	1.57	90.0	90	0.00
C	C90d	14.3	14.5	1.40	80.5	90	9.53
C	C90e	14.5	14.7	1.41	80.5	90	9.46
C	C90f	13.2	13.2	1.57	90.0	90	0.00
C	C90g	15.2	15.2	1.57	90.0	90	0.00
C	C90h	14.2	14.3	1.45	83.2	90	6.78
C	C90i	14.0	14.0	1.57	90.0	90	0.00
C	C90j	13.9	14.5	1.28	73.5	90	16.54
C	C90k	14.3	14.7	1.34	76.6	90	13.40
C	C90l	14.8	15.1	1.37	78.6	90	11.44
C	C90m	14.7	15.1	1.34	76.8	90	13.22
C	C90n	14.1	14.1	1.57	90.0	90	0.00
C	C80a	14.0	14.0	1.57	90.0	82	8.00
C	C80b	13.9	14.0	1.45	83.1	82	1.15
C	C80c	13.6	13.6	1.57	90.0	82	8.00
C	C80d	12.8	13.4	1.27	72.8	82	9.21
C	C80e	13.4	13.7	1.36	78.0	82	4.01
C	C80f	13.3	13.6	1.36	77.9	82	4.06
C	C80g	14.3	14.5	1.40	80.5	82	1.53
C	C80h	13.6	14.1	1.30	74.7	82	7.30
C	C80i	13.9	14.1	1.40	80.3	82	1.66
C	C80j	14.7	15.0	1.37	78.5	82	3.48
C	C80k	14.0	14.3	1.37	78.2	82	3.76
C	C80l	13.7	13.8	1.45	83.1	82	1.10
C	C80m	12.9	13.3	1.32	75.9	82	6.09
C	C80n	13.4	13.5	1.45	83.0	82	1.02
C	C70a	13.9	14.8	1.22	69.9	69	0.92
C	C70b	14.1	15.0	1.22	70.1	69	1.05
C	C70c	13.9	14.8	1.22	69.9	69	0.92
C	C70d	14.1	14.5	1.34	76.5	69	7.51
C	C70e	13.9	14.8	1.22	69.9	69	0.92
C	C70f	13.6	14.5	1.22	69.7	69	0.71
C	C70g	13.5	14.6	1.18	67.6	69	1.38
C	C70h	14.7	15.8	1.20	68.5	69	0.51
C	C70i	12.9	13.5	1.27	72.9	69	3.85
C	C70j	12.8	13.7	1.21	69.1	69	0.12
C	C70k	13.3	14.2	1.21	69.5	69	0.49
C	C70l	15.2	16.3	1.20	68.8	69	0.17
C	C70m	14.2	14.9	1.26	72.4	69	3.37
C	C70n	13.9	14.7	1.24	71.0	69	2.01
C	C70p	12.5	13.5	1.18	67.8	69	1.19

Type	Sample ID	Width (mm)	Length (mm)	Calc Angle (rad)	Calc Angle (deg)	Actual Angle (deg)	Absolute Difference (deg)
C	C60a	12.6	14.0	1.12	64.2	59	5.16
C	C60b	12.9	15.6	0.97	55.8	59	3.22
C	C60c	13.4	16.4	0.96	54.8	59	4.21
C	C60d	14.5	16.8	1.04	59.7	59	0.67
C	C60e	11.8	13.8	1.03	58.8	59	0.23
C	C60f	14.1	16.3	1.05	59.9	59	0.89
C	C60g	13.5	15.7	1.04	59.3	59	0.30
C	C60h	13.5	15.9	1.01	58.1	59	0.89
C	C60i	14.1	16.5	1.02	58.7	59	0.29
C	C60j	13.6	16.5	0.97	55.5	59	3.49
C	C60k	15.6	18.7	0.99	56.5	59	2.46
C	C60l	12.4	14.2	1.06	60.8	59	1.84
C	C60m	13.7	16.4	0.99	56.7	59	2.35
C	C60n	15.5	17.9	1.05	60.0	59	0.99
C	C60p	13.2	15.7	1.00	57.2	59	1.78
C	C50a	13.4	19.3	0.77	44.0	46	2.03
C	C50b	12.5	17.4	0.80	45.9	46	0.08
C	C50c	12.3	17.9	0.76	43.4	46	2.60
C	C50d	12.7	18.5	0.76	43.4	46	2.65
C	C50e	11.9	16.9	0.78	44.8	46	1.24
C	C50f	13.9	20.0	0.77	44.0	46	1.97
C	C50g	12.3	17.7	0.77	44.0	46	1.98
C	C50h	13.0	18.1	0.80	45.9	46	0.09
C	C50i	12.6	17.9	0.78	44.7	46	1.26
C	C50j	12.5	18.1	0.76	43.7	46	2.32
C	C50k	12.3	18.1	0.75	42.8	46	3.19
C	C50l	12.7	19.4	0.71	40.9	46	5.11
C	C50m	12.8	18.9	0.74	42.6	46	3.37
C	C50n	11.6	16.8	0.76	43.7	46	2.33
C	C40a	12.7	17.6	0.81	46.2	41	5.19
C	C40b	12.3	16.8	0.82	47.1	41	6.07
C	C40c	11.9	17.0	0.78	44.4	41	3.43
C	C40d	11.5	18.6	0.67	38.2	41	2.81
C	C40e	11.5	18.7	0.66	37.9	41	3.05
C	C40f	11.8	18.8	0.68	38.9	41	2.12
C	C40g	11.8	17.9	0.72	41.2	41	0.24
C	C40h	11.5	18.8	0.66	37.7	41	3.29
C	C40i	11.6	18.8	0.66	38.1	41	2.90
C	C40j	12.8	20.5	0.67	38.6	41	2.36
C	C40k	12.4	19.9	0.67	38.5	41	2.46
C	C40l	11.2	16.8	0.73	41.8	41	0.81
C	C40m	13.5	20.7	0.71	40.7	41	0.29
C	C40n	13.0	19.7	0.72	41.3	41	0.29

Type	Sample ID	Width (mm)	Length (mm)	Calc Angle (rad)	Calc Angle (deg)	Actual Angle (deg)	Absolute Difference (deg)
C	C30a	10.2	22.1	0.48	27.5	31	3.51
C	C30b	11.7	21.6	0.57	32.8	31	1.80
C	C30c	11.1	21.6	0.54	30.9	31	0.08
C	C30d	12.4	23.7	0.55	31.5	31	0.55
C	C30e	10.1	22.7	0.46	26.4	31	4.58
C	C30f	10.5	21.6	0.51	29.1	31	1.91
C	C30g	10.6	21.0	0.53	30.3	31	0.68
C	C30h	10.4	22.3	0.49	27.8	31	3.20
C	C30i	10.5	21.9	0.50	28.6	31	2.35
C	C30j	11.5	21.4	0.57	32.5	31	1.51
C	C30k	9.4	19.9	0.49	28.2	31	2.81
C	C30l	10.6	22.5	0.49	28.1	31	2.89
C	C30m	10.5	21.7	0.51	28.9	31	2.06
C	C30n	11.1	22.2	0.52	30.0	31	1.00
C	C20a	9.0	25.9	0.35	20.3	21	0.67
C	C20b	9.5	28.8	0.34	19.3	21	1.74
C	C20c	9.3	22.5	0.43	24.4	21	3.41
C	C20d	10.6	22.4	0.49	28.2	21	7.24
C	C20e	9.4	24.6	0.39	22.5	21	1.46
C	C20f	9.1	27.3	0.34	19.5	21	1.53
C	C20g	8.4	26.8	0.32	18.3	21	2.73
C	C20h	7.7	26.2	0.30	17.1	21	3.91
C	C20i	8.0	28.5	0.28	16.3	21	4.70
C	C20j	9.1	28.3	0.33	18.8	21	2.24
C	C20k	7.3	25.7	0.29	16.5	21	4.50
C	C20l	7.8	28.8	0.27	15.7	21	5.29
C	C20m	8.6	27.4	0.32	18.3	21	2.71
C	C20n	8.7	26.7	0.33	19.0	21	1.98
C	C10a	5.6	32.6	0.17	9.9	11	1.11
C	C10b	5.8	31.7	0.18	10.5	11	0.46
C	C10c	6.7	34.2	0.20	11.3	11	0.30
C	C10d	6.3	35.9	0.18	10.1	11	0.89
C	C10e	5.6	33.1	0.17	9.7	11	1.26
C	C10f	6.2	33.0	0.19	10.8	11	0.17
C	C10g	5.8	33.1	0.18	10.1	11	0.91
C	C10h	6.1	32.8	0.19	10.7	11	0.28
C	C10i	6.4	32.0	0.20	11.5	11	0.54
C	C10j	5.8	31.9	0.18	10.5	11	0.52
C	C10k	6.1	34.8	0.18	10.1	11	0.90
C	C10l	6.7	33.3	0.20	11.6	11	0.61
C	C10m	6.2	32.9	0.19	10.9	11	0.14
C	C10n	5.7	33.2	0.17	9.9	11	1.11

Appendix B: Raw Data—Fabric 1

Type	Sample ID	Width (mm)	Length (mm)	Calc Angle (rad)	Calc Angle (deg)	Actual Angle (deg)	Absolute Difference (deg)
F1	1F90a	8.5	10.8	0.91	51.9	90	38.1
F1	1F90b	9.1	10.9	0.99	56.6	90	33.4
F1	1F90c	9.4	10.9	1.04	59.6	90	30.4
F1	1F90d	8.7	11.7	0.84	48.0	90	42.0
F1	1F90e	10.1	13.1	0.88	50.4	90	39.6
F1	1F90f	9.6	10.6	1.13	64.9	90	25.1
F1	1F90g	9.2	10.9	1.00	57.6	90	32.4
F1	1F90h	9.4	10.9	1.04	59.6	90	30.4
F1	1F90i	9.1	9.6	1.25	71.4	90	18.6
F1	1F90j	10.3	12.2	1.01	57.6	90	32.4
F1	1F90k	9.2	11.4	0.94	53.8	90	36.2
F1	1F90l	9.6	10.4	1.18	67.4	90	22.6
F1	1F90m	10.7	12.5	1.03	58.9	90	31.1
F1	1F90n	10.0	12.4	0.94	53.8	90	36.2
F1	1F80a	9.1	9.8	1.19	68.2	82	13.8
F1	1F80b	9.5	10.0	1.25	71.8	82	10.2
F1	1F80c	8.6	9.0	1.27	72.9	82	9.1
F1	1F80d	9.4	11.0	1.02	58.7	82	23.3
F1	1F80e	9.7	11.3	1.03	59.1	82	22.9
F1	1F80f	8.6	9.0	1.27	72.9	82	9.1
F1	1F80g	8.5	8.5	1.57	90.0	82	8.0
F1	1F80h	8.3	9.5	1.06	60.9	82	21.1
F1	1F80i	7.2	9.2	0.90	51.5	82	30.5
F1	1F80j	7.9	8.8	1.11	63.9	82	18.1
F1	1F80k	7.9	8.7	1.14	65.2	82	16.8
F1	1F80l	8.1	9.0	1.12	64.2	82	17.8
F1	1F80m	10.3	11.1	1.19	68.1	82	13.9
F1	1F80n	8.7	9.5	1.16	66.3	82	15.7
F1	1F70a	8.6	13.8	0.67	38.5	69	30.5
F1	1F70b	10.6	12.8	0.98	55.9	69	13.1
F1	1F70c	9.3	11.3	0.97	55.4	69	13.6
F1	1F70d	9.5	12.3	0.88	50.6	69	18.4
F1	1F70e	9.4	11.1	1.01	57.9	69	11.1
F1	1F70f	10.0	12.0	0.99	56.4	69	12.6
F1	1F70g	9.2	13.3	0.76	43.8	69	25.2
F1	1F70h	8.9	11.5	0.88	50.7	69	18.3
F1	1F70i	9.4	12.6	0.84	48.2	69	20.8
F1	1F70j	10.4	14.4	0.81	46.2	69	22.8
F1	1F70k	9.0	12.0	0.85	48.6	69	20.4
F1	1F70l	9.3	12.5	0.84	48.1	69	20.9
F1	1F70m	8.7	12.0	0.81	46.5	69	22.5
F1	1F70n	9.6	11.2	1.03	59.0	69	10.0

Type	Sample ID	Width (mm)	Length (mm)	Calc Angle (rad)	Calc Angle (deg)	Actual Angle (deg)	Absolute Difference (deg)
F1	1F60a	8.7	13.8	0.68	39.1	59	19.9
F1	1F60b	9.3	12.4	0.85	48.6	59	10.4
F1	1F60c	8.4	12.5	0.74	42.2	59	16.8
F1	1F60d	8.6	12.9	0.73	41.8	59	17.2
F1	1F60e	8.7	12.4	0.78	44.6	59	14.4
F1	1F60f	8.4	12.2	0.76	43.5	59	15.5
F1	1F60g	7.2	11.7	0.66	38.0	59	21.0
F1	1F60h	9.8	14.9	0.72	41.1	59	17.9
F1	1F60i	8.4	13.9	0.65	37.2	59	21.8
F1	1F60j	9.0	15.0	0.64	36.9	59	22.1
F1	1F60k	8.0	10.9	0.82	47.2	59	11.8
F1	1F60l	8.1	11.2	0.81	46.3	59	12.7
F1	1F60m	8.3	13.6	0.66	37.6	59	21.4
F1	1F60n	8.1	13.5	0.64	36.9	59	22.1
F1	1F50a	11.8	14.9	0.91	52.4	46	6.4
F1	1F50b	9.8	13.0	0.85	48.9	46	2.9
F1	1F50c	10.4	13.5	0.88	50.4	46	4.4
F1	1F50d	9.7	14.4	0.74	42.3	46	3.7
F1	1F50e	9.3	14.1	0.72	41.3	46	4.7
F1	1F50f	11.2	13.9	0.94	53.7	46	7.7
F1	1F50g	11.6	11.7	1.44	82.5	46	36.5
F1	1F50h	9.1	11.7	0.89	51.1	46	5.1
F1	1F50i	9.2	12.1	0.86	49.5	46	3.5
F1	1F50j	9.8	12.7	0.88	50.5	46	4.5
F1	1F50k	8.2	12.5	0.72	41.0	46	5.0
F1	1F50l	10.3	14.2	0.81	46.5	46	0.5
F1	1F50m	10.5	11.3	1.19	68.3	46	22.3
F1	1F50n	9.2	12.4	0.84	47.9	46	1.9
F1	1F40a	11.0	14.6	0.85	48.9	41	7.9
F1	1F40b	9.7	14.6	0.73	41.6	41	0.6
F1	1F40o	8.5	13.5	0.68	39.0	41	2.0
F1	1F40d	10.2	15.8	0.70	40.2	41	0.8
F1	1F40e	9.5	10.2	1.20	68.6	41	27.6
F1	1F40f	9.0	12.1	0.84	48.1	41	7.1
F1	1F40g	9.1	13.9	0.71	40.9	41	0.1
F1	1F40h	9.8	14.0	0.78	44.4	41	3.4
F1	1F40i	9.5	15.8	0.65	37.0	41	4.0
F1	1F40j	9.5	14.4	0.72	41.3	41	0.3
F1	1F40k	10.9	15.4	0.79	45.1	41	4.1
F1	1F40l	10.2	15.7	0.71	40.5	41	0.5
F1	1F40m	10.9	16.3	0.73	42.0	41	1.0
F1	1F40n	9.0	14.4	0.68	38.7	41	2.3

Type	Sample ID	Width (mm)	Length (mm)	Calc Angle (rad)	Calc Angle (deg)	Actual Angle (deg)	Absolute Difference (deg)
F1	1F30a	7.4	13.5	0.58	33.2	31	2.2
F1	1F30b	7.3	15.4	0.49	28.3	31	2.7
F1	1F30c	8.4	17.4	0.50	28.9	31	2.1
F1	1F30d	7.8	14.8	0.56	31.8	31	0.8
F1	1F30e	7.3	14.0	0.55	31.4	31	0.4
F1	1F30f	8.0	17.2	0.48	27.7	31	3.3
F1	1F30g	8.3	18.5	0.47	26.7	31	4.3
F1	1F30h	8.8	15.8	0.59	33.8	31	2.8
F1	1F30i	7.8	17.0	0.48	27.3	31	3.7
F1	1F30j	7.8	14.3	0.58	33.1	31	2.1
F1	1F30k	7.9	17.2	0.48	27.3	31	3.7
F1	1F30l	9.6	21.4	0.47	26.7	31	4.3
F1	1F30m	9.3	19.2	0.51	29.0	31	2.0
F1	1F30n	7.1	14.6	0.51	29.1	31	1.9
F1	1F20a	6.3	19.6	0.33	18.7	21	2.3
F1	1F20b	6.0	19.3	0.32	18.1	21	2.9
F1	1F20c	6.1	16.4	0.38	21.8	21	0.8
F1	1F20d	5.5	18.8	0.30	17.0	21	4.0
F1	1F20e	5.6	17.8	0.32	18.3	21	2.7
F1	1F20f	5.8	18.2	0.32	18.6	21	2.4
F1	1F20g	6.3	17.4	0.37	21.2	21	0.2
F1	1F20h	5.9	17.6	0.34	19.6	21	1.4
F1	1F20i	5.6	17.7	0.32	18.4	21	2.6
F1	1F20j	5.8	17.5	0.34	19.4	21	1.6
F1	1F20k	5.6	14.0	0.41	23.6	21	2.6
F1	1F20l	5.6	16.0	0.36	20.5	21	0.5
F1	1F20m	5.4	16.9	0.33	18.6	21	2.4
F1	1F20p	5.8	15.7	0.38	21.7	21	0.7
F1	1F10a	5.5	34.2	0.16	9.3	11	1.7
F1	1F10b	5.3	25.4	0.21	12.0	11	1.0
F1	1F10c	5.2	26.7	0.20	11.2	11	0.2
F1	1F10d	6.1	32.7	0.19	10.8	11	0.2
F1	1F10e	5.0	40.7	0.12	7.1	11	3.9
F1	1F10f	6.0	34.5	0.17	10.0	11	1.0
F1	1F10g	5.3	24.0	0.22	12.8	11	1.8
F1	1F10h	5.5	25.6	0.22	12.4	11	1.4
F1	1F10i	5.6	28.0	0.20	11.5	11	0.5
F1	1F10j	4.4	24.4	0.18	10.4	11	0.6
F1	1F10k	4.9	22.5	0.22	12.6	11	1.6
F1	1F10l	5.6	20.9	0.27	15.5	11	4.5
F1	1F10m	4.7	24.7	0.19	11.0	11	0.0
F1	1F10n	6.6	25.2	0.26	15.2	11	4.2

Appendix C: Raw Data—Fabric 2

Type	Sample ID	Width (mm)	Length (mm)	Calc Angle (rad)	Calc Angle (deg)	Actual Angle (deg)	Absolute Difference (deg)
F2	2F90a	7.7	7.8	1.41	80.82	90	9.18
F2	2F90b	7.6	7.8	1.34	77.00	90	13.00
F2	2F90c	7.6	7.8	1.34	77.00	90	13.00
F2	2F90d	7.6	7.8	1.34	77.00	90	13.00
F2	2F90e	7.7	7.8	1.41	80.82	90	9.18
F2	2F90f	6.7	7.2	1.20	68.52	90	21.48
F2	2F90g	5.8	6.0	1.31	75.16	90	14.84
F2	2F90h	7.6	7.6	1.57	90.00	90	0.00
F2	2F90i	8.0	8.3	1.30	74.55	90	15.45
F2	2F90j	7.2	7.8	1.18	67.38	90	22.62
F2	2F90k	7.2	7.4	1.34	76.65	90	13.35
F2	2F90l	7.1	7.5	1.24	71.20	90	18.80
F2	2F90m	7.2	7.2	1.57	90.00	90	0.00
F2	2F90n	6.9	7.1	1.33	76.37	90	13.63
F2	2F80a	7.6	7.8	1.34	77.00	82	5.00
F2	2F80b	6.1	6.7	1.14	65.57	82	16.43
F2	2F80c	8.1	8.3	1.35	77.40	82	4.60
F2	2F80d	8.9	9.2	1.31	75.33	82	6.67
F2	2F80e	7.6	7.6	1.57	90.00	82	8.00
F2	2F80f	8.0	8.5	1.23	70.25	82	11.75
F2	2F80g	7.4	8.1	1.15	66.00	82	16.00
F2	2F80h	7.7	8.5	1.13	64.94	82	17.06
F2	2F80i	6.8	7.5	1.14	65.05	82	16.95
F2	2F80j	8.1	8.1	1.57	90.00	82	8.00
F2	2F80k	8.8	9.4	1.21	69.42	82	12.58
F2	2F80l	7.6	7.6	1.57	90.00	82	8.00
F2	2F80m	7.9	8.8	1.11	63.86	82	18.14
F2	2F80n	7.9	7.9	1.57	90.00	82	8.00
F2	2F70a	7.0	7.8	1.11	63.82	69	5.18
F2	2F70b	7.2	7.8	1.18	67.38	69	1.62
F2	2F70c	7.3	8.2	1.10	62.90	69	6.10
F2	2F70d	7.0	7.9	1.09	62.38	69	6.62
F2	2F70e	6.9	8.0	1.04	59.60	69	9.40
F2	2F70f	7.1	8.7	0.95	54.70	69	14.30
F2	2F70g	7.8	9.0	1.05	60.07	69	8.93
F2	2F70h	7.4	8.2	1.13	64.48	69	4.52
F2	2F70i	7.1	8.3	1.03	58.81	69	10.19
F2	2F70j	7.8	8.6	1.14	65.09	69	3.91
F2	2F70k	8.4	9.1	1.18	67.38	69	1.62
F2	2F70l	7.4	9.1	0.95	54.41	69	14.59
F2	2F70m	7.1	8.6	0.97	55.65	69	13.35
F2	2F70n	6.9	8.3	0.98	56.24	69	12.76

Type	Sample ID	Width (mm)	Length (mm)	Calc Angle (rad)	Calc Angle (deg)	Actual Angle (deg)	Absolute Difference (deg)
F2	2F60a	7.3	8.2	1.10	62.90	59	3.90
F2	2F60b	7.2	8.0	1.12	64.16	59	5.16
F2	2F60c	7.0	7.9	1.09	62.38	59	3.38
F2	2F60d	7.1	8.2	1.05	59.98	59	0.98
F2	2F60e	7.5	8.3	1.13	64.64	59	5.64
F2	2F60f	7.0	7.6	1.17	67.08	59	8.08
F2	2F60g	6.9	8.5	0.95	54.27	59	4.73
F2	2F60h	7.3	8.0	1.15	65.85	59	6.85
F2	2F60i	7.4	8.1	1.15	66.00	59	7.00
F2	2F60j	7.8	9.1	1.03	59.00	59	0.00
F2	2F60k	7.1	8.3	1.03	58.81	59	0.19
F2	2F60l	6.8	8.0	1.02	58.21	59	0.79
F2	2F60m	7.6	8.6	1.08	62.09	59	3.09
F2	2F60n	7.1	8.3	1.03	58.81	59	0.19
F2	2F50a	6.1	8.3	0.83	47.30	46	1.30
F2	2F50b	7.3	9.4	0.89	50.95	46	4.95
F2	2F50c	7.0	8.9	0.91	51.86	46	5.86
F2	2F50d	6.9	9.3	0.84	47.90	46	1.90
F2	2F50e	7.1	9.0	0.91	52.08	46	6.08
F2	2F50f	7.1	9.3	0.87	49.77	46	3.77
F2	2F50g	7.6	9.8	0.89	50.85	46	4.85
F2	2F50h	7.4	9.2	0.93	53.55	46	7.55
F2	2F50i	7.3	9.9	0.83	47.51	46	1.51
F2	2F50j	7.6	10.2	0.84	48.17	46	2.17
F2	2F50k	6.9	9.8	0.78	44.76	46	1.24
F2	2F50l	7.3	9.5	0.88	50.21	46	4.21
F2	2F50m	7.6	9.7	0.90	51.58	46	5.58
F2	2F50n	6.9	9.6	0.80	45.95	46	0.05
F2	2F40a	6.3	10.4	0.65	37.28	41	3.72
F2	2F40b	6.8	10.9	0.67	38.60	41	2.40
F2	2F40c	6.3	9.9	0.69	39.52	41	1.48
F2	2F40d	6.8	10.1	0.74	42.32	41	1.32
F2	2F40e	6.4	10.4	0.66	37.98	41	3.02
F2	2F40f	7.0	10.3	0.75	42.81	41	1.81
F2	2F40g	6.8	11.4	0.64	36.62	41	4.38
F2	2F40h	6.6	10.1	0.71	40.80	41	0.20
F2	2F40i	6.6	9.7	0.75	42.88	41	1.88
F2	2F40j	7.2	10.4	0.76	43.81	41	2.81
F2	2F40k	6.5	10.4	0.68	38.68	41	2.32
F2	2F40l	6.3	9.6	0.72	41.01	41	0.01
F2	2F40m	6.6	10.8	0.66	37.67	41	3.33
F2	2F40n	6.6	11.0	0.64	36.87	41	4.13

Type	Sample ID	Width (mm)	Length (mm)	Calc Angle (rad)	Calc Angle (deg)	Actual Angle (deg)	Absolute Difference (deg)
F2	2F30a	6.0	12.6	0.50	28.44	31	2.56
F2	2F30b	6.6	12.1	0.58	33.06	31	2.06
F2	2F30c	6.5	11.5	0.60	34.42	31	3.42
F2	2F30d	7.1	14.0	0.53	30.47	31	0.53
F2	2F30e	6.4	13.5	0.49	28.30	31	2.70
F2	2F30f	6.3	12.4	0.53	30.53	31	0.47
F2	2F30g	7.1	12.4	0.61	34.93	31	3.93
F2	2F30h	7.0	12.5	0.59	34.06	31	3.06
F2	2F30i	6.5	11.9	0.58	33.11	31	2.11
F2	2F30j	6.0	12.6	0.50	28.44	31	2.56
F2	2F30k	6.1	11.5	0.56	32.03	31	1.03
F2	2F30l	6.1	12.4	0.51	29.47	31	1.53
F2	2F30m	6.5	11.7	0.59	33.75	31	2.75
F2	2F30n	6.4	11.9	0.57	32.54	31	1.54
F2	2F20a	5.2	16.5	0.32	18.37	21	2.63
F2	2F20b	5.8	16.9	0.35	20.07	21	0.93
F2	2F20c	6.3	14.5	0.45	25.75	21	4.75
F2	2F20d	5.4	17.7	0.31	17.76	21	3.24
F2	2F20e	6.2	16.1	0.40	22.65	21	1.65
F2	2F20f	5.2	16.1	0.33	18.84	21	2.16
F2	2F20g	5.7	14.5	0.40	23.15	21	2.15
F2	2F20h	5.7	18.7	0.31	17.75	21	3.25
F2	2F20i	4.6	16.6	0.28	16.09	21	4.91
F2	2F20j	5.7	17.3	0.34	19.24	21	1.76
F2	2F20k	6.1	15.1	0.42	23.83	21	2.83
F2	2F20l	5.7	16.4	0.35	20.34	21	0.66
F2	2F20m	5.9	16.3	0.37	21.22	21	0.22
F2	2F20n	5.8	15.4	0.39	22.12	21	1.12
F2	2F10a	5.7	29.6	0.19	11.10	11	0.10
F2	2F10b	4.8	28.9	0.17	9.56	11	1.44
F2	2F10c	5.2	21.9	0.24	13.74	11	2.74
F2	2F10d	5.6	23.3	0.24	13.91	11	2.91
F2	2F10e	5.4	23.4	0.23	13.34	11	2.34
F2	2F10f	5.3	21.8	0.25	14.07	11	3.07
F2	2F10g	4.8	23.4	0.21	11.84	11	0.84
F2	2F10h	4.5	22.1	0.21	11.75	11	0.75
F2	2F10i	4.8	21.2	0.23	13.09	11	2.09
F2	2F10j	5.6	24.4	0.23	13.27	11	2.27
F2	2F10k	5.6	25.7	0.22	12.59	11	1.59
F2	2F10l	5.3	29.0	0.18	10.53	11	0.47
F2	2F10m	5.2	22.4	0.23	13.42	11	2.42
F2	2F10n	5.6	23.0	0.25	14.09	11	3.09

Appendix D: Raw Data—Fabric 3

Type	Sample ID	Width (mm)	Length (mm)	Calc Angle (rad)	Calc Angle (deg)	Actual Angle (deg)	Absolute Difference (deg)
F3	3F90a	12.5	12.7	1.39	79.82	90	10.18
F3	3F90b	12.2	12.5	1.35	77.42	90	12.58
F3	3F90c	10.9	12.9	1.01	57.67	90	32.33
F3	3F90d	10.4	12.4	0.99	57.00	90	33.00
F3	3F90e	10.8	12.5	1.04	59.77	90	30.23
F3	3F90f	10.5	11.7	1.11	63.82	90	26.18
F3	3F90g	9.7	11.4	1.02	58.31	90	31.69
F3	3F90h	10.0	11.9	1.00	57.18	90	32.82
F3	3F90i	9.4	11.7	0.93	53.46	90	36.54
F3	3F90j	11.2	12.6	1.09	62.73	90	27.27
F3	3F90k	10.1	11.8	1.03	58.86	90	31.14
F3	3F90l	10.8	12.0	1.12	64.16	90	25.84
F3	3F90m	10.6	12.7	0.99	56.58	90	33.42
F3	3F90n	10.0	11.6	1.04	59.55	90	30.45
F3	3F80a	10.4	11.7	1.09	62.73	82	19.27
F3	3F80b	10.1	12.3	0.96	55.20	82	26.80
F3	3F80c	9.6	10.3	1.20	68.75	82	13.25
F3	3F80d	9.7	11.1	1.06	60.91	82	21.09
F3	3F80e	10.1	12.1	0.99	56.59	82	25.41
F3	3F80f	10.5	11.3	1.19	68.31	82	13.69
F3	3F80g	10.5	11.6	1.13	64.85	82	17.15
F3	3F80h	9.2	12.0	0.87	50.06	82	31.94
F3	3F80i	10.2	12.8	0.92	52.83	82	29.17
F3	3F80j	11.9	12.5	1.26	72.18	82	9.82
F3	3F80k	10.2	10.6	1.30	74.21	82	7.79
F3	3F80l	9.8	11.8	0.98	56.15	82	25.85
F3	3F80m	10.1	11.7	1.04	59.68	82	22.32
F3	3F80n	10.9	11.4	1.27	72.97	82	9.03
F3	3F80p	10.1	10.4	1.33	76.20	82	5.80
F3	3F70a	11.7	12.7	1.17	67.11	69	1.89
F3	3F70b	10.3	11.0	1.21	69.45	69	0.45
F3	3F70c	10.5	10.8	1.33	76.46	69	7.46
F3	3F70d	10.4	10.6	1.38	78.85	69	9.85
F3	3F70e	10.6	11.7	1.13	64.96	69	4.04
F3	3F70f	9.9	10.7	1.18	67.70	69	1.30
F3	3F70g	10.1	10.3	1.37	78.69	69	9.69
F3	3F70h	10.1	10.9	1.19	67.91	69	1.09
F3	3F70i	10.6	11.5	1.17	67.18	69	1.82
F3	3F70j	10.7	10.9	1.38	79.01	69	10.01
F3	3F70k	10.0	11.2	1.10	63.23	69	5.77
F3	3F70l	11.0	11.5	1.27	73.04	69	4.04
F3	3F70m	11.5	11.5	1.57	90.00	69	21.00
F3	3F70n	11.7	12.4	1.23	70.66	69	1.66

Type	Sample ID	Width (mm)	Length (mm)	Calc Angle (rad)	Calc Angle (deg)	Actual Angle (deg)	Absolute Difference (deg)
F3	3F60a	10.8	11.5	1.22	69.91	59	10.91
F3	3F60b	10.6	10.8	1.38	78.96	59	19.96
F3	3F60c	10.3	11.1	1.19	68.11	59	9.11
F3	3F60d	10.4	11.7	1.09	62.73	59	3.73
F3	3F60e	9.6	10.9	1.08	61.73	59	2.73
F3	3F60f	9.8	11.0	1.10	62.99	59	3.99
F3	3F60g	10.6	11.5	1.17	67.18	59	8.18
F3	3F60h	9.2	10.4	1.09	62.20	59	3.20
F3	3F60i	10.0	11.6	1.04	59.55	59	0.55
F3	3F60j	9.9	11.0	1.12	64.16	59	5.16
F3	3F60k	10.6	11.9	1.10	62.97	59	3.97
F3	3F60l	9.9	10.5	1.23	70.54	59	11.54
F3	3F60m	9.7	10.3	1.23	70.35	59	11.35
F3	3F60n	9.4	10.9	1.04	59.59	59	0.59
F3	3F50a	9.7	13.9	0.77	44.25	46	1.75
F3	3F50b	10.1	13.1	0.88	50.44	46	4.44
F3	3F50c	9.7	12.6	0.88	50.34	46	4.34
F3	3F50d	9.3	12.9	0.81	46.13	46	0.13
F3	3F50e	9.4	12.4	0.86	49.29	46	3.29
F3	3F50f	9.7	12.7	0.87	49.80	46	3.80
F3	3F50g	9.7	14.3	0.75	42.71	46	3.29
F3	3F50h	8.9	12.9	0.76	43.62	46	2.38
F3	3F50i	9.8	14.0	0.78	44.43	46	1.57
F3	3F50j	9.1	12.2	0.84	48.24	46	2.24
F3	3F50k	8.6	13.2	0.71	40.66	46	5.34
F3	3F50l	11.1	13.1	1.01	57.92	46	11.92
F3	3F50m	11.1	13.2	1.00	57.24	46	11.24
F3	3F50n	9.7	13.1	0.83	47.77	46	1.77
F3	3F50p	9.0	13.9	0.70	40.35	46	5.65
F3	3F40a	8.5	12.4	0.76	43.27	41	2.27
F3	3F40b	9.4	13.5	0.77	44.13	41	3.13
F3	3F40c	9.0	12.7	0.79	45.13	41	4.13
F3	3F40d	9.1	13.4	0.75	42.77	41	1.77
F3	3F40e	8.6	14.3	0.65	36.97	41	4.03
F3	3F40f	8.8	13.8	0.69	39.62	41	1.38
F3	3F40g	9.0	12.6	0.80	45.58	41	4.58
F3	3F40h	9.7	16.2	0.64	36.78	41	4.22
F3	3F40i	9.9	13.9	0.79	45.42	41	4.42
F3	3F40j	8.1	10.8	0.85	48.59	41	7.59
F3	3F40k	9.3	15.8	0.63	36.06	41	4.94
F3	3F40l	8.6	10.5	0.96	54.99	41	13.99
F3	3F40m	10.4	14.7	0.79	45.03	41	4.03
F3	3F40n	8.7	13.8	0.68	39.08	41	1.92

Type	Sample ID	Width (mm)	Length (mm)	Calc Angle (rad)	Calc Angle (deg)	Actual Angle (deg)	Absolute Difference (deg)
F3	3F30a	7.7	16.5	0.49	27.82	31	3.18
F3	3F30b	7.5	14.3	0.55	31.63	31	0.63
F3	3F30c	8.1	18.3	0.46	26.27	31	4.73
F3	3F30d	7.6	17.3	0.45	26.06	31	4.94
F3	3F30e	7.9	15.9	0.52	29.79	31	1.21
F3	3F30f	7.2	16.5	0.45	25.87	31	5.13
F3	3F30g	7.8	14.3	0.58	33.06	31	2.06
F3	3F30h	7.6	16.4	0.48	27.61	31	3.39
F3	3F30i	7.2	18.8	0.39	22.52	31	8.48
F3	3F30j	8.0	18.1	0.46	26.23	31	4.77
F3	3F30k	7.7	13.9	0.59	33.64	31	2.64
F3	3F30l	7.2	16.6	0.45	25.70	31	5.30
F3	3F30m	6.9	15.8	0.45	25.89	31	5.11
F3	3F30n	7.7	16.5	0.49	27.82	31	3.18
F3	3F20a	6.0	21.6	0.28	16.13	21	4.87
F3	3F20b	7.1	22.7	0.32	18.23	21	2.77
F3	3F20c	6.3	18.2	0.35	20.25	21	0.75
F3	3F20d	6.8	20.7	0.33	19.18	21	1.82
F3	3F20e	6.6	17.1	0.40	22.70	21	1.70
F3	3F20f	6.5	18.4	0.36	20.69	21	0.31
F3	3F20g	5.7	21.0	0.27	15.75	21	5.25
F3	3F20h	6.9	22.7	0.31	17.70	21	3.30
F3	3F20i	6.6	20.5	0.33	18.78	21	2.22
F3	3F20j	7.5	19.7	0.39	22.38	21	1.38
F3	3F20k	5.8	20.8	0.28	16.19	21	4.81
F3	3F20l	7.0	20.6	0.35	19.87	21	1.13
F3	3F20m	6.1	17.2	0.36	20.77	21	0.23
F3	3F20n	6.7	20.1	0.34	19.47	21	1.53
F3	3F10a	5.2	28.1	0.19	10.66	11	0.34
F3	3F10b	5.6	31.5	0.18	10.24	11	0.76
F3	3F10c	6.3	26.2	0.24	13.91	11	2.91
F3	3F10d	6.8	33.1	0.21	11.86	11	0.86
F3	3F10e	5.7	24.7	0.23	13.34	11	2.34
F3	3F10f	5.9	23.3	0.26	14.67	11	3.67
F3	3F10g	4.1	28.6	0.14	8.24	11	2.76
F3	3F10h	5.3	23.8	0.22	12.87	11	1.87
F3	3F10i	6.8	31.1	0.22	12.63	11	1.63
F3	3F10j	6.1	34.9	0.18	10.07	11	0.93
F3	3F10k	5.4	28.4	0.19	10.96	11	0.04
F3	3F10l	5.5	28.1	0.20	11.29	11	0.29
F3	3F10m	5.2	27.4	0.19	10.94	11	0.06
F3	3F10n	5.7	28.1	0.20	11.70	11	0.70
F3	3F10p	5.1	30.9	0.17	9.50	11	1.50

Appendix E: Bloodstain Photos—Control

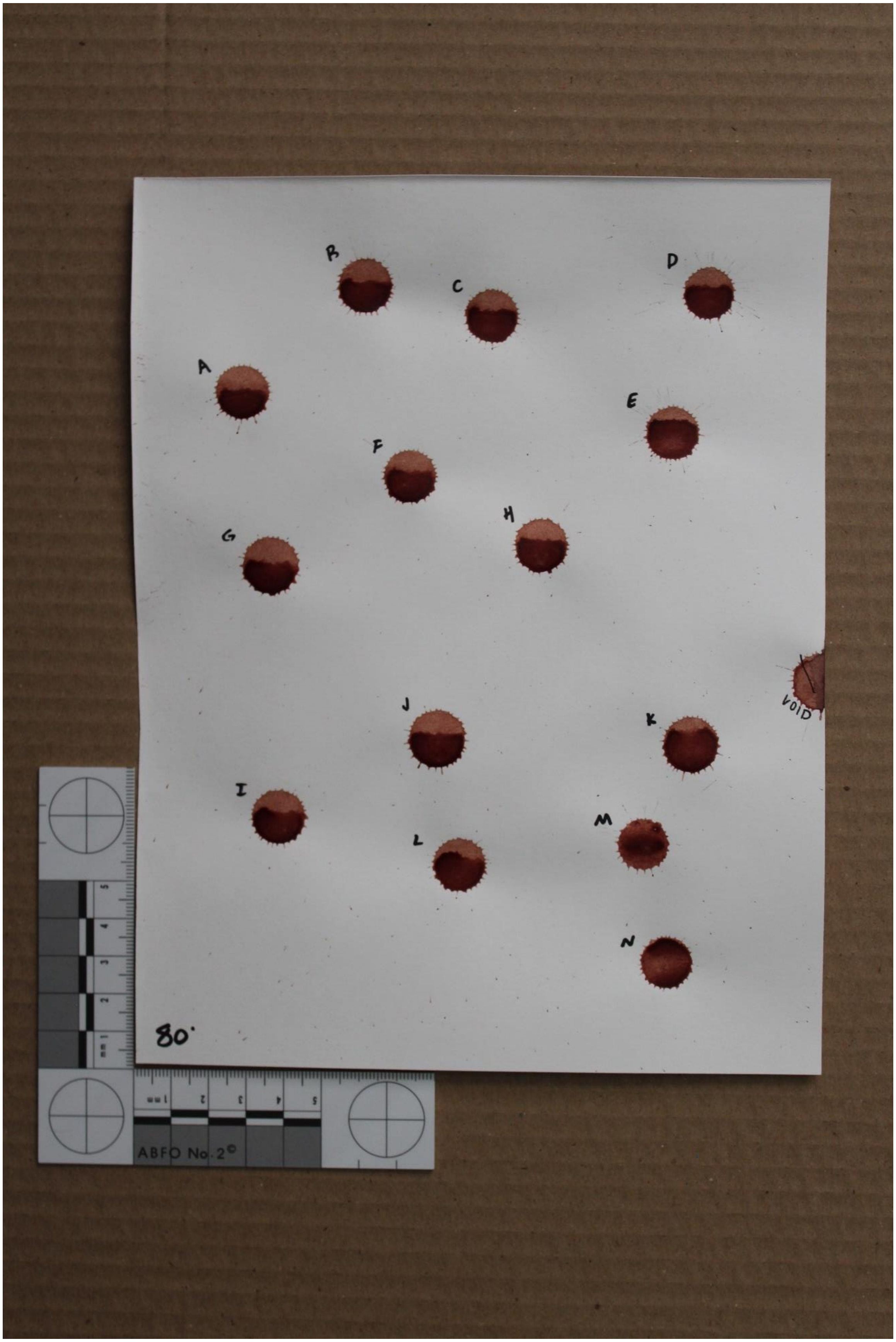
B
C
D
A
E
F
H
G
VOID
J
K
I
M
L
N
80°
ABFO No. 2©

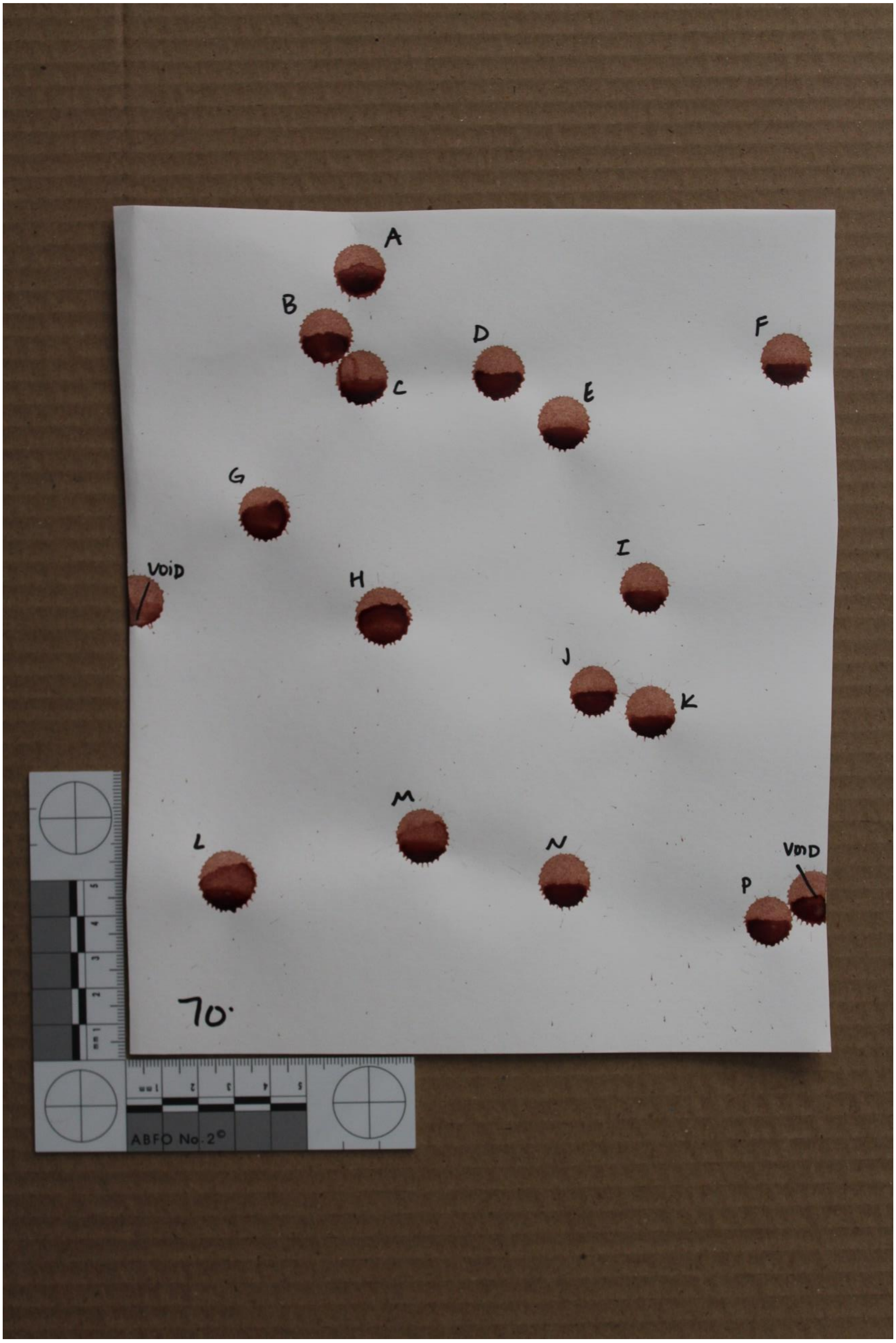
A
B
C
D
E
F
G
VOID
H
I
J
K
M
L
N
VOID
P
70°
ABFO No. 2©

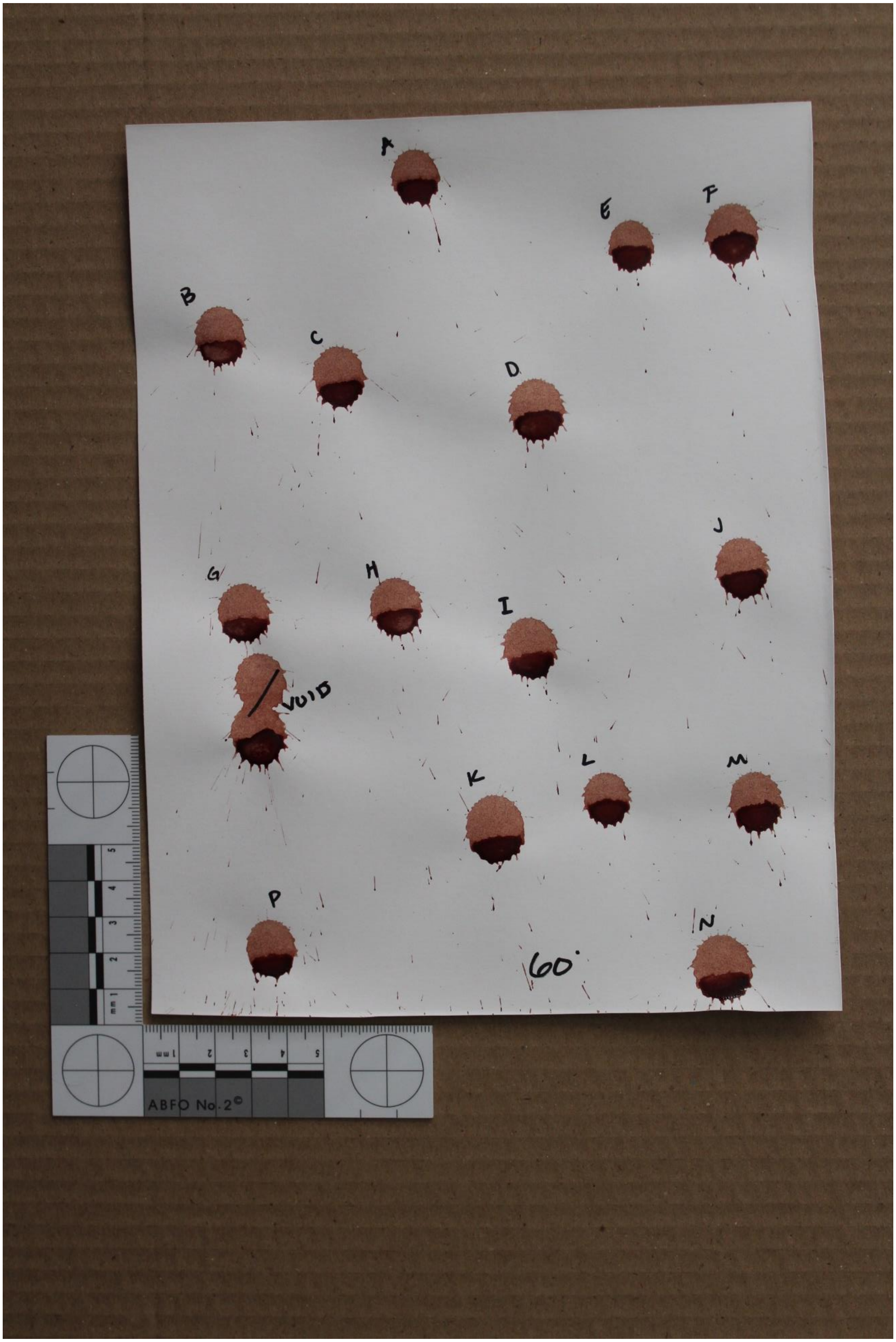
A
E
F
B
C
D
J
G
H
I
VOID
K
L
M
P
N
60°
ABFO No. 2©

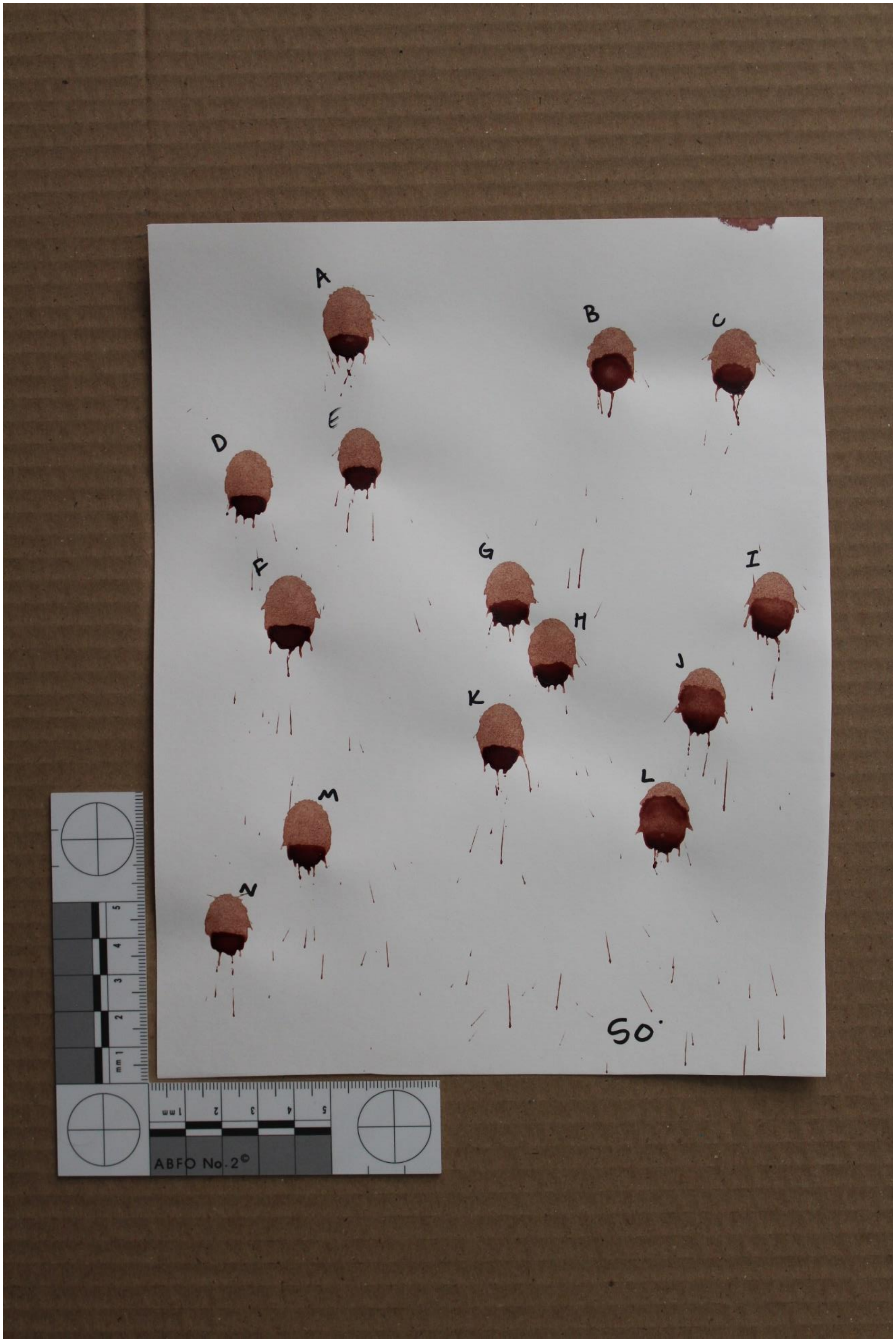
A
B
C
D
E
F
G
H
I
J
K
L
M
N
50°
ABFO No. 2©

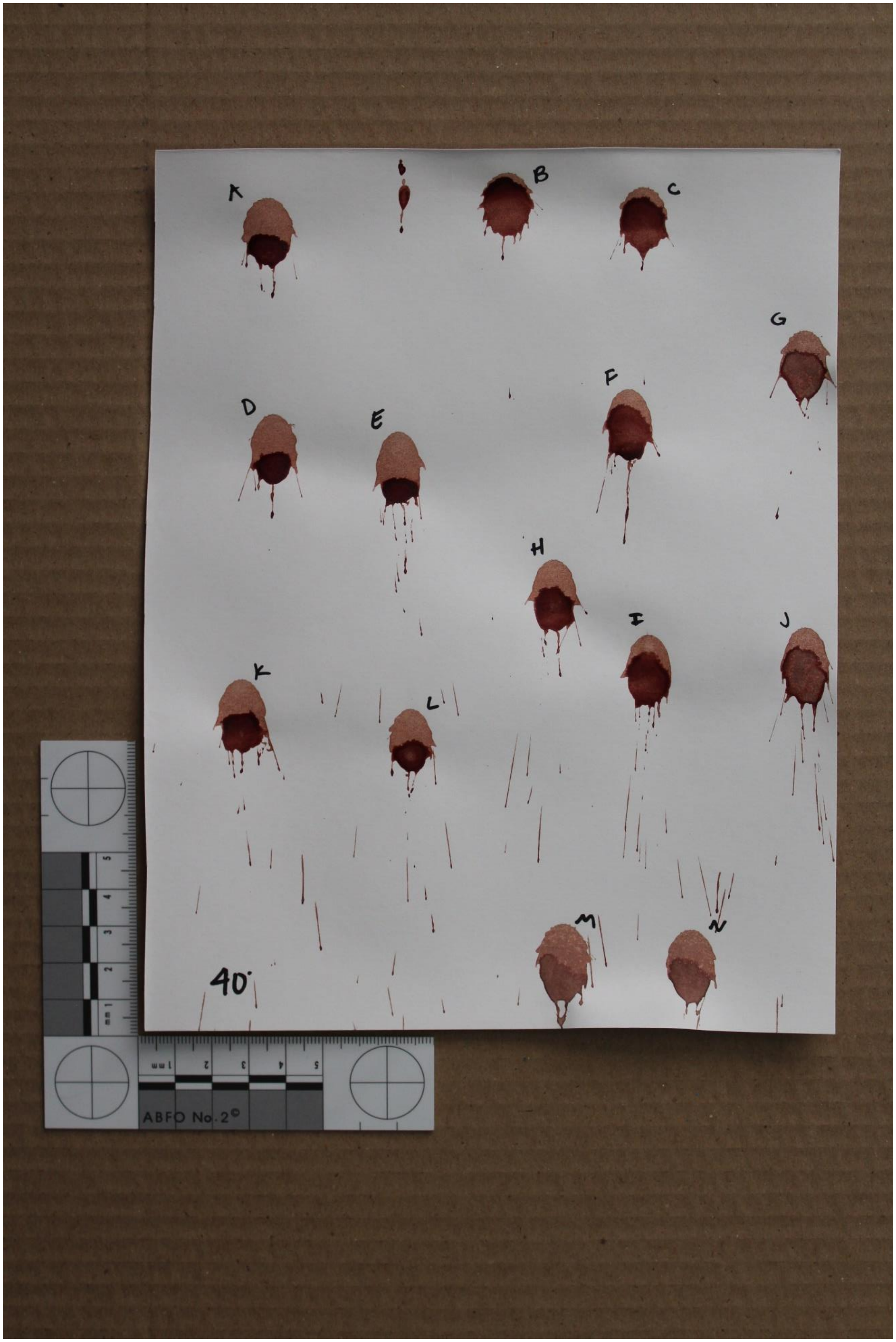
A
B
C
D
E
F
G
H
I
J
K
L
M
N
40°
ABFO No. 2©

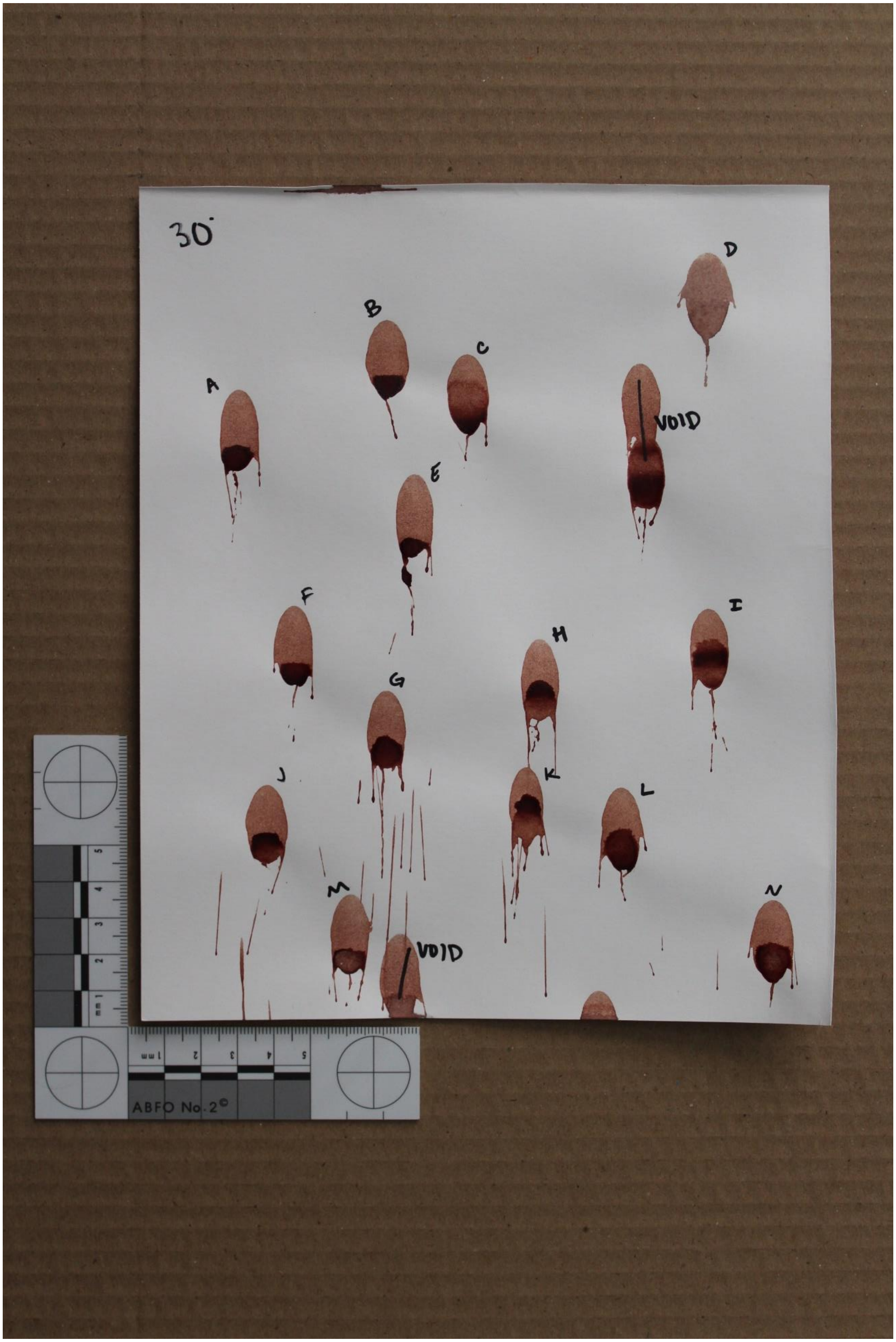
30°
A
B
C
D
E
VOID
F
G
H
I
J
K
L
M
N
VOID
ABFO No. 2©

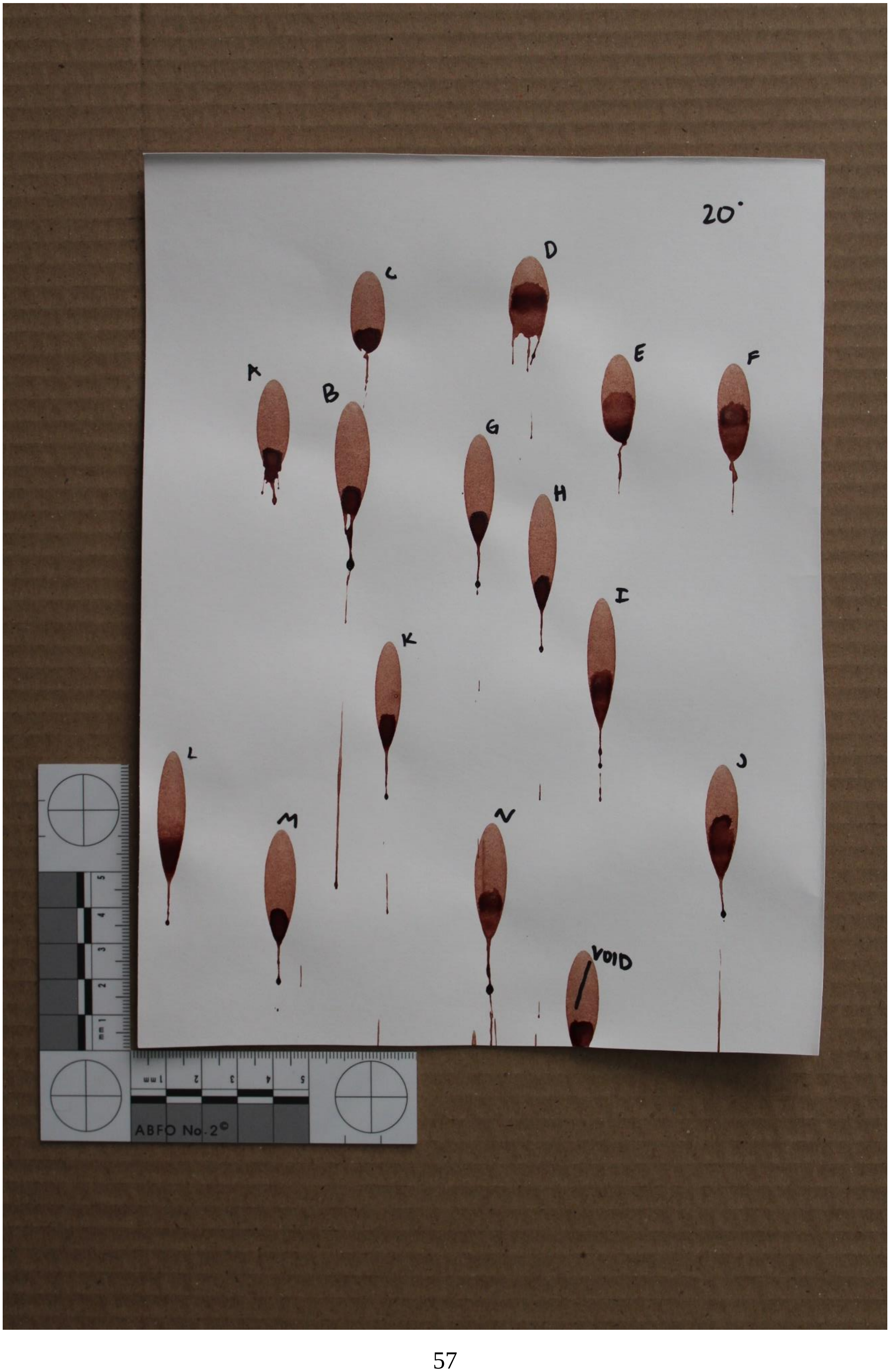
20°
A
B
C
D
E
F
G
H
I
J
K
L
M
N
VOID
ABFO No. 2©

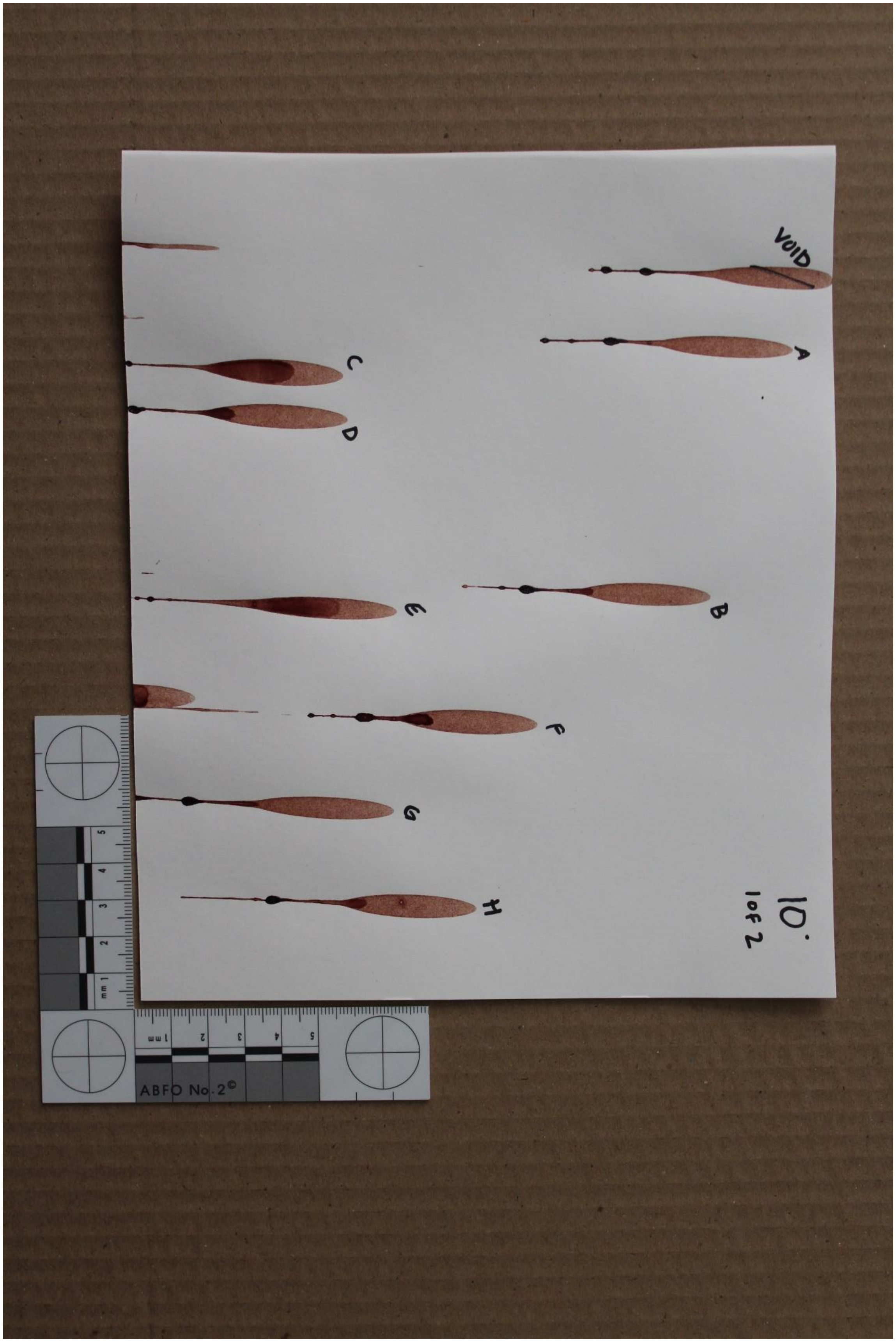
VOID
A
B
C
D
E
F
G
H
10°
1 of 2
ABFO No. 2©

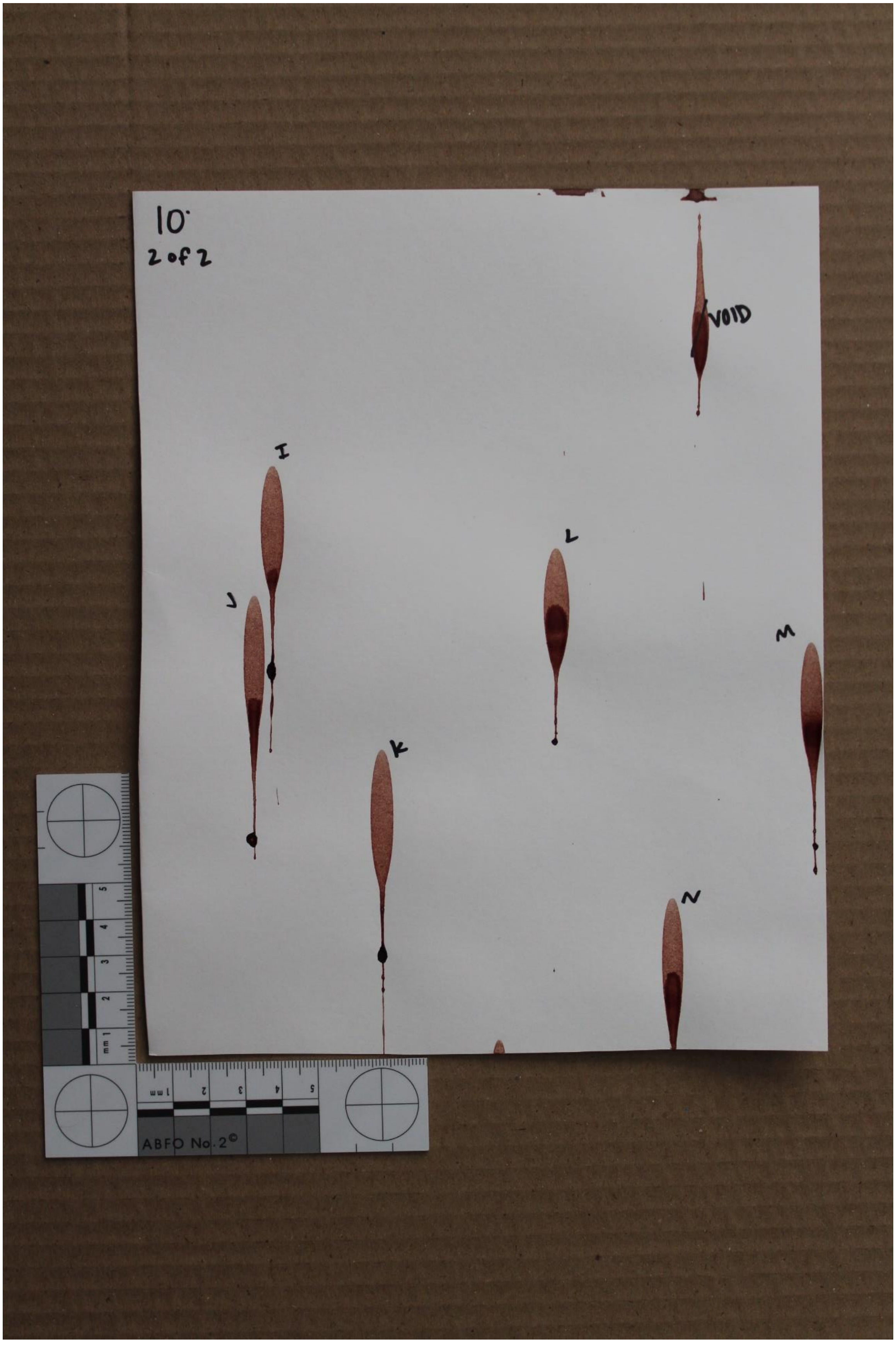
10°
2 of 2
VOID
I
J
K
L
M
N
ABFO No. 2©

Appendix F: Bloodstain Photos—Fabric 1

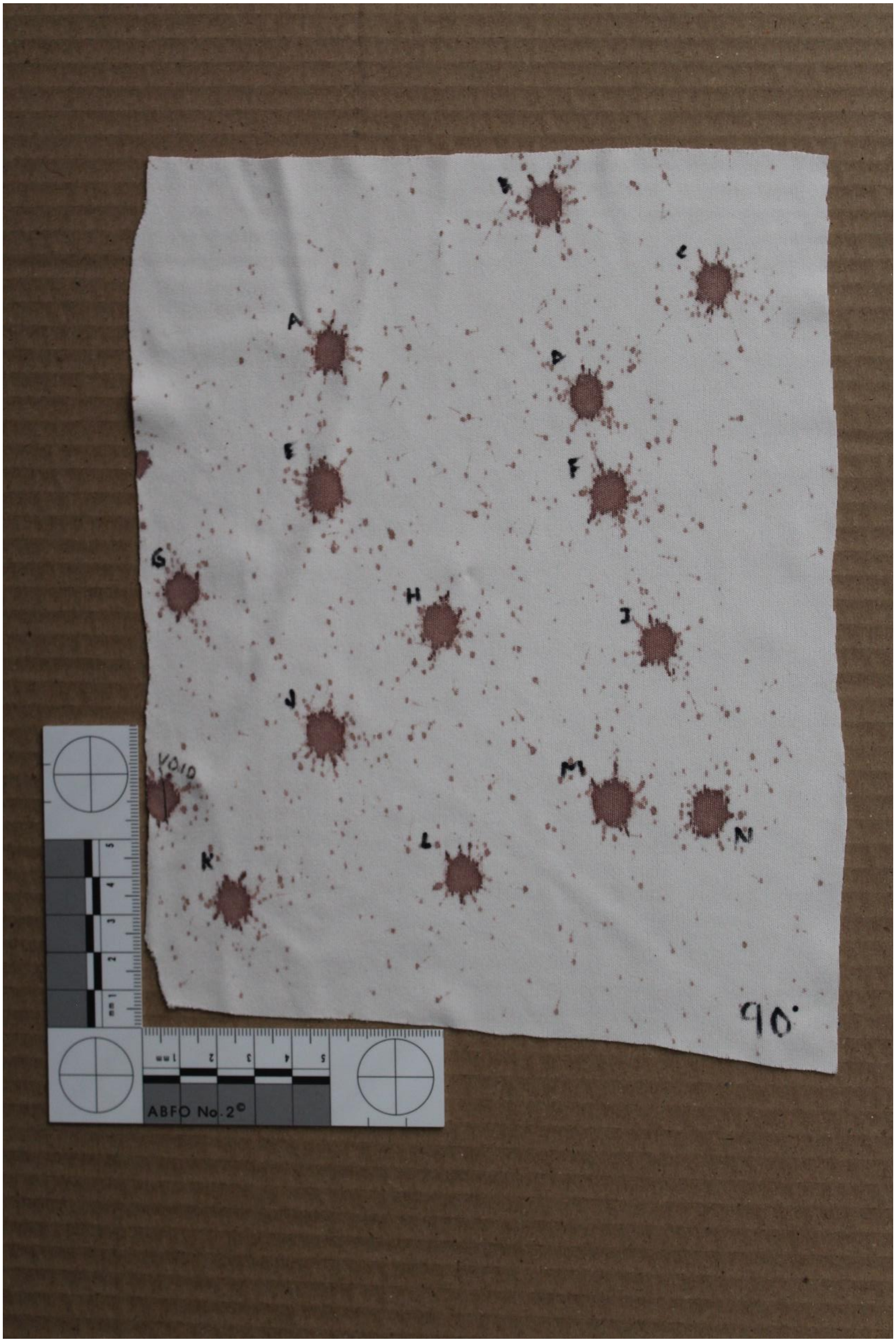

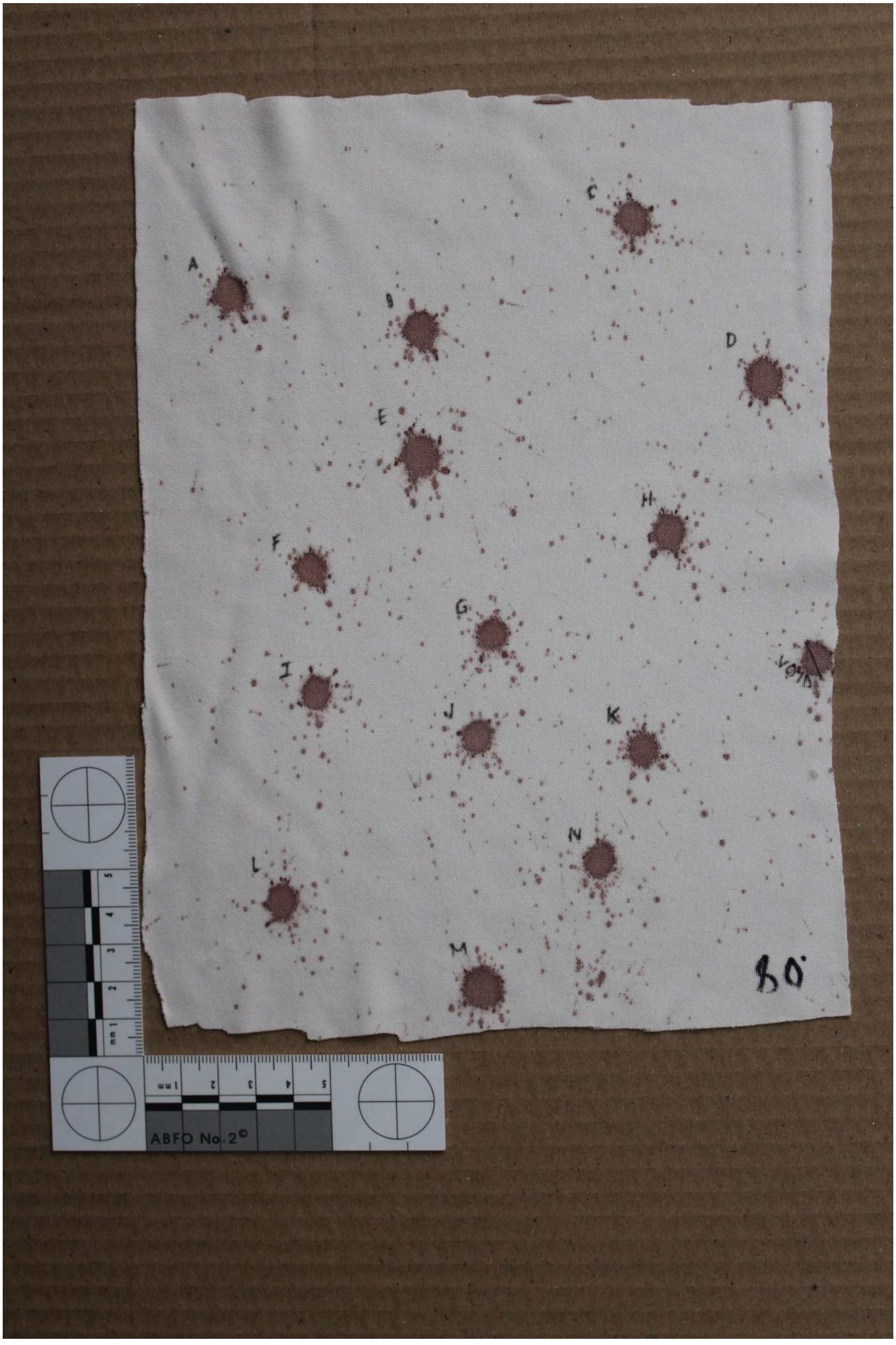
ABFO No. 2©


ABFO No 2©


ABFO No. 2©

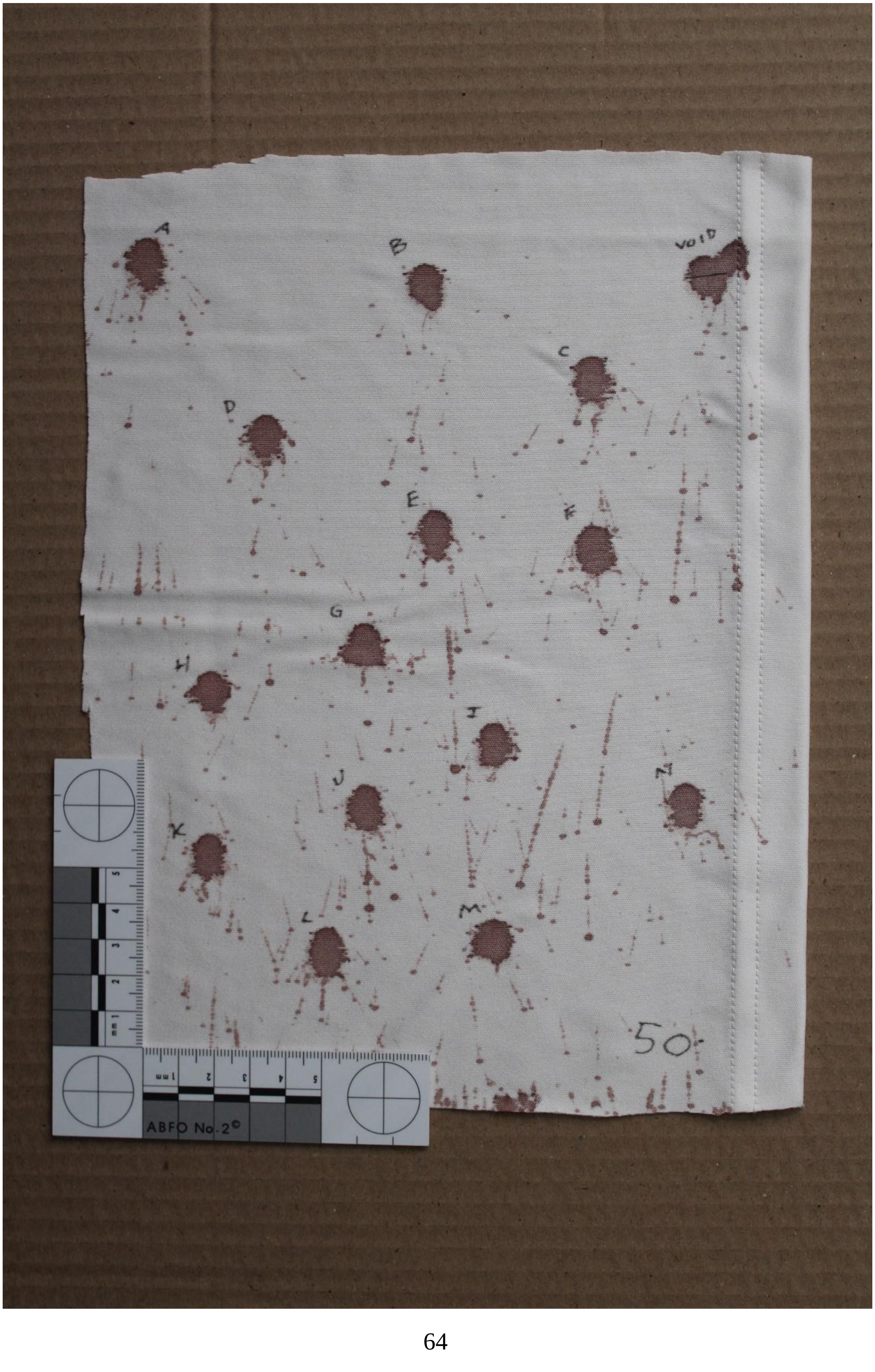
A
B
VOID
C
D
E
F
G
H
I
J
K
L
M
N
50
ABFO No. 2©

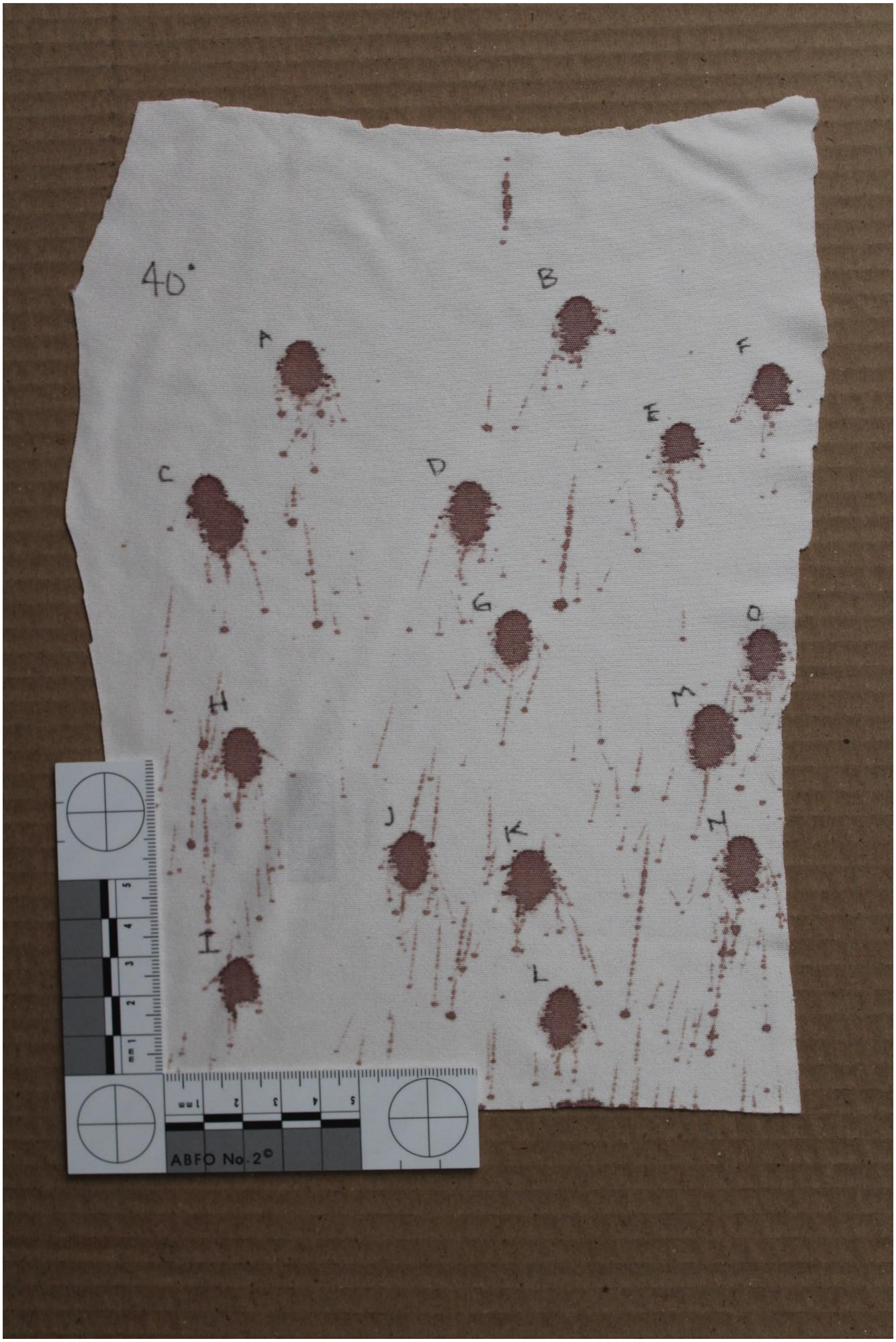
40°
A
B
C
D
E
F
G
H
I
J
K
L
M
N
O
ABFO No. 2©

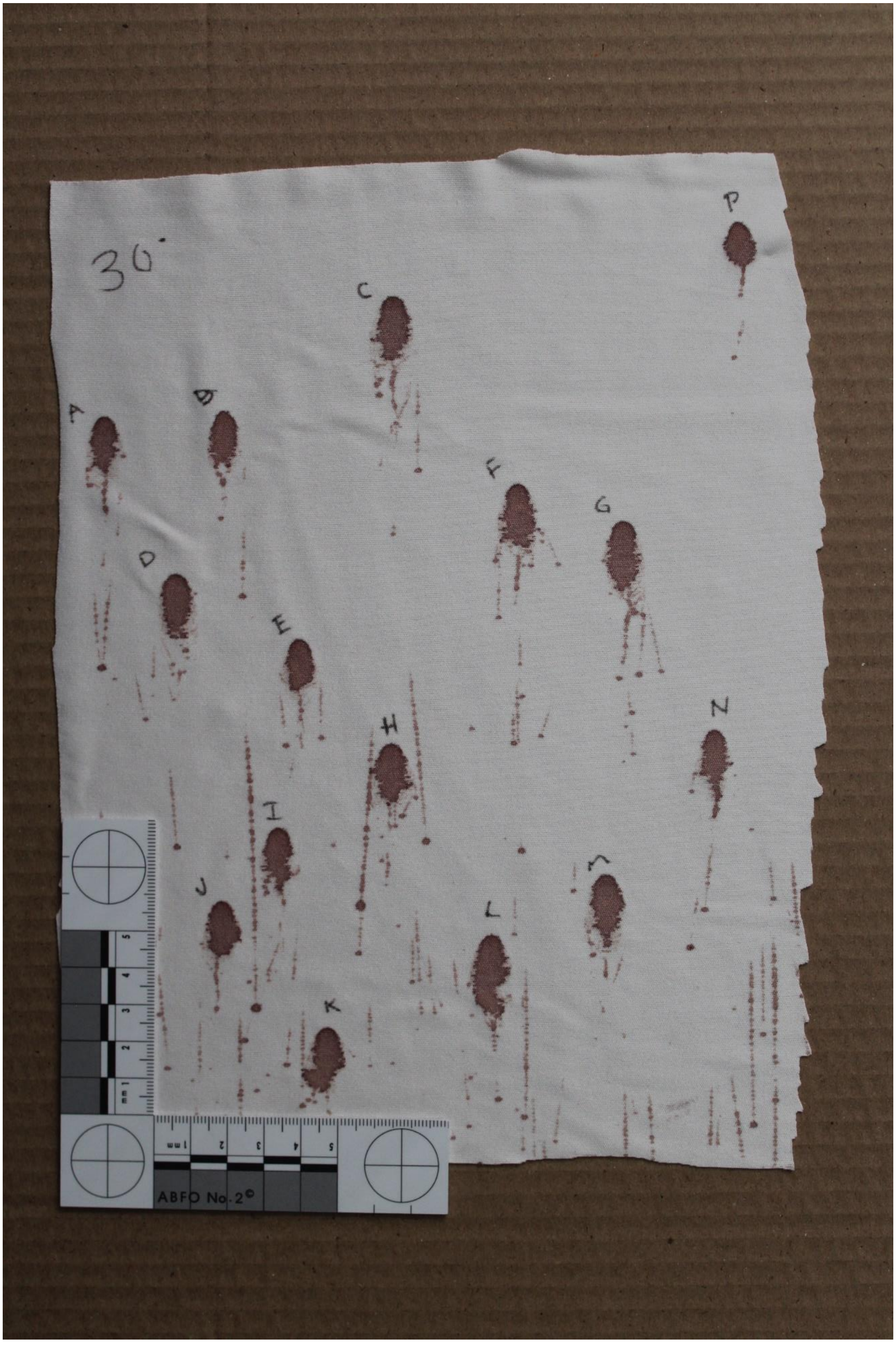
30°
P
C
A
B
F
G
D
E
N
H
I
M
J
L
K
ABFO No. 2©

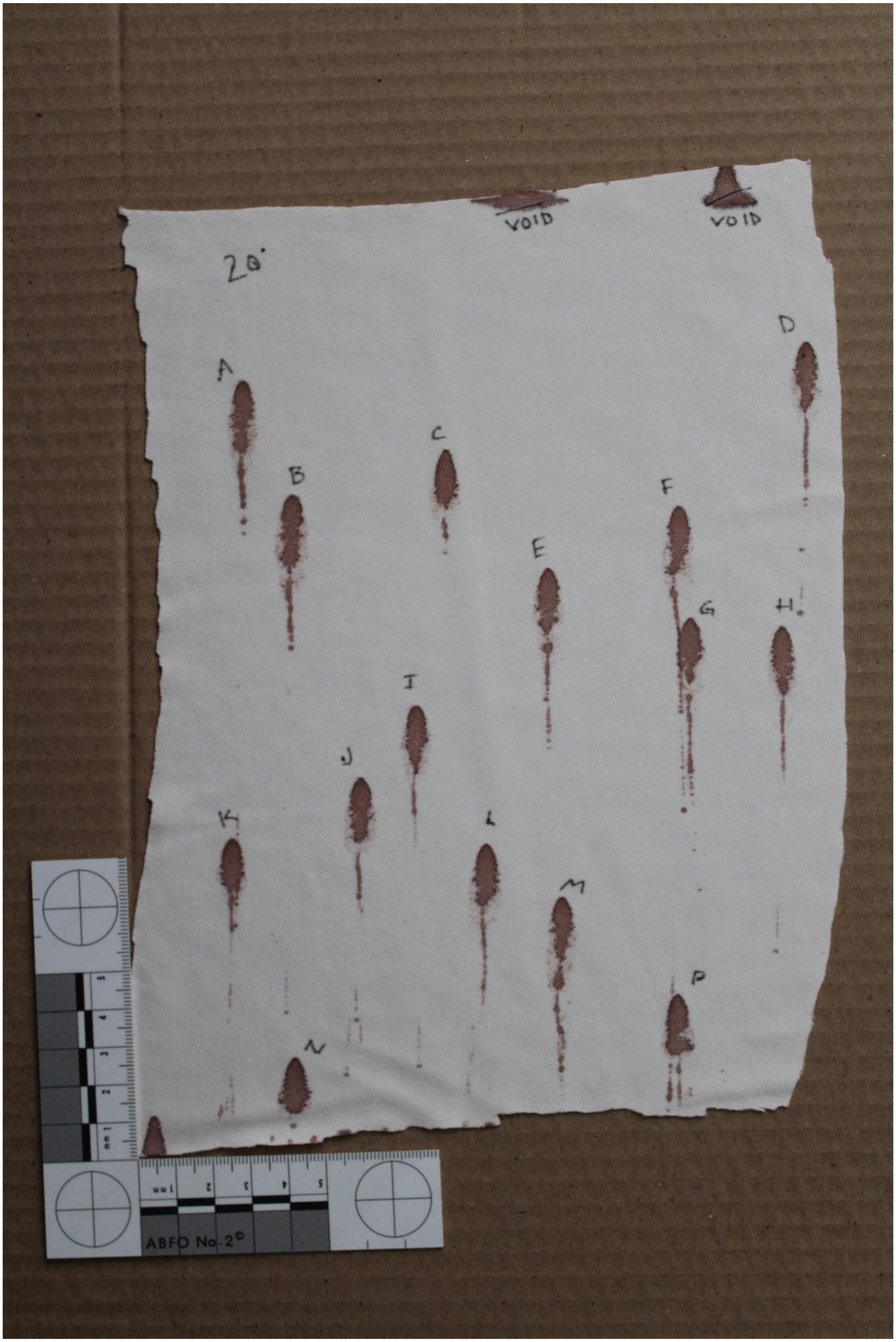
VOID
VOID
20°
A
B
C
D
E
F
G
H
I
J
K
L
M
N
P
ABFO No. 2©

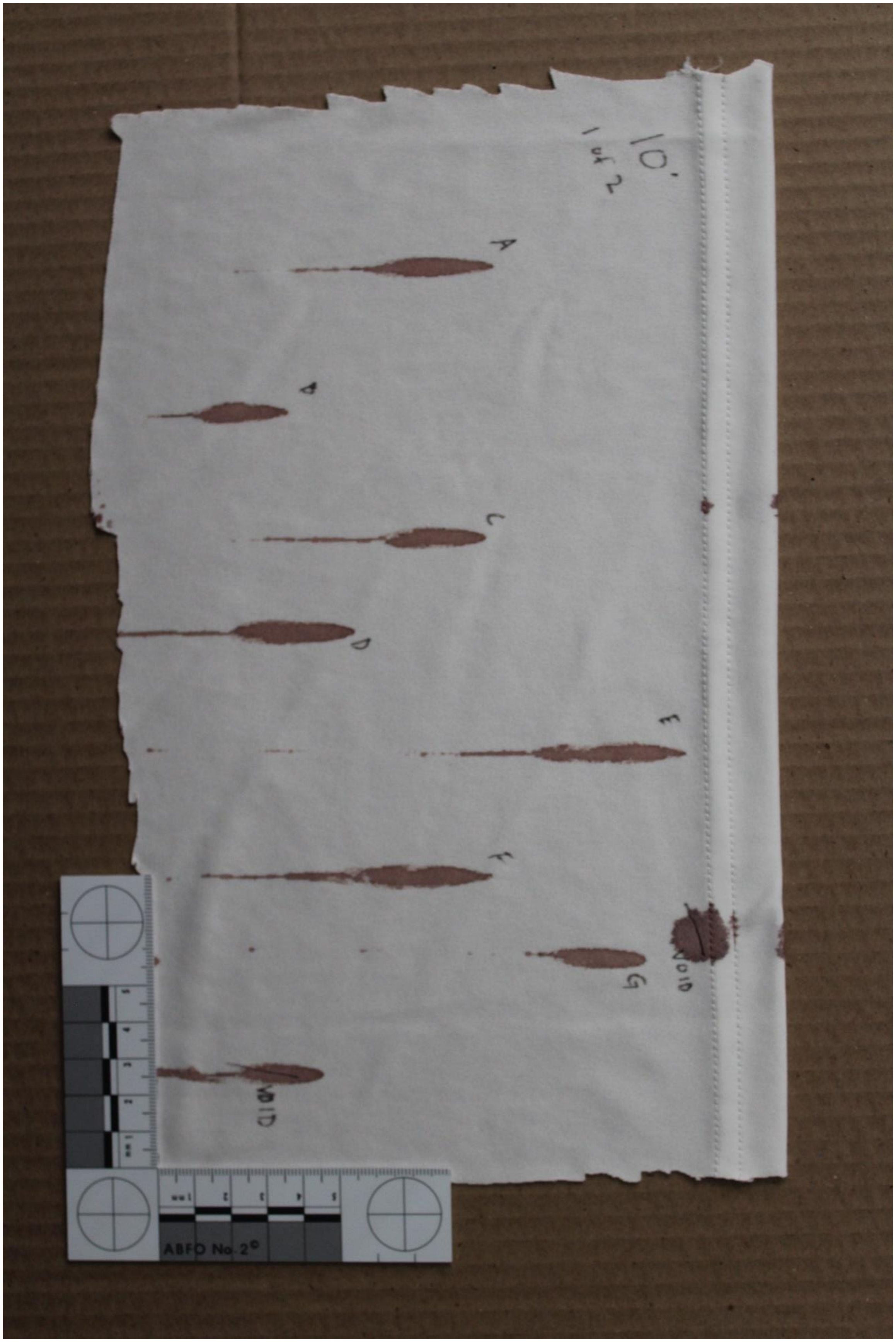

ABFO No. 2©

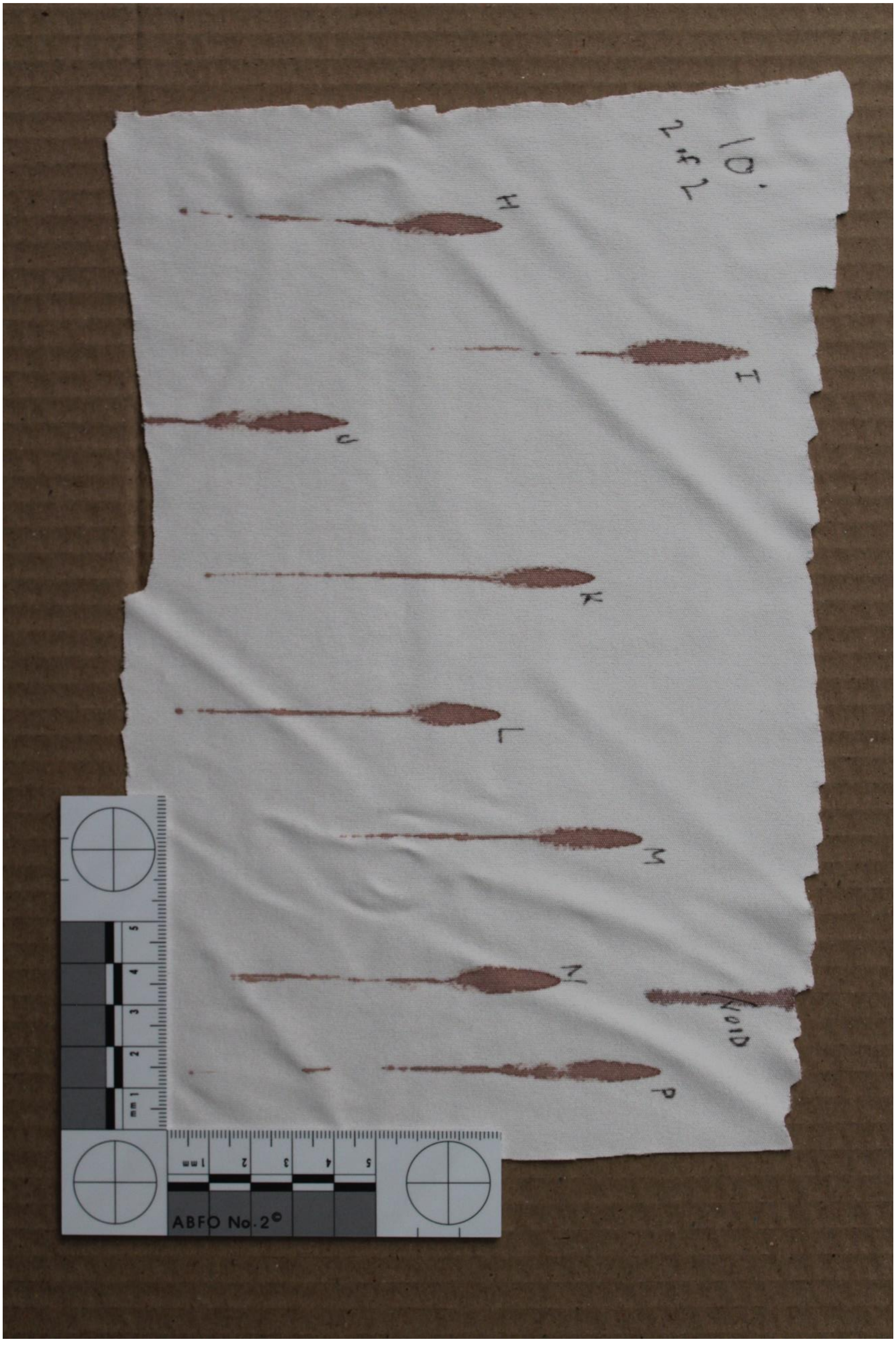
10'
2 of 2
H
I
J
K
L
M
N
VOID
P
ABFO No. 2©

Appendix G: Bloodstain Photos—Fabric 2

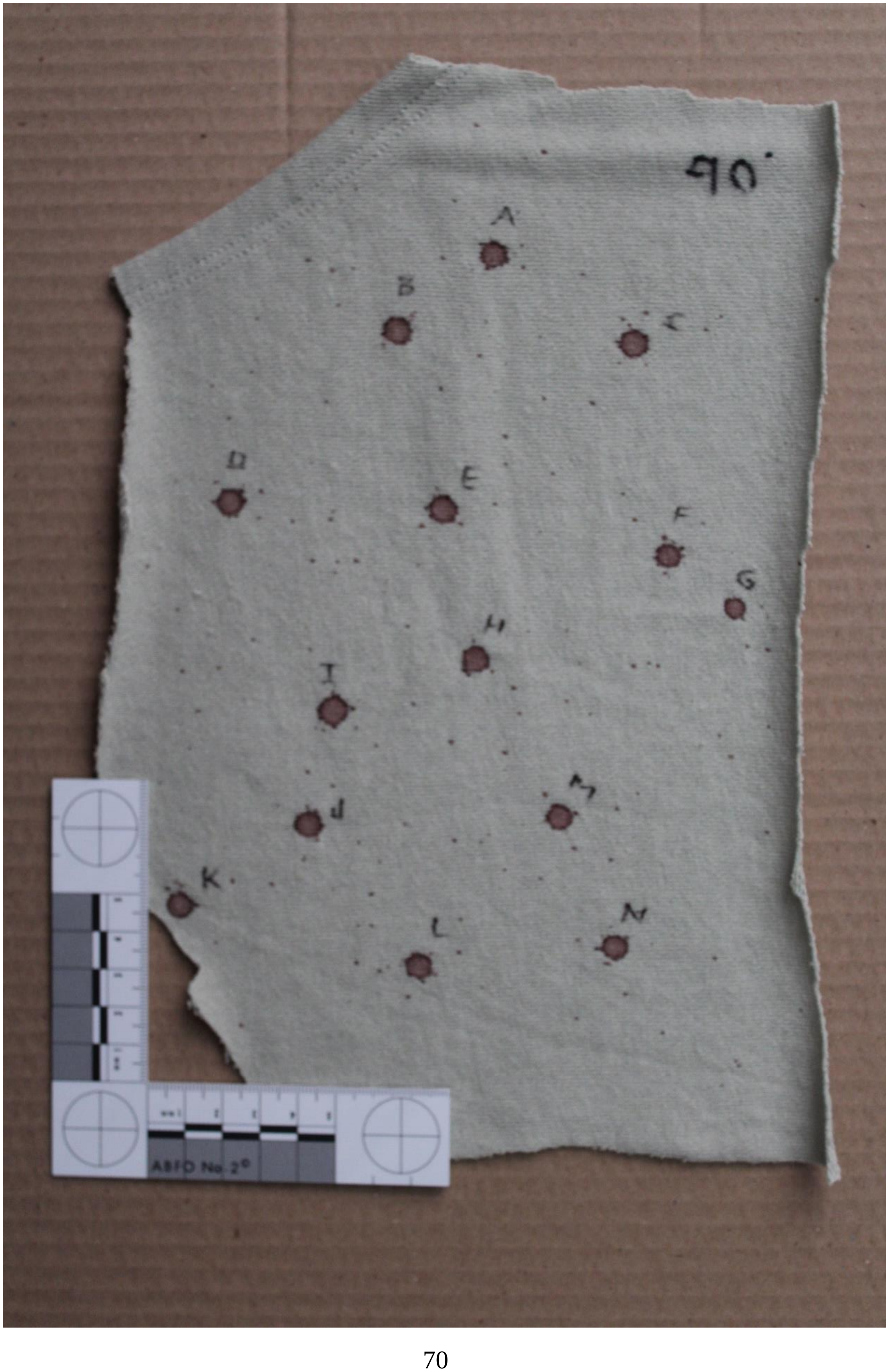

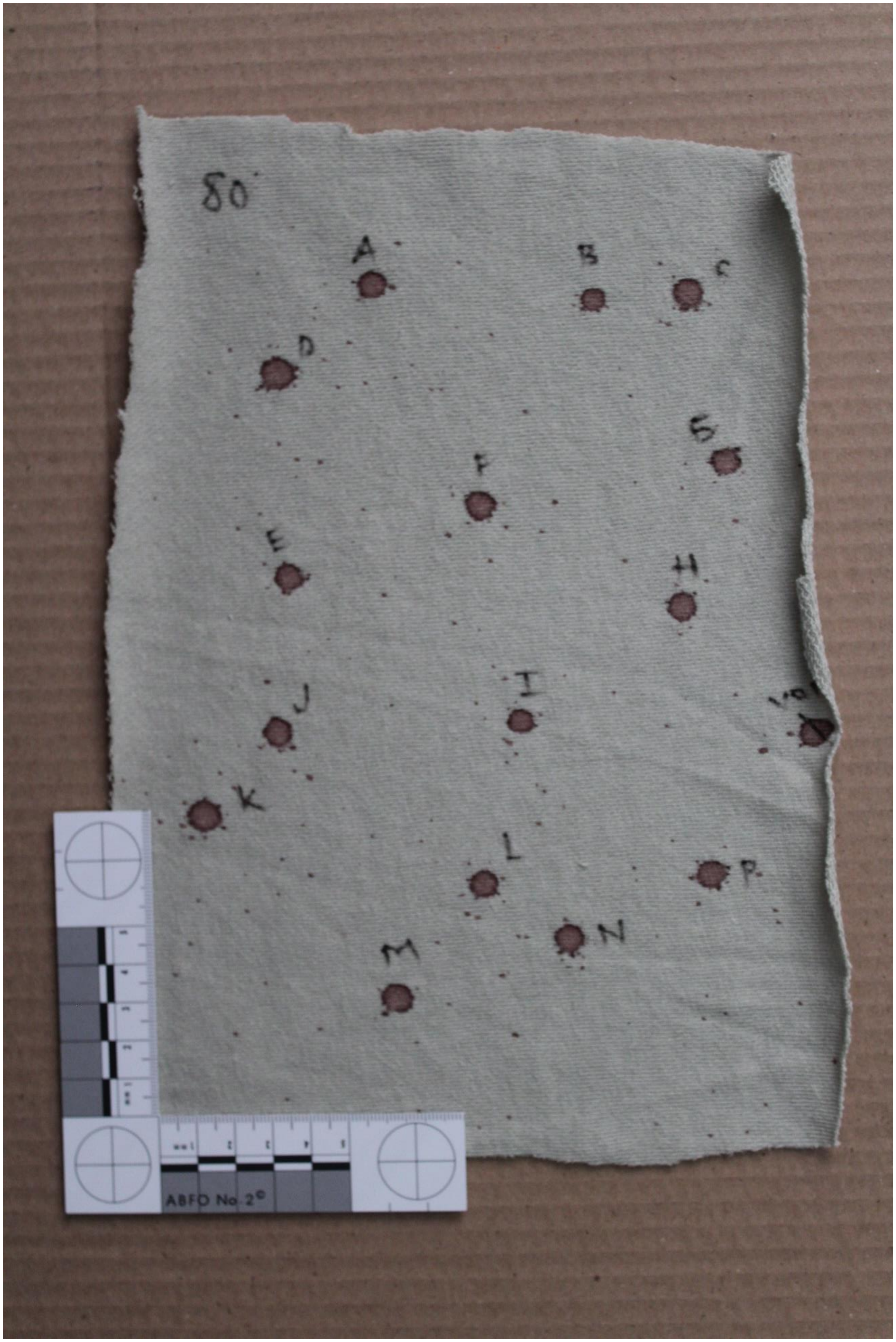
80
A
B
C
D
G
F
E
H
I
J
K
L
P
N
M
ABFO No. 2©

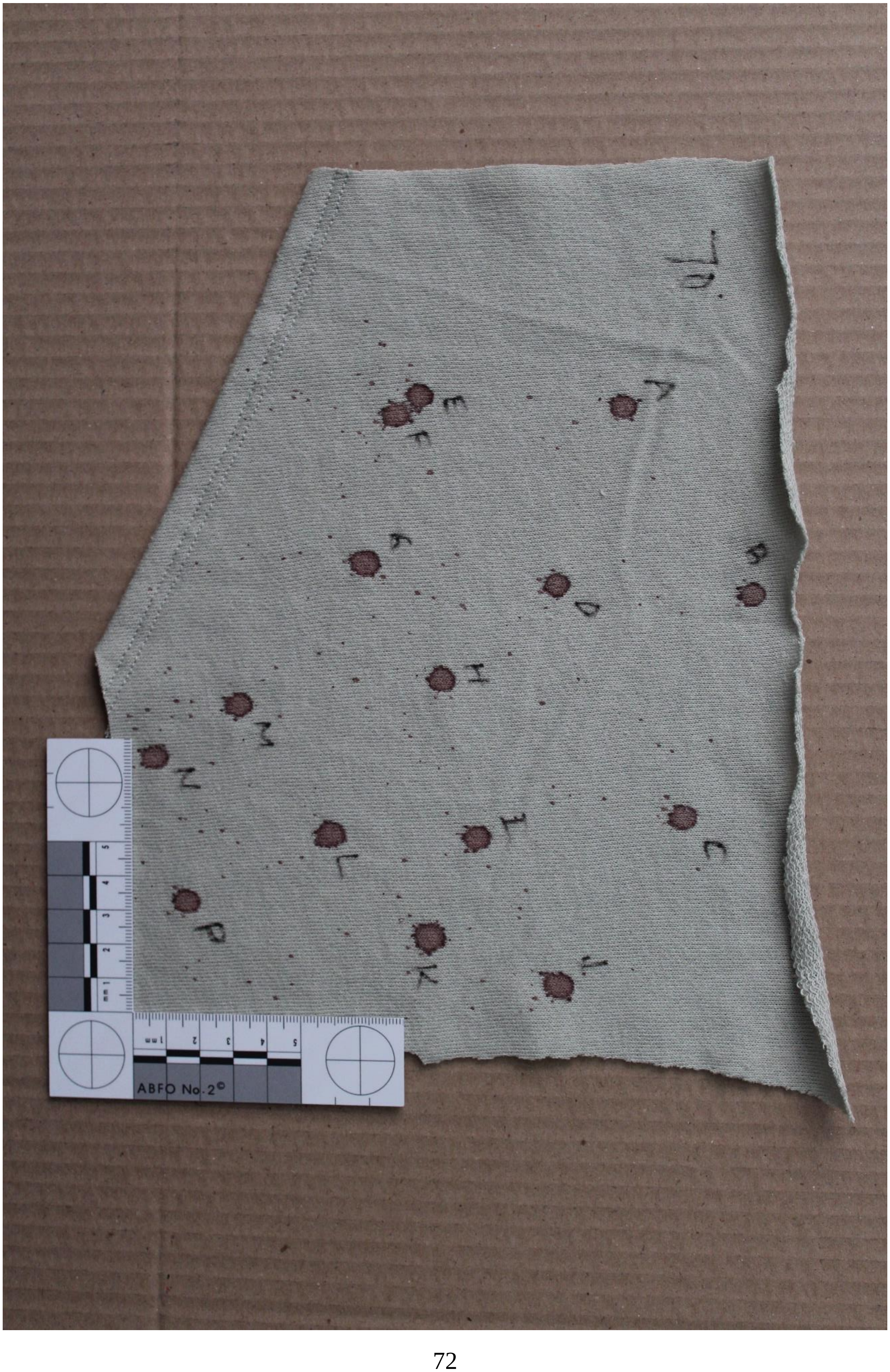
ABFO No. 2©

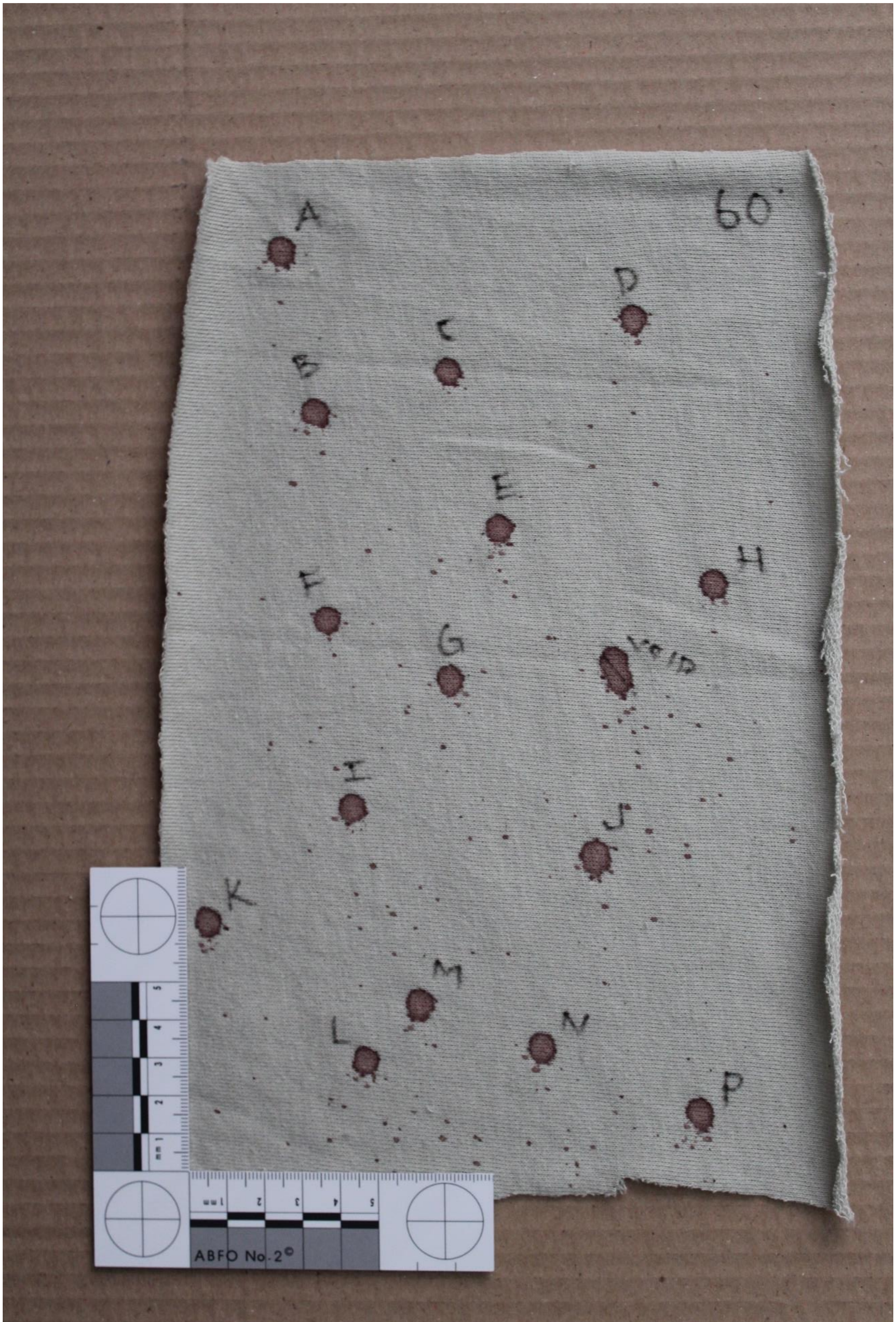
60
A
D
C
B
E
H
F
G
Void
I
J
K
M
L
N
P
ABFO No. 2©


50
C
D
A
B
E
F
G
N
H
I
K
M
J
L
ABFO No. 2©

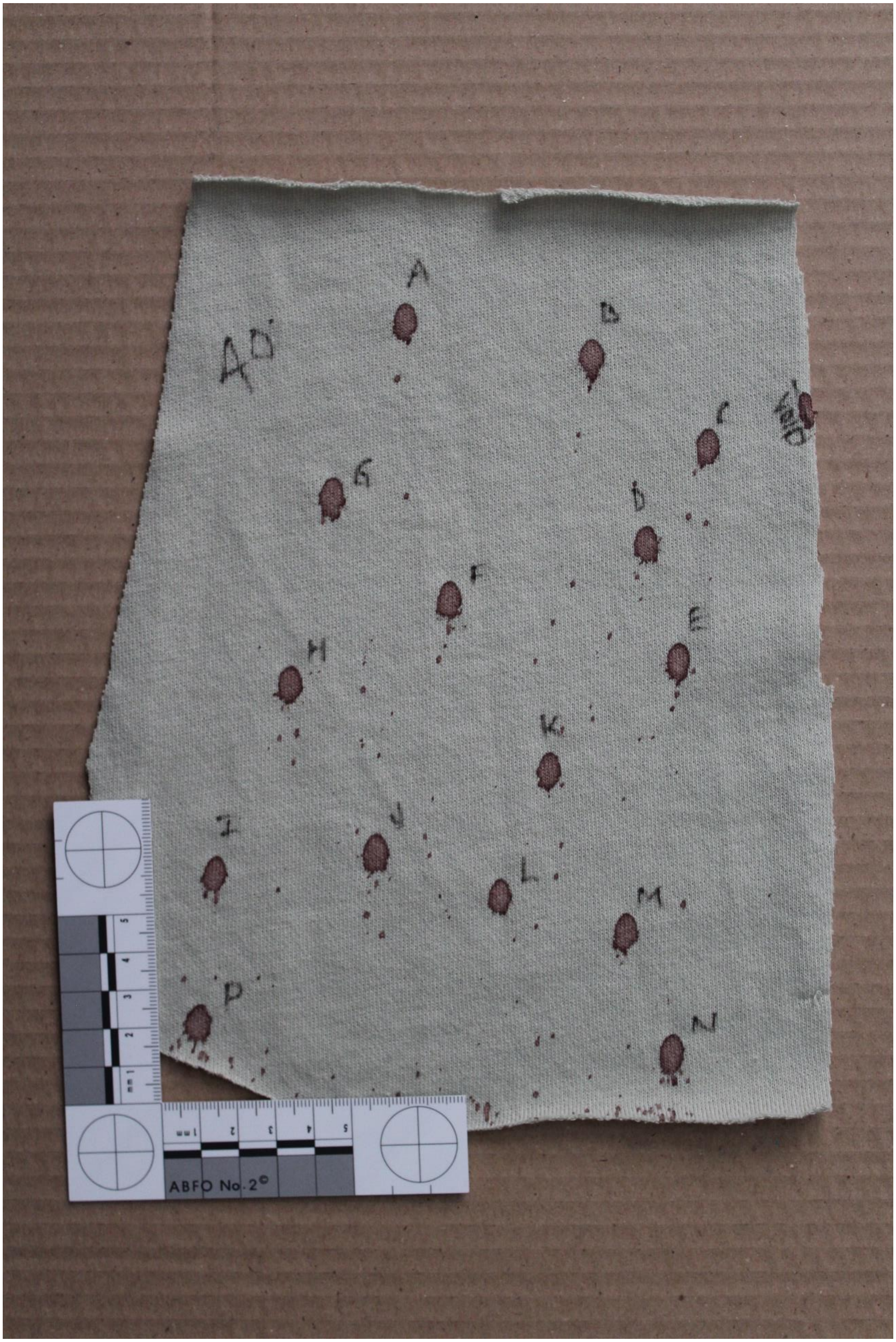
ABFO No. 2©

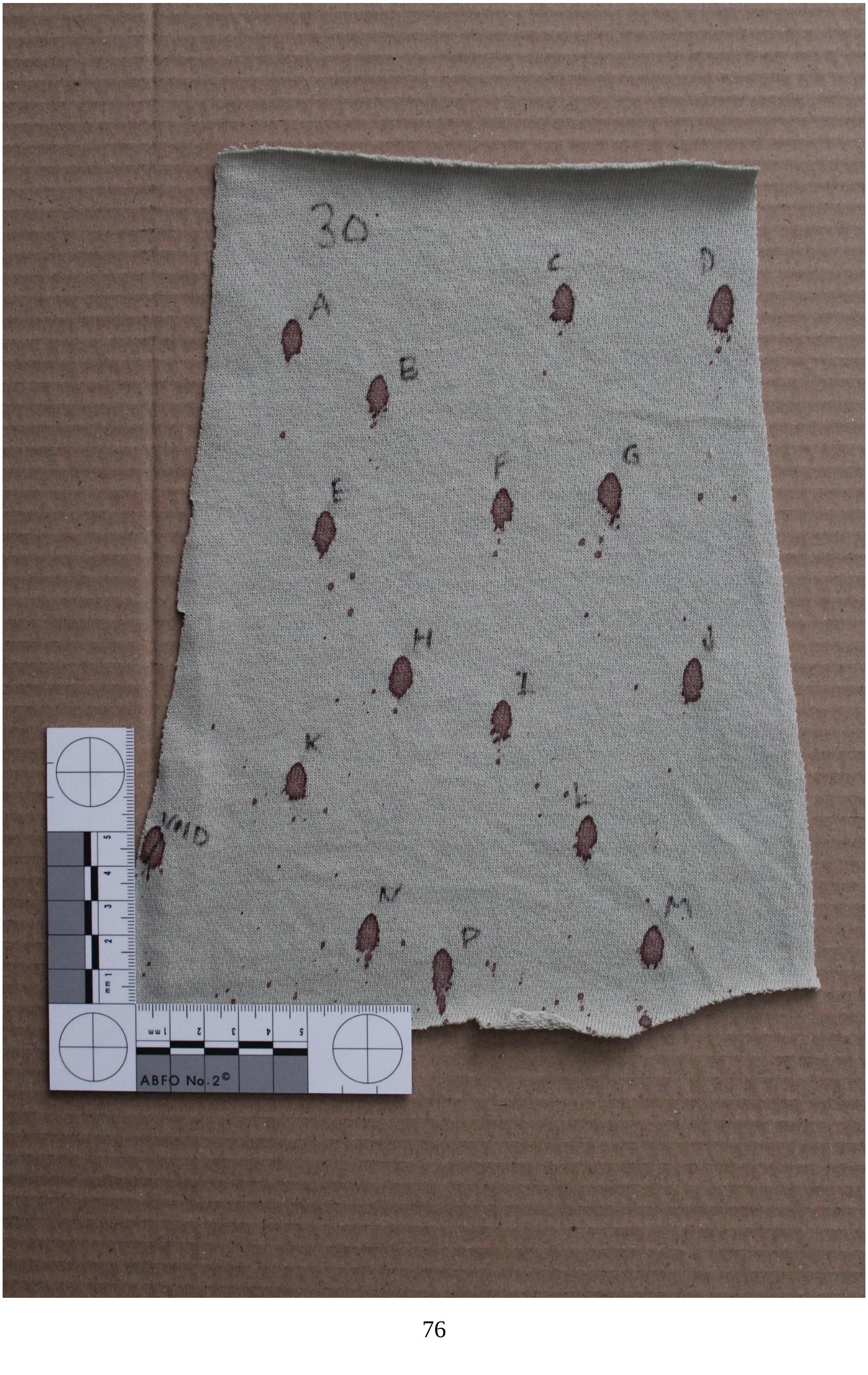
30
A
B
C
D
E
F
G
H
I
J
K
L
M
N
P
VOID
ABFO No. 2©

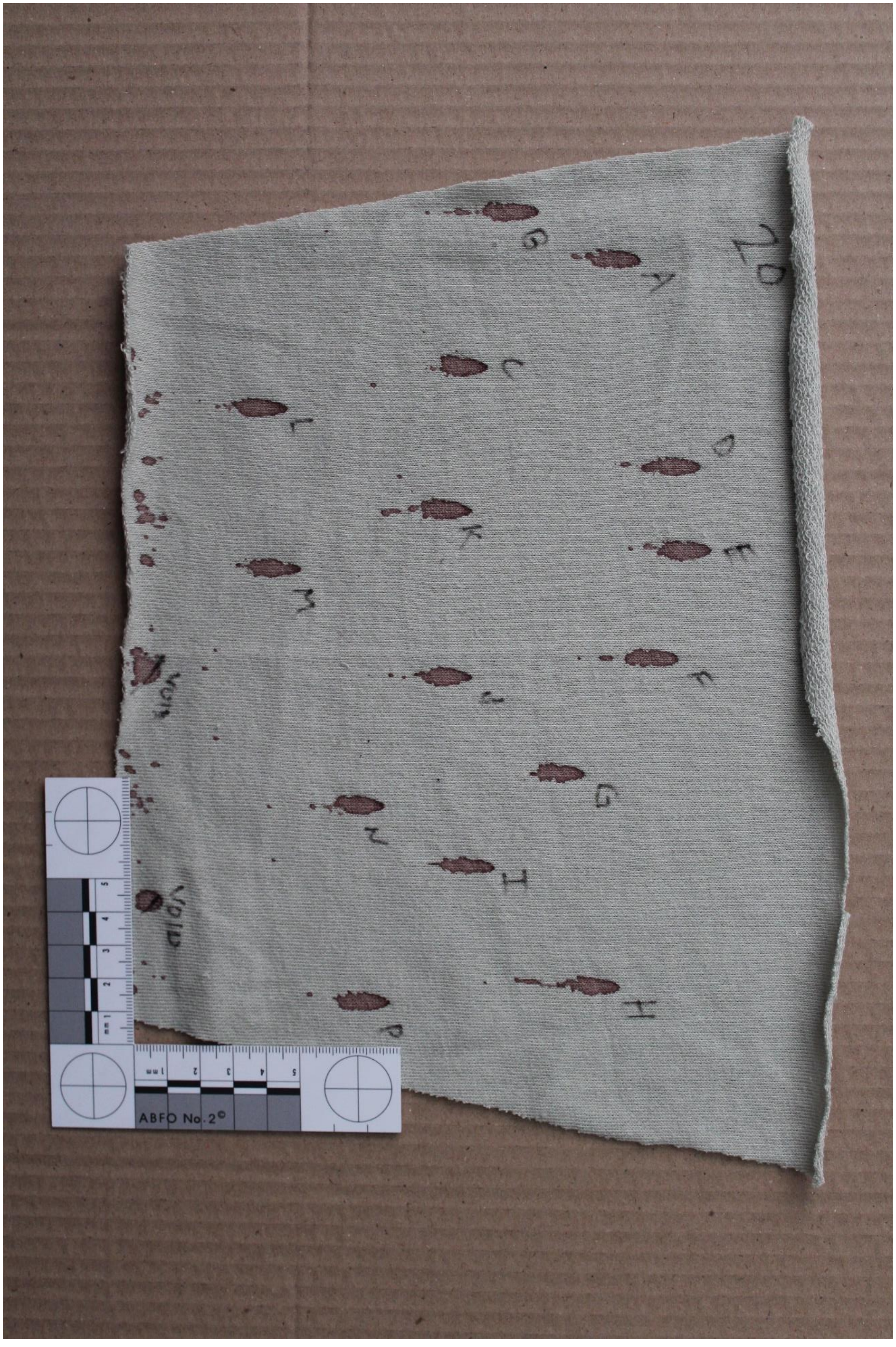

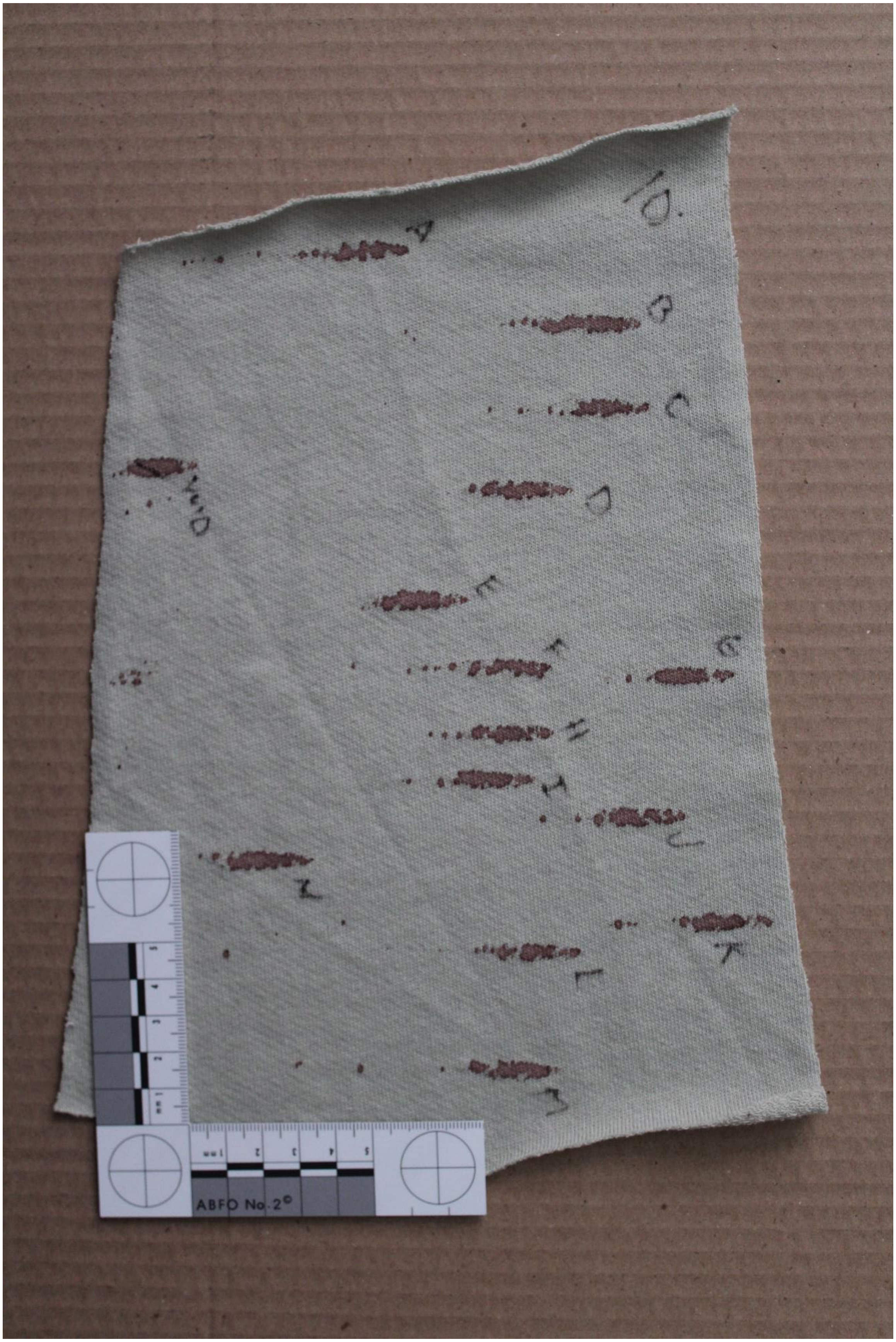
ABFO No. 2©

Appendix H: Bloodstain Photos—Fabric 3

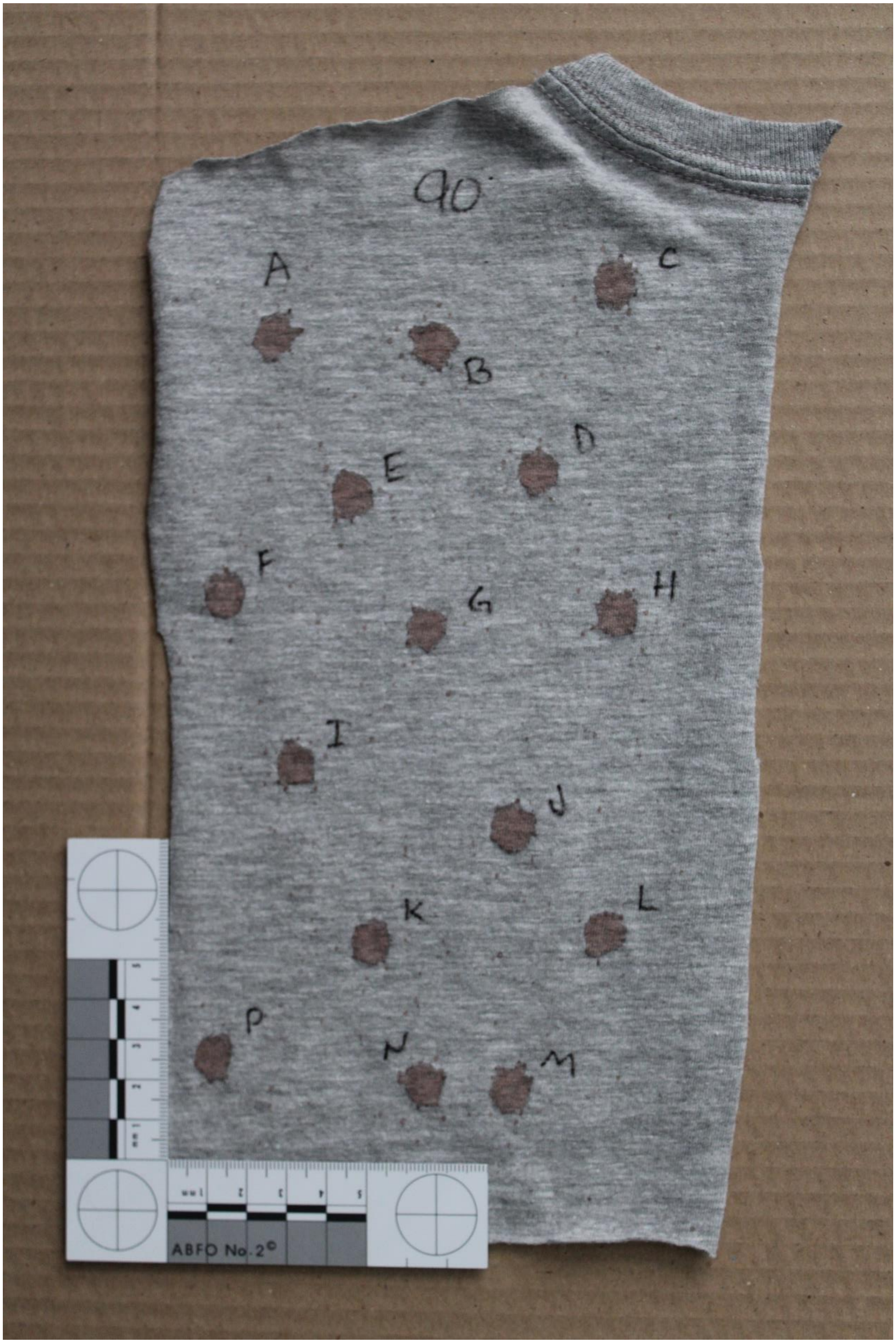


80
A
B
C
D
E
F
G
H
I
J
K
L
M
N
P
ABFO No. 2©


70°
B
C
D
A
G
E
F
H
I
J
K
M
L
N
ABFO No. 2©

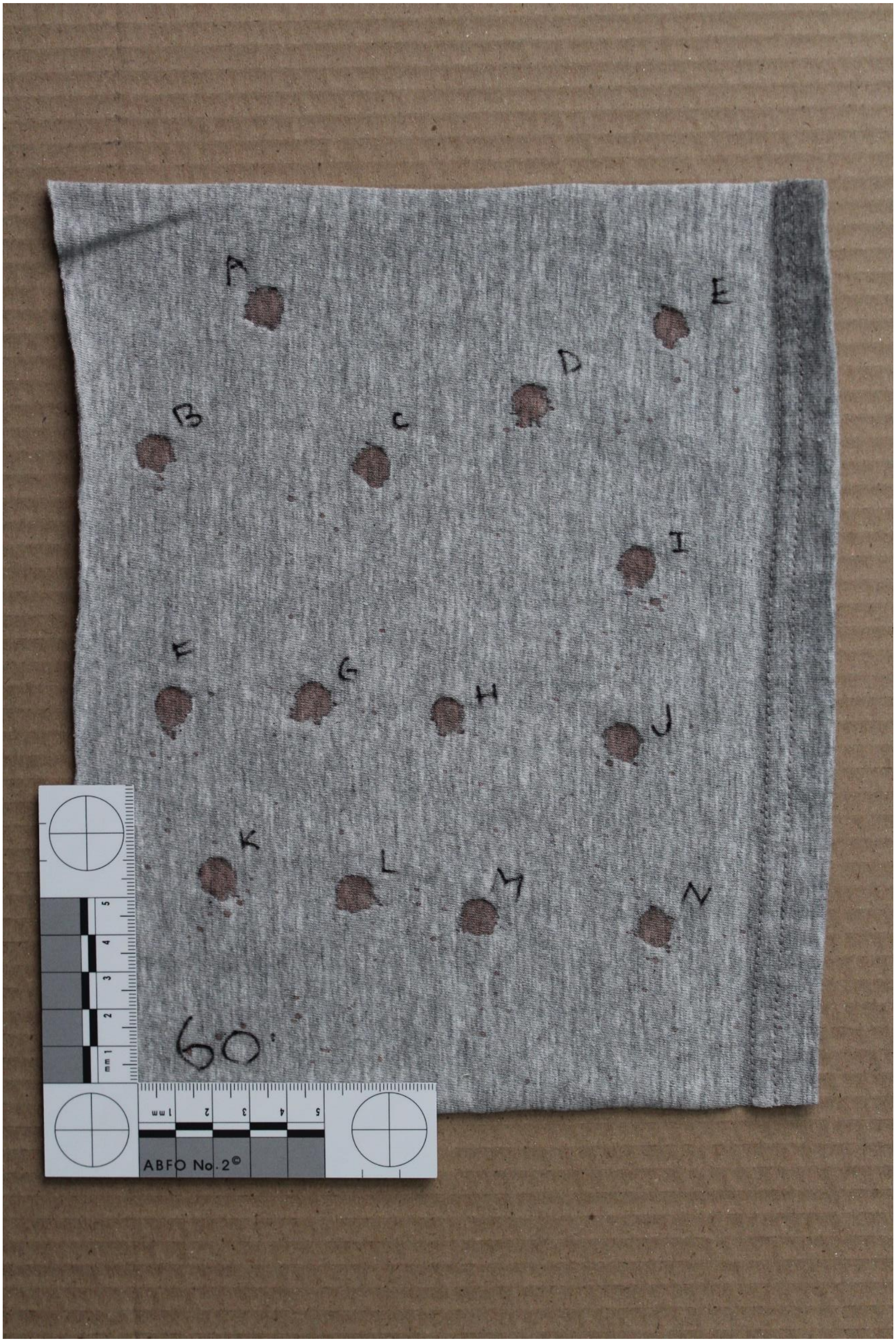
A
E
D
B
C
I
F
G
H
J
K
L
M
N
60°
ABFO No. 2©

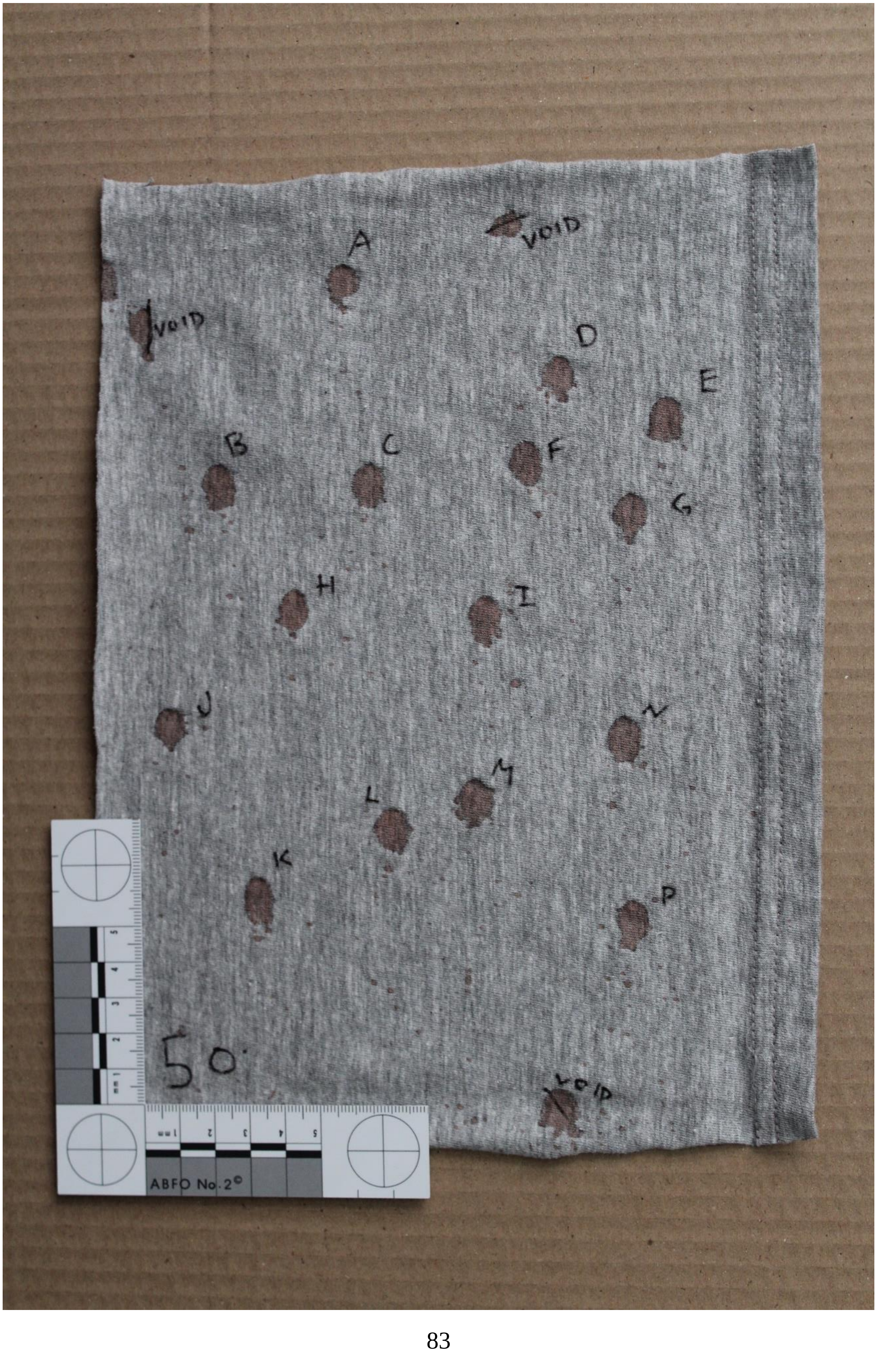
A
VOID
VOID
D
E
B
C
F
G
H
I
J
N
M
L
K
P
50
VOID
ABFO No. 2©

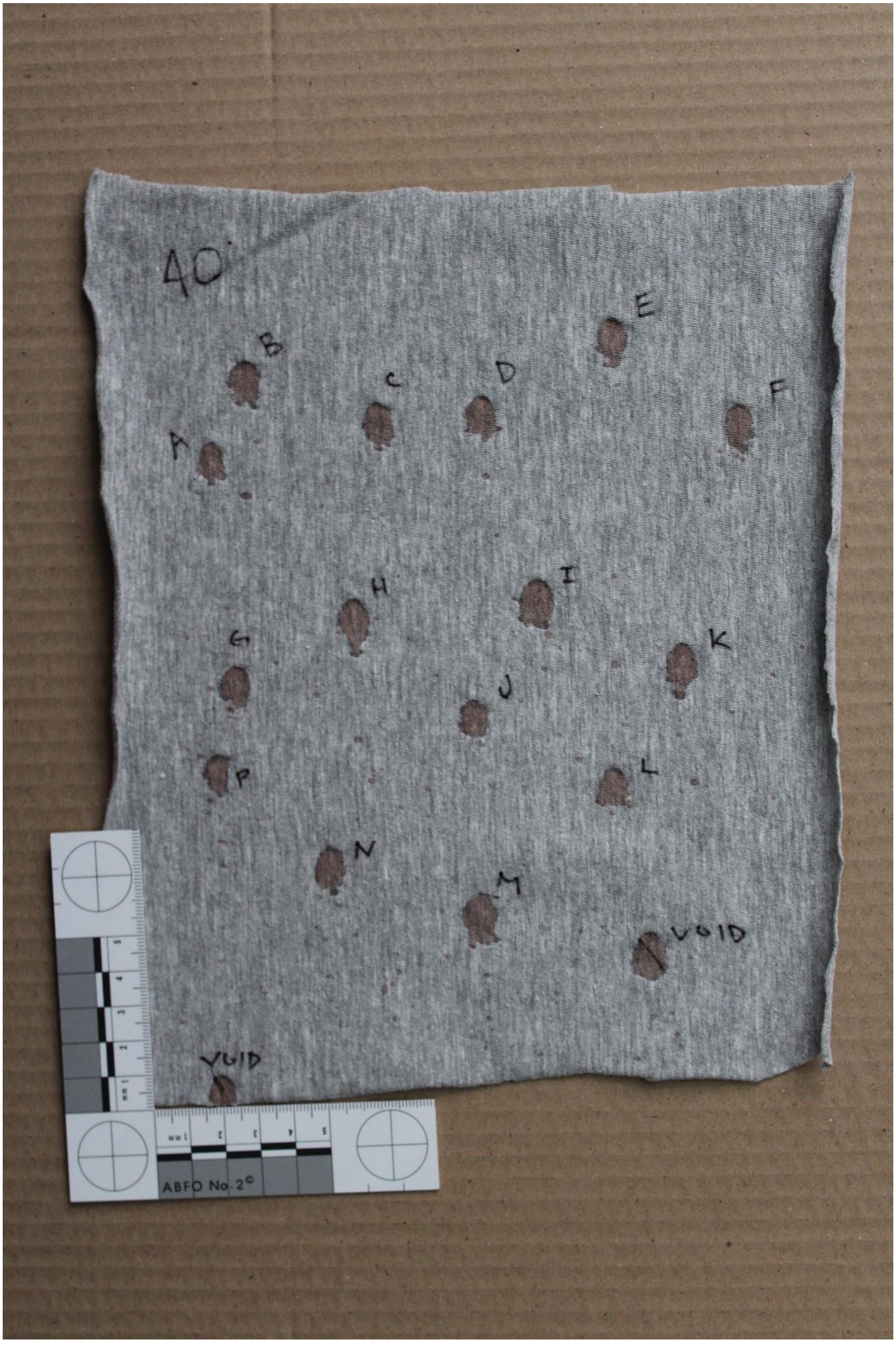
40
A
B
C
D
E
F
G
H
I
J
K
L
M
N
P
VOID
VOID
ABFO No. 2©

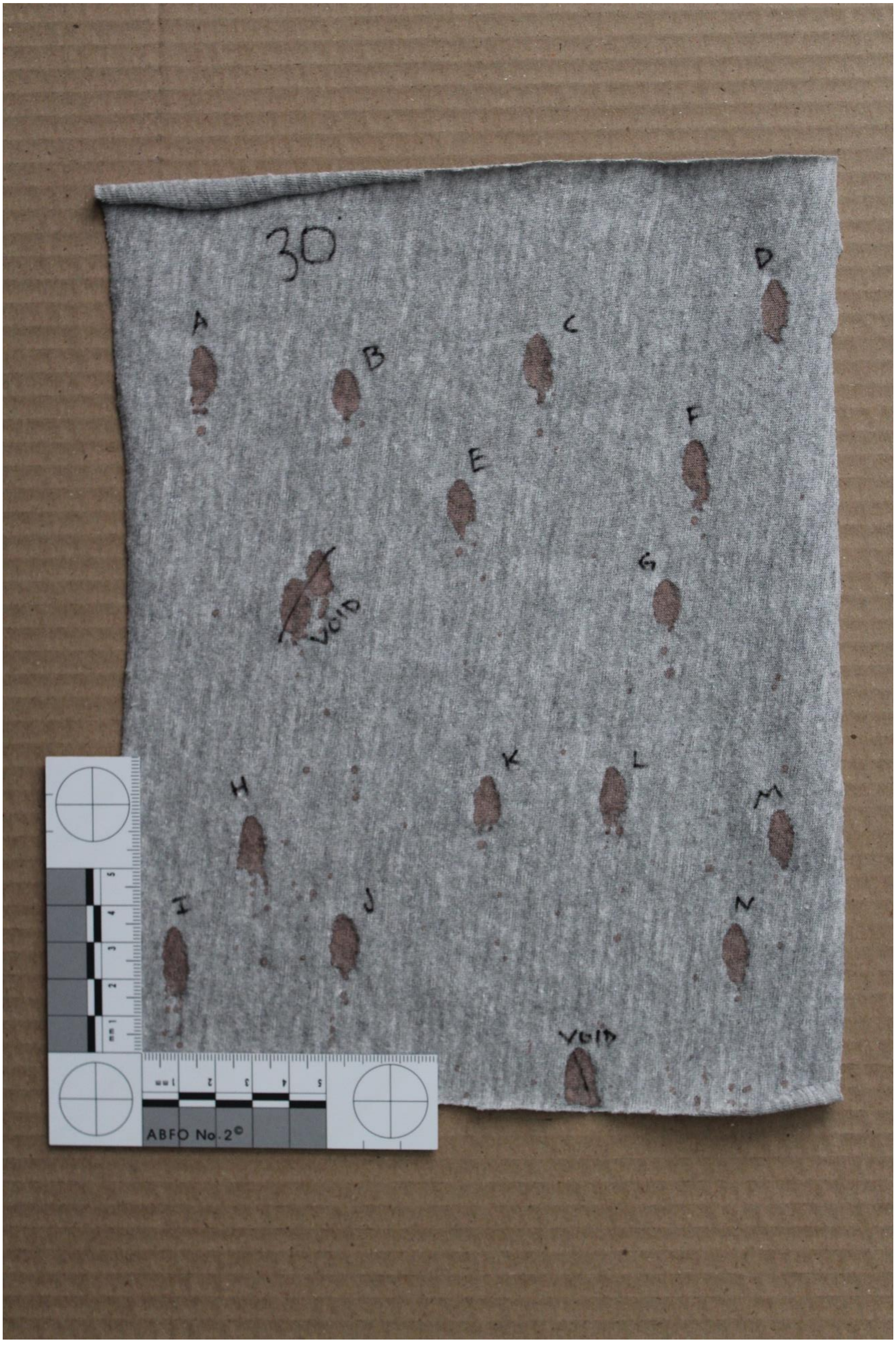
30
A
B
C
D
E
F
G
VOID
H
K
L
M
I
J
N
VOID
ABFO No. 2©


ABFO No. 2©

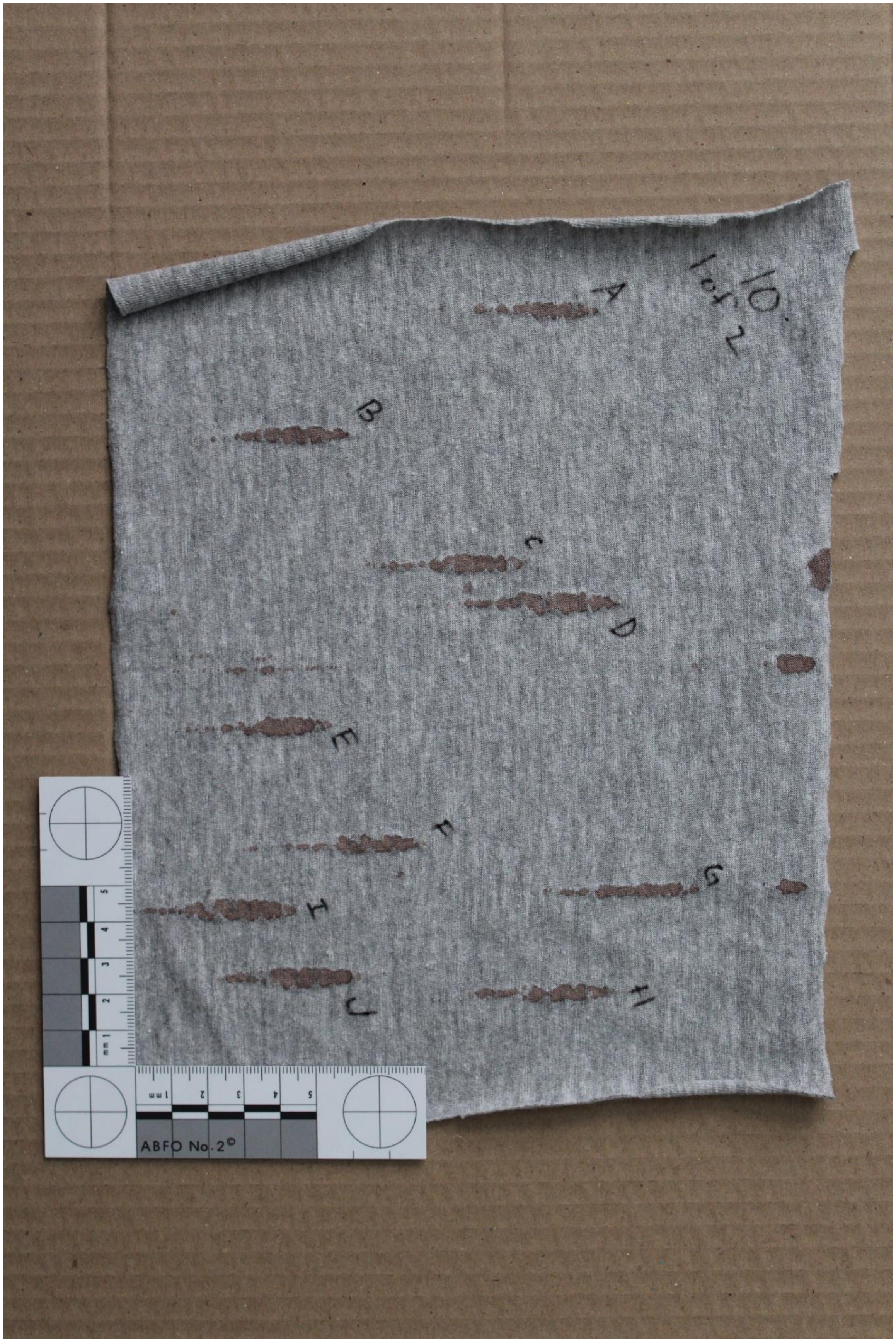
10
1 of 2
A
B
C
D
E
F
G
H
I
J
ABFO No. 2©

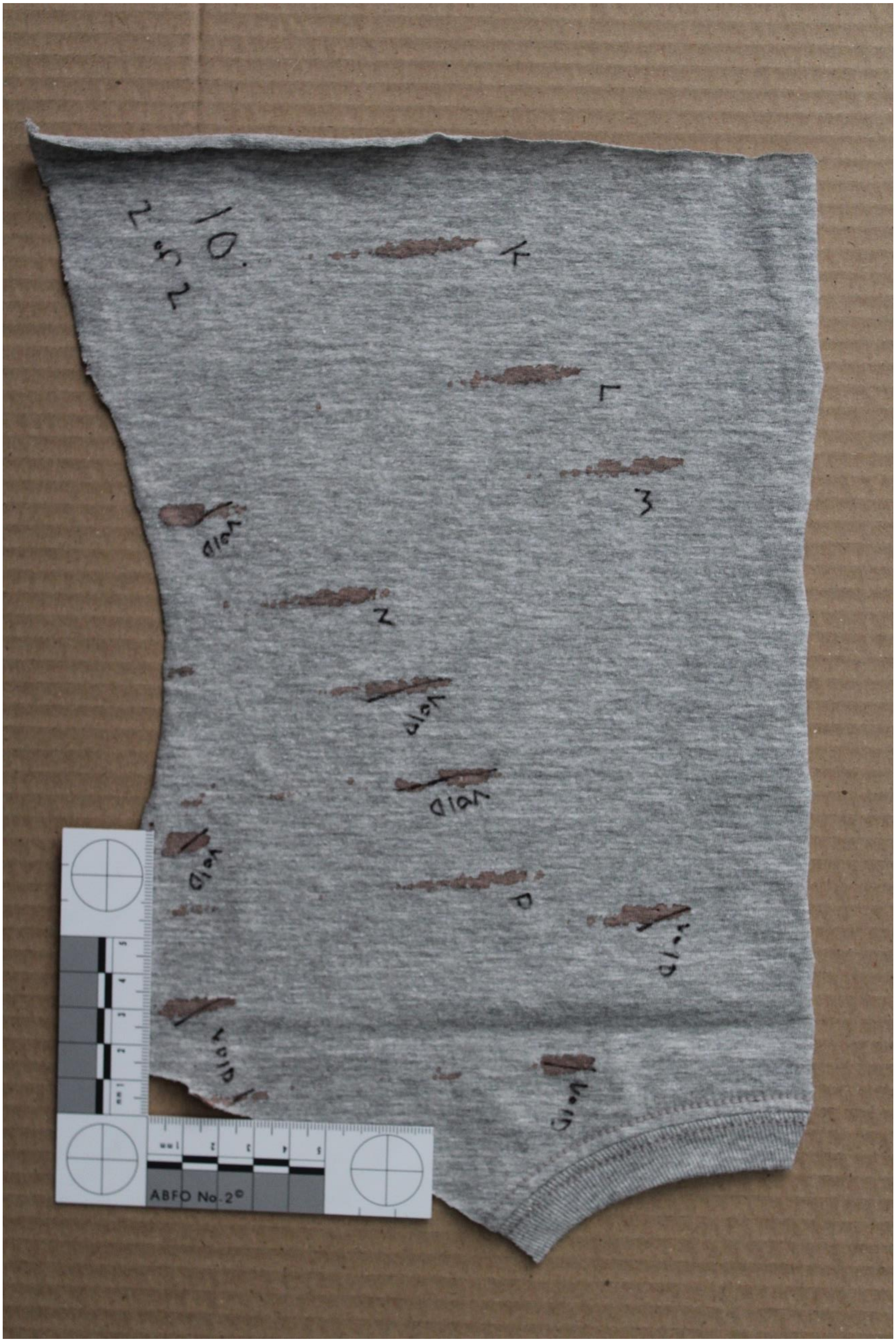
ABFO No. 2©